



Ministry of Energy and Mines
BC Geological Survey

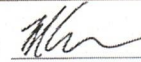
Assessment Report
Title Page and Summary

TYPE OF REPORT [type of survey(s)]: Helicopter Airborne Survey

TOTAL COST: 80,000.00

AUTHOR(S): Michael Cunningham

SIGNATURE(S):



NOTICE OF WORK PERMIT NUMBER(S)/DATE(S): April 13/2021 , April 14/2021

YEAR OF WORK: 2021

STATEMENT OF WORK - CASH PAYMENTS EVENT NUMBER(S)/DATE(S): 5848526

PROPERTY NAME: McNulty

CLAIM NAME(S) (on which the work was done): 107339(McNaulty Creek) , 1081411(McNaulty Creek 2) , 1081412(McNaulty Creek 3)

COMMODITIES SOUGHT: Copper,Gold,Silver,Lead,Zinc,Molybdenum

MINERAL INVENTORY MINFILE NUMBER(S), IF KNOWN: None

MINING DIVISION: Similkameen & Osoyoos Divisions

NTS/BCGS: 092-H08 , 092-H09

LATITUDE: 49 ° 30 '38.61 " LONGITUDE: 120 ° 10 '1.72 " (at centre of work)

OWNER(S):

1) Platinum Belt Resources Inc

2)

MAILING ADDRESS:

8899 Michael Drive

Coldstream B.C.

OPERATOR(S) [who paid for the work]:

1) Max Investments

2)

MAILING ADDRESS:

3750 West 49th Ave

Vancouver B.C.

PROPERTY GEOLOGY KEYWORDS (lithology, age, stratigraphy, structure, alteration, mineralization, size and attitude):

Intermontane Belt, Mid-Jurassic, Okanagan Batholith, Porphyry Copper, Molybdenum, Gold, chalcocopyrite, pyrrhotite, arsenopyrite,

Skarn Altered Diorites, granite, granodiorite, syenite

REFERENCES TO PREVIOUS ASSESSMENT WORK AND ASSESSMENT REPORT NUMBERS: N/A

TYPE OF WORK IN THIS REPORT	EXTENT OF WORK (IN METRIC UNITS)	ON WHICH CLAIMS	PROJECT COSTS APPORTIONED (incl. support)
GEOLOGICAL (scale, area)			
Ground, mapping	_____	_____	_____
Photo interpretation	_____	_____	_____
GEOPHYSICAL (line-kilometres)			
Ground			
Magnetic	337.9	107339,1081411,1081412	80,000.00
Electromagnetic	_____	_____	_____
Induced Polarization	_____	_____	_____
Radiometric	_____	_____	_____
Seismic	_____	_____	_____
Other	_____	_____	_____
Airborne			
GEOCHEMICAL (number of samples analysed for...)			
Soil	_____	_____	_____
Silt	_____	_____	_____
Rock	_____	_____	_____
Other	_____	_____	_____
DRILLING (total metres; number of holes, size)			
Core	_____	_____	_____
Non-core	_____	_____	_____
RELATED TECHNICAL			
Sampling/assaying	_____	_____	_____
Petrographic	_____	_____	_____
Mineralographic	_____	_____	_____
Metallurgic	_____	_____	_____
PROSPECTING (scale, area)			
PREPARATORY / PHYSICAL			
Line/grid (kilometres)	_____	_____	_____
Topographic/Photogrammetric (scale, area)	_____	_____	_____
Legal surveys (scale, area)	_____	_____	_____
Road, local access (kilometres)/trail	_____	_____	_____
Trench (metres)	_____	_____	_____
Underground dev. (metres)	_____	_____	_____
Other	_____	_____	_____
TOTAL COST:			80,000.00

**REPORT ON A HELICOPTER-BORNE
MAGNETIC GRADIOMETER SURVEY
NEAR PRINCETON, BC**

- Property Name -

McNulty

NTS Areas: 092 H08 and 092 H09

- Location -

49° 30' 38.61" N, 120° 10' 1.72" W

705,062 m E, 5,488,090 m N, UTM Zone 10

- Prepared for -

Max Investments Ltd.

- Prepared by -

Balch Exploration Consulting Inc.

- Written by -

Michael Cunningham, P.Geo.

F-3070 Councillor's Way, Ottawa, Ontario, K1T 2S6

- Completion Date –

Survey: April 14, 2021

Report: May 10, 2021

TABLE OF CONTENTS

1.0 INTRODUCTION	1
1.1 CONTRACTOR.....	1
1.2 CLIENT	1
1.3 SURVEY OBJECTIVES.....	1
2.0 SURVEY AREA	2
2.1 LOCATION AND ACCESS	2
2.2 INFRASTRUCTURE.....	3
2.3 CLIMATE	3
2.4 TOPOGRAPHY	3
2.5 MINERAL AND MINING CLAIMS	3
2.6 FLIGHT AND TIE LINES	4
2.7 DATUM AND PROJECTION.....	5
3.0 PERSONNEL AND CALENDAR.....	6
3.1 PERSONNEL	6
3.2 CALENDAR	6
3.3 SUMMARY OF COSTS	6
4.0 SURVEY SYSTEM	8
4.1 HELICOPTER.....	8
4.2 AIRBORNE SYSTEM	8
4.2.1 IMPAC and AGIS	9
4.3 LASER ALTIMETER.....	11
4.4 PILOT GUIDANCE UNIT	11
4.5 GPS NAVIGATION	12
4.6 MAGNETOMETER SENSOR	13
4.7 MAGNETIC GRADIOMETER.....	16
4.8 FLUXGATE MAGNETOMETER	16
4.9 BASE STATION MAGNETOMETER.....	19
5.0 DATA ACQUISITION AND PROCESSING	21
5.1 DATA ACQUISITION EQUIPMENT CHECKS	21
5.2 LASER ALTIMETER CALIBRATION	21
5.3 LAG TEST.....	21
5.4 MAGNETOMETER TESTS.....	22
5.4.1 Compensation Flight Test.....	22
5.4.2 Heading Correction Test.....	23
5.5 FIELD PROCESSING AND QUALITY CONTROL	23
5.6 DATA PROCESSING.....	24
5.6.1 Position Corrections.....	24
5.6.2 Flight Height and Digital Terrain Model.....	26
5.6.3 Magnetic Processing	26
5.6.4 Magnetic Gradient	28
6.0 RESULTS	31
7.0 INTERPRETATION	41

7.1 OVERVIEW41
7.2 McNULTY MAGNETIC SURVEY.....43
8.0 QUALIFICATIONS 47
9.0 REFERENCES 48
APPENDIX A – OUTLINE OF SURVEY POLYGONS..... 49
APPENDIX B - LIST OF DATABASE COLUMNS (.GDB FORMAT)..... 50
APPENDIX C – PRECISION GEOSURVEYS LOGISTICS REPORT..... 51

List of Figures

FIGURE 1 – LOCATION MAP OF THE McNULTY SURVEY AREA.....	2
FIGURE 2 - MAP OF CLAIM OUTLINES OVER THE SURVEY AREA.....	4
FIGURE 3 - FLIGHT AND TIE LINES OVER THE McNULTY CLAIMS.	5
FIGURE 4 – THE SURVEY USED AN AIRBUS AS350 AS SHOWN ABOVE.....	8
FIGURE 5 - SURVEY HELICOPTER EQUIPPED WITH THREE MAGNETIC SENSORS FOR GRADIENT MAGNETIC DATA ACQUISITION.	9
FIGURE 6 - IMPAC DATA ACQUISITION SYSTEM.....	9
FIGURE 7 – AGIS OPERATOR DISPLAY, SHOWING REAL-TIME FLIGHT LINE RECORDING AND NAVIGATION PARAMETERS. ADDITIONAL WINDOWS DISPLAY REAL-TIME GEOPHYSICAL DATA TO THE OPERATOR.	10
FIGURE 8 – OPTI-LOGIC RS800 RANGEFINDER LASER ALTIMETER.	11
FIGURE 9 – PGU SCREEN DISPLAYING NAVIGATION INFORMATION.	12
FIGURE 10 - HEMISPHERE R220 GPS RECEIVER.	13
FIGURE 11 – (LEFT) SCINTREX CESIUM (CS-3) MAGNETOMETER. (RIGHT) GEOMETRICS G-822A Cs VAPOR MAGNETOMTER.	13
FIGURE 12 – VIEW OF TRIPLE MAGNETIC BOOM SYSTEM.....	16
FIGURE 13 - BILLINGSLEY TRIAXIAL FLUXGATE MAGNETOMETER.....	17
FIGURE 14 – GEM GSM-19T PROTON PRECESSION MAGNETOMETER.	19
FIGURE 15 - GSM 19 BASE STATIONS USED TO RECORD DIURNAL VARIATIONS. GEM 3 – LEFT AND GEM 4 – RIGHT.....	20
FIGURE 16 – MAGNETIC DATA PROCESSING FLOW.	25
FIGURE 17 - SHADED IMAGE OF THE TOTAL MAGNETIC INTENSITY (TMI) OVER THE SURVEY BLOCK.	31
FIGURE 18 - SHADED IMAGE OF THE GRADIENT ENHANCED TOTAL MAGNETIC INTENSITY (TMI) OVER THE SURVEY BLOCK.....	32
FIGURE 19 - SHADED IMAGE OF THE RESIDUAL MAGNETIC INTENSITY (RMI) OVER THE SURVEY BLOCK.....	33
FIGURE 20 - SHADED IMAGE OF THE GRADIENT ENHANCED RESIDUAL MAGNETIC INTENSITY (RMI) OVER THE SURVEY BLOCK.	34
FIGURE 21 - SHADED IMAGE OF THE GRADIENT ENHANCED REDUCED-TO-POLE (RTP) OVER THE SURVEY BLOCK.	35
FIGURE 22 – SHADED IMAGE OF THE IN-LINE HORIZONTAL GRADIENT OVER THE SURVEY BLOCK.	36
FIGURE 23 – SHADED IMAGE OF THE CROSS-LINE HORIZONTAL GRADIENT OVER THE SURVEY BLOCK.	37
FIGURE 24 – SHADED IMAGE OF THE VERTICAL GRADIENT OVER THE SURVEY BLOCK.	38
FIGURE 25 – SHADED IMAGE OF THE TOTAL HORIZONTAL GRADIENT OVER THE SURVEY BLOCK.	39
FIGURE 26 - IMAGE OF THE DTM OVER THE SURVEY BLOCK.	40
FIGURE 27 – BEDROCK GEOLOGY MAP OF THE McNULTY SURVEY BLOCK (RED OUTLINE). GEOLOGICAL ROCK UNITS NEAR THE McNULTY PROPERTY: EPEMK – EOCENE UNDIVIDED VOLCANIC ROCKS; KGR – CRETACEOUS GRANITES; MJGR – MIDDLE JURASSIC GRANITE; MJOgd – MIDDLE JURASSIC GRANODIORITE; LTJGD – LATE TRIASSIC TO EARLY JURASSIC GRANODIORITE; TRJN – TRIASSIC TO JURASSIC CALC-ALKALINE VOLCANIC ROCKS; UTRNE/UTNE – UPPER TRIASSIC BASALTIC VOLCANIC ROCKS; UTNSF – UPPER TRIASSIC MUDSTONE, SILTSTONE, AND SHALES;	42
FIGURE 28 - TOTAL MAGNETIC INTENSITY MAP OF THE McNULTY BLOCK WITH BEDROCK GEOLOGY: MJGR – MIDDLE JURASSIC GRANITE; MJOgd – MIDDLE JURASSIC GRANODIORITE; LTJGD – LATE TRIASSIC TO EARLY JURASSIC GRANODIORITE; AND UTNE – UPPER TRIASSIC BASALTIC VOLCANIC ROCKS. (1) INTERPRETED N-W TRENDING STRUCTURES NEAR CONTACT BETWEEN MJGR AND MJOgd. (2) E-W TRENDING STRUCTURE. (3) HIGH MAGNETIC REGION.	44
FIGURE 29 – CALCULATED VERTICAL GRADIENT MAP OF THE McNULTY BLOCK WITH BEDROCK GEOLOGY: MJGR – MIDDLE JURASSIC GRANITE; MJOgd – MIDDLE JURASSIC GRANODIORITE; LTJGD – LATE TRIASSIC TO EARLY JURASSIC GRANODIORITE; AND UTNE – UPPER TRIASSIC BASALTIC VOLCANIC ROCKS.	45
FIGURE 30 – TOTAL MAGNETIC INTENSITY PROFILES ALONG THREE SURVEY LINES (T19060, L350, AND L40) WITH SOME POTENTIAL TARGET REGIONS (PT1, PT3, AND PT4).....	46

List of Tables

TABLE 1 - SUMMARY OF MINING CLAIMS INCLUDING OWNERSHIP AND DUE DATE.	3
TABLE 2 - SUMMARY OF FLIGHT AND TIE LINE SPECIFICATIONS.	5
TABLE 3 - LIST OF SURVEY PERSONNEL.	6
TABLE 4 - TIME SCHEDULE FOR SURVEY.	6
TABLE 5 - SUMMARY OF COSTS.	7
TABLE 6 - SCINTREX CS-3 SPECIFICATIONS.	14
TABLE 7 – GEOMETRICS G-822A SPECIFICATIONS.	15
TABLE 8 – MAGNETOMETER DETAILS. CROSS-LINE GRADIENT MEASURED BETWEEN MAG 1 AND MAG 2.	16
TABLE 9 – GEOMETRICS G-822A SPECIFICATIONS.	18
TABLE 10 - GSM-19 BASE STATION SPECIFICATIONS.	19
TABLE 11 - MAGNETIC BASE STATION LOCATIONS.	20
TABLE 12 – SURVEY LAG CORRECTION VALUES. MAGNETIC DATA AT 20 HZ; LASER ALTIMETER WAS RESAMPLED TO 20 HZ.	21
TABLE 13 – RESULTS OF COMPENSATION FLIGHT FOR MAG 1.	22
TABLE 14 – RESULTS OF COMPENSATION FLIGHT FOR MAG 2.	22
TABLE 15 – RESULTS OF COMPENSATION FLIGHT FOR MAG 3.	23
TABLE 16 – MAGNETIC SENSOR HEADING CORRECTIONS FOR HEADINGS 000°/090°/180°/270°.	23
TABLE 17 – CONTRACT SURVEY SPECIFICATIONS.	24
TABLE 18 – MAGNETIC SENSOR RELATIONSHIP USED TO CALCULATE MAGNETIC GRADIENTS. TOTAL MAGNETIC INTENSITY (TMI) WAS DETERMINED FROM MAG 2, AND SUCCESSIVE VALUES OF THE TMI WERE USED TO DETERMINE THE LONGITUDINAL (Y AXIS) GRADIENT.	28
TABLE 19 – POTENTIAL AREAS OF INTEREST LOCATIONS IN UTM ZONE 10 AND DATUM WGS84.	43
TABLE 20 – MCNULTY BLOCK POLYGON CORNERS.	49

1.0 INTRODUCTION

1.1 CONTRACTOR

Balch Exploration Consulting Inc. (“BECI”, the “Contractor”) having its head office at 11500 Fifth Line, Rockwood, Ontario, Canada, N0B 2K0, has performed a helicopter-borne triaxial gradient magnetometer survey.

1.2 CLIENT

Max Investments Ltd. (“Max Investments”, or the “Client”) having its head office at 3750 West 49th Ave, Vancouver, B.C., V6N3TB.

1.3 SURVEY OBJECTIVES

To identify geologic features, contacts and outlines that could be related to copper-rich porphyry, VMS, and skarn deposits and gold deposits.

2.0 SURVEY AREA

2.1 LOCATION AND ACCESS

The McNulty survey block is located approximately 21 km east-northeast of Princeton, British Columbia, 15 km northwest of Hedley, British Columbia, and 38 km west of Penticton, British Columbia. The block is located within NTS topographic sheets 092-H08, and 092-H09. Figure 1 shows the location of the survey block.

There are forestry roads throughout the area potentially providing access to the survey block. Access to the forestry roads could be found off Highway 3, Crowsnest Highway, approximately 4 km west of Hedley, BC.

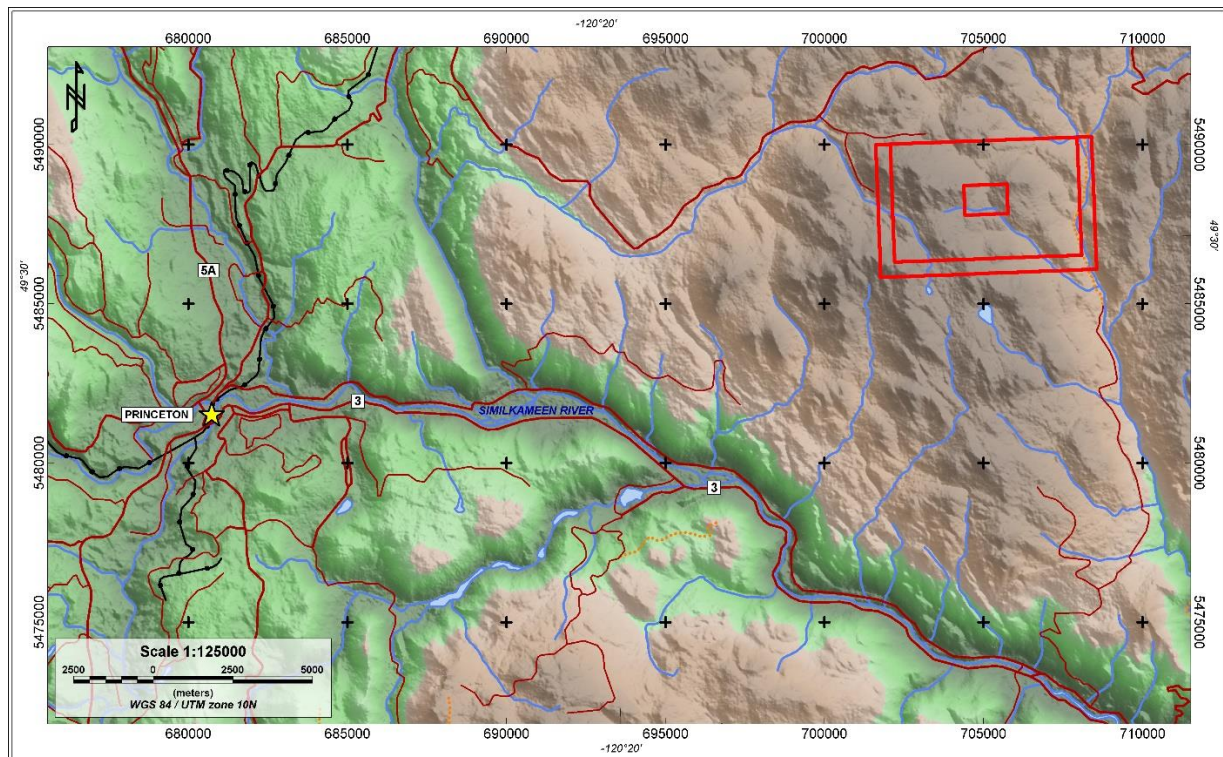


Figure 1 – Location map of the McNulty survey area.

2.2 INFRASTRUCTURE

Forestry roads and clear-cuts are throughout the survey area.

2.3 CLIMATE

The average daily temperature varies from a high of +23°C in August to a low of -14°C in February. During the survey, the weather conditions were sunny.

2.4 TOPOGRAPHY

The topography is hilly to mountainous, with an elevation variation under 500 m from east to west (Figure 2).

2.5 MINERAL AND MINING CLAIMS

The mineral claims for the McNulty block are shown in Figure 2 and tabulated in Table 1.

Table 1 - Summary of Mining claims including ownership and due date.

McNULTY CREEK PROPERTY CLAIMS									
TENURE NO.	CLAIM NAME	OWNER #	OWNER NAME	DATE ISSUED	EXPIRES	AREA (HA)	OWNERSHIP (%)	TENURE TYPE	TITLE TYPE
1073339	McNULTY CREEK	250001	PLATINUM BELT RESOURCES INC.	DEC 17/2019	FEB 26/2022	125.85	100%	CLAIM	MCX
1081411	McNULTY CREEK 2	250001	PLATINUM BELT RESOURCES INC.	FEB 26/2021	FEB 26/2022	2055.61	100%	CLAIM	MCX
1081412	McNULTY CREEK 3	250001	PLATINUM BELT RESOURCES INC.	FEB 26/2021	FEB 26/2022	650.38	100%	CLAIM	MCX

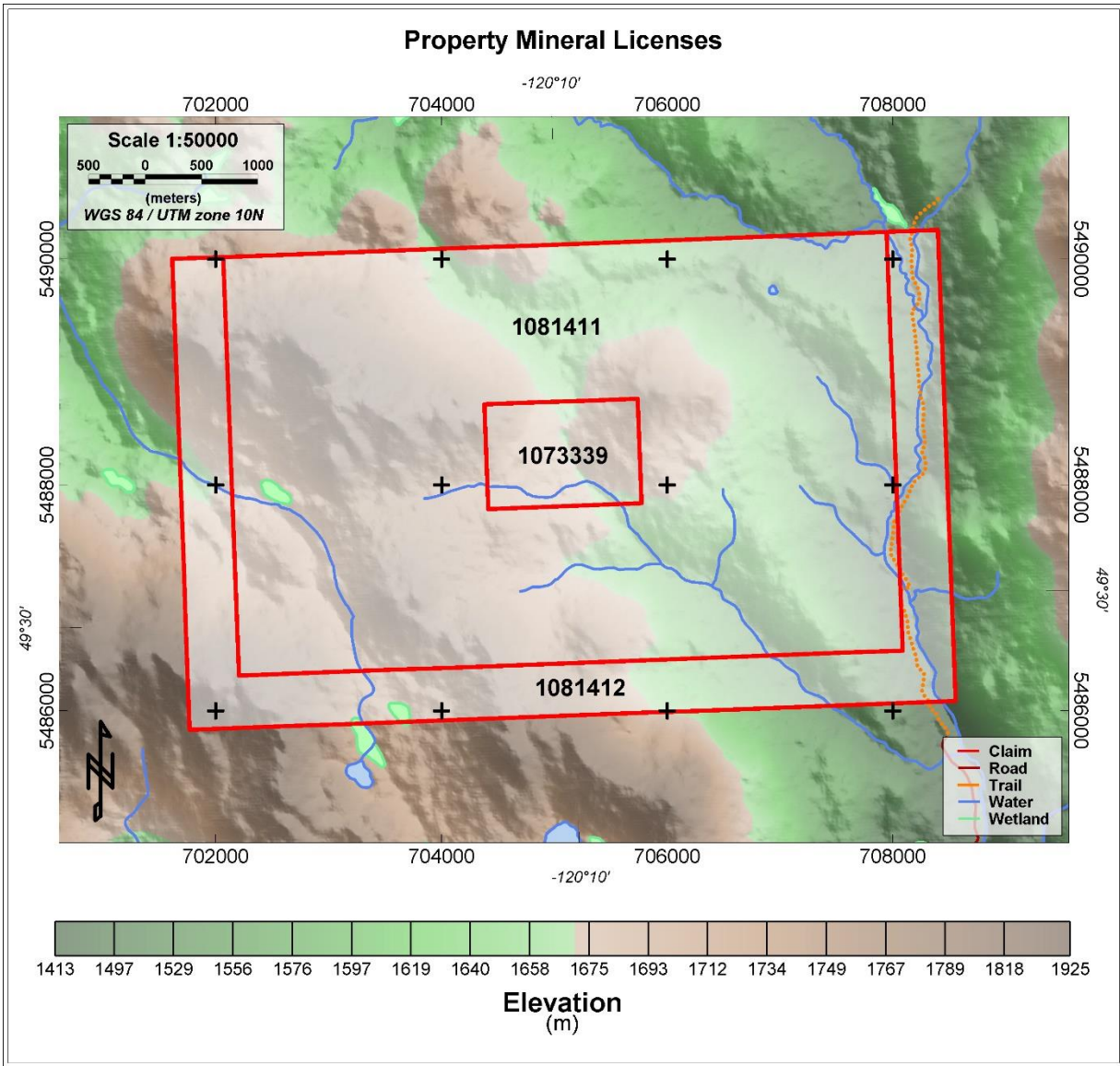


Figure 2 - Map of claim outlines over the survey area.

2.6 FLIGHT AND TIE LINES

The survey was flown in one block with flight and tie line specifications summarized in Table 2. Figure 3 shows the survey lines superimposed over the mineral claims. The lines were clipped to the survey boundary post-flight from the Geosoft database.

A nominal altitude of 40 m AGL was employed while draping the topography.

2.7 DATUM AND PROJECTION

The survey was flown using the WGS 84 Datum. The Datum used to produce this report as well as the map products, grids and database is WGS 84. The projection is UTM ZONE 10 N. All references to UTM coordinates in this report are based on the WGS 84 Datum.

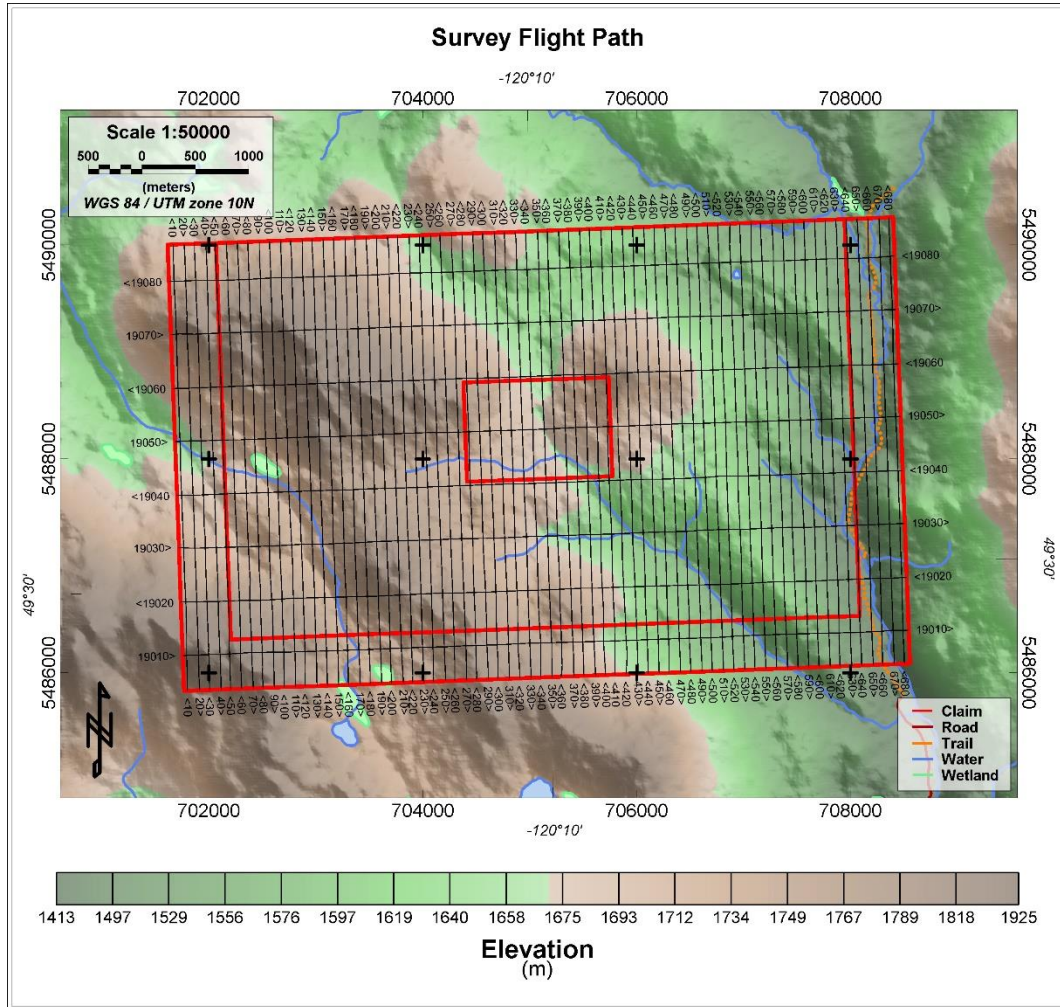


Figure 3 - Flight and tie lines over the McNulty claims.

Table 2 - Summary of flight and tie line specifications.

Survey Block	Area (km ²)	Line Type	Planned No. of Lines	Line Spacing (m)	Line Orientation	Survey Height (m)		Total Planned (km)	Total Actual (km)
						Nominal	Mean		
McNulty	28.3	Survey	68	100	178°/358°	40.0	41.4	284	283.6
		Tie	8	500	088°/268°	40.0	41.4	54	54.3
		Total:	76			40.0	41.4	338	337.9

3.0 PERSONNEL AND CALENDAR

3.1 PERSONNEL

The following personal participated in the survey (see Table 3 below):

Table 3 - List of survey personnel.

Individual	Position	Description
Harmen Keyser, P.Geo.	Pilot and project manager	Helicopter pilot(s)
Melissa Sparrow	Operator and pilot	Operated and maintained the equipment
Jenny Poon, B.Sc., P.Geo.	Processing, mapping, reporting	Line-leveling, drift correction, diurnal corrections, tie-line leveling
Mike Cunningham	Reporting, interpretation	Report write-up
Steve Balch	Supervision	Liaison with Max Investments Ltd.
Chris Balch	Mapping	Plotting maps, printing report, folding, and binding
Chris Dyakowski	Client	President of Max Investments Ltd.

3.2 CALENDAR

Data was acquired over a 2-day period on April 13th and 14th (Table 4).

Table 4 - Time Schedule for survey.

Sunday	Monday	Tuesday	Wednesday	Thursday	Friday	Saturday
Apr 11, 2021	Apr. 12, 2021	Apr. 13, 2021	Apr. 14, 2021	Apr. 15, 2021	Apr. 16, 2021	Apr. 17, 2021
-	-	Flt-01	Flt-02	-	-	-

3.3 SUMMARY OF COSTS

The total cost of the survey was \$90,000 plus taxes. Table 5 summarizes the costs.

Table 5 - Summary of Costs.

Item		Amount
Labour		\$ 18,000.00
Mobilization		\$ 7,000.00
Data acquisition		\$ 50,000.00
Instrumentation rental		\$ 6,000.00
Data processing		\$ 4,000.00
Maps & GIS		\$ 2,400.00
Report & Interpretation		\$ 2,600.00
		\$ 90,000.00

4.0 SURVEY SYSTEM

4.1 HELICOPTER

The helicopter used was an Airbus AS350 (Figure 4) with registration C-GSVY, owned and operated by Precision GeoSurveys, based in Langley, British Columbia, Canada.



Figure 4 – The survey used an Airbus AS350 as shown above.

4.2 AIRBORNE SYSTEM

The survey aircraft (Figure 5) was equipped with a data acquisition system, GPS navigation system, pilot guidance unit (PGU), laser altimeter, triple magnetic gradient boom system, and fluxgate magnetometer. In addition, two magnetic base stations were used to record temporal magnetic variations.



Figure 5 - Survey helicopter equipped with three magnetic sensors for gradient magnetic data acquisition.

4.2.1 IMPAC and AGIS

The Integrated Multi-Parameter Acquisition Console (IMPAC) (Figure 6), manufactured by Nuvia Dynamics Inc. (previously Pico Envirotec Inc.), is the main computer used in integrated data recording, data synchronizing, providing real-time quality control data for the geophysical operator display, and the generation of navigation information for the pilot and operator display systems.



Figure 6 - IMPAC data acquisition system.

IMPAC uses the Microsoft Windows operating system and geophysical parameters are based on Nuvia's Airborne Geophysical Information System (AGIS) software. Depending on survey specifications, information such as magnetic field, electromagnetic data, total gamma count, counts of various radioelements (K, U, Th, etc.), temperature, cosmic radiation, barometric pressure, atmospheric humidity, navigation parameters, and GPS status can all be monitored on the AGIS on-board display (Figure 7).

While in flight, the geophysical operator can view raw magnetic response, magnetic fourth difference, compensated and uncompensated data, radiometric spectra, aircraft position, and gradient bird position, survey altitude, cross track error, and other parameters for immediate QC (quality control) of the geophysical data. Additional software allows for post or real time magnetic compensation.

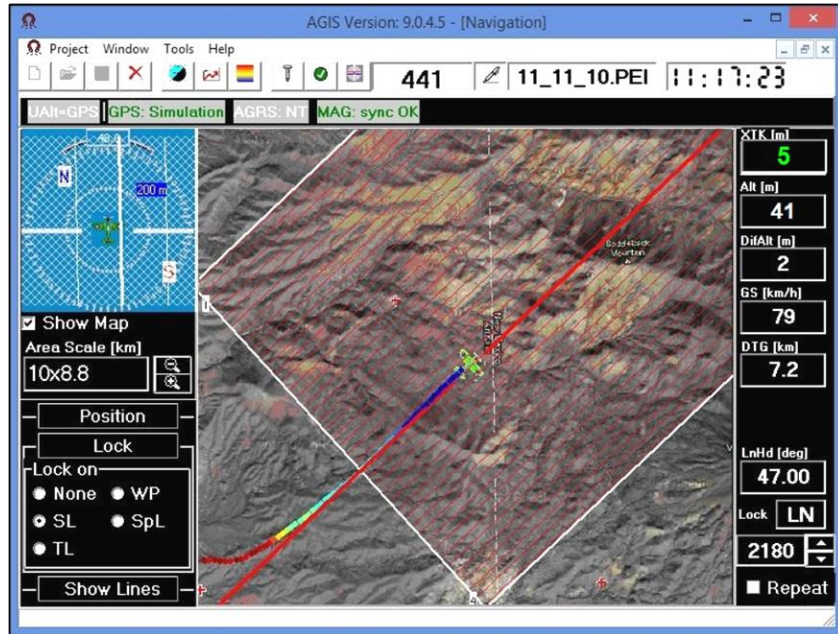


Figure 7 – AGIS operator display, showing real-time flight line recording and navigation parameters. Additional windows display real-time geophysical data to the operator.

4.3 LASER ALTIMETER

Terrain clearance is measured by an Opti-Logic RS800 Rangefinder laser altimeter (Figure 8) attached to the aft end of the magnetometer boom. The RS800 laser is a time-of-flight sensor that measures distance by a rapidly modulated and collimated laser beam that creates a dot on the target surface. The maximum range of the laser altimeter is 700 m off natural surfaces with accuracy of ± 1 m on 1 x 1 m diffuse target with 50% ($\pm 20\%$) reflectivity. Within the sensor unit, reflected signal light is collected by the lens and focused onto a photodiode. Through serial communications and digital outputs, ground clearance data are transmitted to an RS-232 compatible port and recorded and displayed by the AGIS and PGU at 10 Hz in meters.

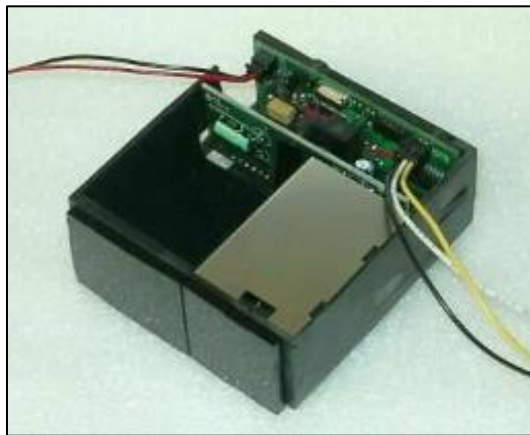


Figure 8 – Opti-Logic RS800 Rangefinder laser altimeter.

4.4 PILOT GUIDANCE UNIT

Steering and elevation (ground clearance) information is continuously provided to the pilot by the Pilot Guidance Unit (PGU). The graphical display is mounted on top of the aircraft's instrument panel, remotely from the data acquisition system. The PGU is the primary navigation aid (Figure 9) to assist the pilot in keeping the aircraft on the planned flight path, heading, speed, and at the desired ground clearance.

PGU information is displayed on a full VGA 600 x 800 pixel 7 inch (17.8 cm) LCD display. The CPU for the PGU is contained in a PC-104 console and uses Microsoft Windows operating system control, with input from the GPS antenna on the aircraft, laser altimeter, and AGIS.

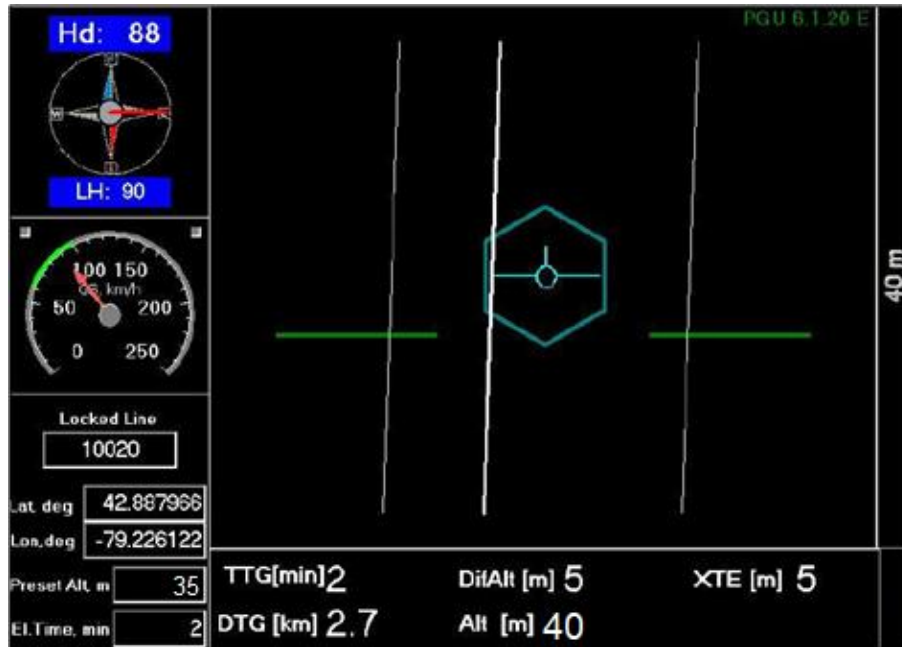


Figure 9 – PGU screen displaying navigation information.

4.5 GPS NAVIGATION

A Hemisphere R220 GPS receiver (Figure 10) and a Novatel GPS antenna on the aircraft integrated with the AGIS navigation system and pilot display (PGU) provide accurate navigational information and control. The R220 GPS receiver supports fast updates and outputs messages at a rate of up to 20 Hz (20 times per second); delivering sub-meter positioning accuracy in three dimensions. It supports GNSS (GPS/GLONASS) L1 and L2 signals.

The receiver supports differential correction methods including L-Band, RTK, SBAS, and Beacon. The R220 employs innovative Hemisphere GPS Eclipse SureTrack technology, which allows it to model the phase on satellites that the airborne unit is currently tracking. With SureTrack technology, dropouts are reduced, and speed of the signal reacquisitions is increased; enhancing accurate positioning when base corrections are not available.

An additional Novatel GPS antenna is located on the triaxial magnetic gradient bird airframe to provide position data for the bird independent of pilot navigation. Positional data of the bird are sampled and recorded at 10 Hz with differential corrections using a second R220 receiver.



Figure 10 - Hemisphere R220 GPS receiver.

4.6 MAGNETOMETER SENSOR

The magnetometer sensors used are model CS-3 by Scintrex Limited, and the G-822A by Geometrics. Both are an optical split-beam cesium magnetometer and consists of a sensor head with a cable connected to a sensor driver. The output of the sensor driver is a larmour frequency which is linearly proportional to the earth's magnetic field. The CS-3 is shown in Figure 11 with specifications provided in Table 6. The G-822A is shown in Figure 11 with specifications provided in Table 7.



**Figure 11 – (Left) Scintrex cesium (CS-3) magnetometer.
(Right) Geometrics G-822A Cs Vapor magnetomter.**

Table 6 - Scintrex CS-3 specifications.

Operating Principal	Self-oscillation split-beam Cesium Vapor (non-radioactive Cs-133)
Operating Range	15,000 to 105,000 nT
Gradient Tolerance	40,000 nT/meter
Operating Zones	10° to 85° and 95° to 170°
Hemisphere Switching	a) Automatic b) Control voltage c) Manual
Sensitivity	0.0006 nT $\sqrt{\text{Hz}}$ rms
Noise Envelope	Typically, 0.002 nT P-P, 0.1 to 1 Hz bandwidth
Heading Error	+/- 0.25 nT (inside the optical axis to the field direction angle range 15° to 75° and 105° to 165°)
Absolute Accuracy	<2.5 nT throughout range
Output	a) Continuous Larmor frequency proportional to the magnetic field (3.49857 Hz/nT) sine wave signal amplitude modulated on the power supply voltage b) Square wave signal at the I/O connector, TTL/CMOS compatible
Information Bandwidth	Only limited by the magnetometer processor used
Sensor Head	Diameter: 63 mm (2.5") Length: 160 mm (6.3") Weight: 1.15 kg (2.6 lb)
Sensor Electronics	Diameter: 63 mm (2.5") Length: 350 mm (13.8") Weight: 1.5 kg (3.3 lb)
Cable, Sensor to Sensor Electronics	3 m (9' 8"), lengths up to 5 m (16' 4") available
Operating Temperature	-40°C to +50°C
Humidity	Up to 100%, splash proof
Supply Power	24 to 35 Volts DC
Supply Current	Approx. 1.5 A at start up, decreasing to 0.5 A at 20°C
Power Up Time	Less than 15 minutes at -30°C

Table 7 – Geometrics G-822A specifications.

Operating Principal	Self-oscillation split-beam Cesium Vapor (non radioactive Cs-133)
Operating Range	20,000 nT to 100,000 nT
Operating Zones	Earth's field vector should be at an angle greater than 6° from the sensor's equator and greater than 6° away from the sensor's long axis.
Hemisphere Switching	Automatic
Sensitivity	<0.0005 nT $\sqrt{\text{Hz}}$ rms.
Noise Envelope	Typically 0.002 nT peak to peak at a 0.1 second sample rate (90% of all readings falling within the peak to peak envelope) using a 822A super-counter
Heading Error	<0.15 nT over entire 360° polar and equatorial spin
Absolute Accuracy	Better than 3 nT throughout range
Output	Cycle of Larmor frequency = 3.498572 Hz/nT, RS-232 data at 9600 baud, concatenated data streams from up to 6 sensors
Information Bandwidth	Only limited by the magnetometer processor used
Sensor Head	Diameter: 60.32 mm (2.375") Length: 158.75 mm (6.25") Weight: 680 g (24 oz)
Sensor Electronics	Diameter: 63.5 mm (2.5") Length: 279.4 mm (11") Weight: 680 g (24 oz)
Cable, Sensor to Sensor Electronics	Standard: 2.77 m (109") Cable length can be increased by 1.10 m (43") for a total length of 3.87 m (152")
Cable, Sensor Electronics to Counter	Standard: 10 m (33') Cable length can be increased up to 50 m (164')
Operating Temperature	-35°C to +50°C (-30°F to +122°F)
Altitude	Up to 9,000 m (30,000 ft)
Water Tight	Sealed for up to 0.9 m (2 ft) water depth)
Supply Power	24 to 35 Volts DC, 0.75 amp at turn-on and 0.5 amp thereafter

4.7 MAGNETIC GRADIOMETER

The primary geophysical technology used on this survey was a magnetic gradiometer system (Figure 12). Three widely spaced split-beam cesium vapor magnetometers mounted in a non-magnetic and non-conductive triple boom configuration provide total magnetic intensity as well as magnetic gradient in the crossline (X or lateral or transverse) and in-line (Y or longitudinal) directions (Table 8). The magnetometer sensors were orientated at 45 degrees with respect to the horizontal to couple with local magnetic field at the McNulty survey block.



Figure 12 – View of triple magnetic boom system

Table 8 – Magnetometer details. Cross-line gradient measured between Mag 1 and Mag 2.

Magnetometer	Model	Serial #	Gradient Direction	Separation (m)
Mag 1	Geometrics G-822A	75656	X or Cross-line	11.5
Mag 2	Scintrex CS-3	612211	Total Field and in-line	7.3
Mag 3	Geometrics G-822A	823063	X or cross-line	11.5

4.8 FLUXGATE MAGNETOMETER

As the survey helicopter flies along a survey line, small attitude changes (pitch, roll, and yaw) are recorded by a triaxial fluxgate magnetometer (Figure 13, Table 9). The fluxgate consists of three magnetic sensors, X, Y, and Z, operating independently and simultaneously. Each sensor has an analog output corresponding to the component of the ambient magnetic field along its axis. Response of the sensors is proportional to the cosine of the angle between the applied field and the sensor's sensitive axis.



Figure 13 - Billingsley Triaxial fluxgate magnetometer.

Table 9 – Geometrics G-822A specifications.

Axial Alignment	Orthogonality better than $\pm 1^\circ$
Input Voltage Options	15 to 34 VDC @ 30 mA
Field Measurement Range Options	$\pm 100 \mu\text{T} = \pm 10 \text{ V}$
Accuracy	$\pm 0.75\%$ of full scale (0.5% typical)
Linearity	$\pm 0.015\%$ of full scale
Sensitivity	100 $\mu\text{V/nT}$
Scale Factor Temperature Shift	0.007% full scale/ $^\circ\text{C}$
Noise	$\leq 12 \text{ pT rms}/\sqrt{\text{Hz}}$ @ 1 Hz
Output Ripple	3 mV peak to peak @ 2nd harmonic
Analog Output at Zero Field	$\pm 0.025 \text{ V}$
Zero Shift with Temperature	$\pm 0.6 \text{ nT}/^\circ\text{C}$
Susceptibility to Perming	$\pm 8 \text{ nT}$ shift with $\pm 5 \text{ Gs}$ applied
Output Impedance	$332 \Omega \pm 5\%$
Frequency Response	3 dB @ $>500 \text{ Hz}$ (to $>4 \text{ kHz}$ wide band)
Over Load Recovery	$\pm 5 \text{ Gs}$ slew $< 2 \text{ ms}$
Random Vibration	$> 20 \text{ G rms}$ 20 Hz to 2 kHz
Temperature Range	-55°C to $+85^\circ\text{C}$
Acceleration	$> 60 \text{ G}$
Weight	100 g
Size	3.51 cm x 3.23 cm x 8.26 cm
Connector	Chassis mounted 9 pin male "D" type

4.9 BASE STATION MAGNETOMETER

A GSM-19T base station magnetometer (manufactured by Gem Systems) was used to record variations in the earth’s magnetic field and referenced into the master database using a GPS UTC time stamp. This system is based on the Overhauser principle and records total magnetic field to within +/- 0.02 nT at a one (1) second time interval. The unit used is shown in Figure 14 with specifications shown in Table 10.

The magnetic base stations were installed in an area (Table 11, Figures 15) of low magnetic noise away from metallic items such as ferromagnetic objects, vehicles, and power lines that could affect the base stations and ultimately the survey data. Magnetic readings were reviewed at regular intervals to ensure that no airborne data were collected during periods of high magnetic activity (in excess of 10 nT from a linear chord of five minutes).



Figure 14 – GEM GSM-19T proton precession magnetometer.

Table 10 - GSM-19 base station specifications.

Configuration Options	Set to Base station mode
Cycle Time	1.0 sec
Environmental	-40°C to +60°C
Gradient Tolerance	7,000 nT/m
Magnetic Readings	299,593
Operating Range	10,000 to 120,000 nT
Power	12 V @ 0.62 A
Sensitivity	0.1 nT @ 1 sec
Weight (Console/Sensor)	3.2 Kg
Integrated GPS	Yes



Figure 15 - GSM 19 base stations used to record diurnal variations. GEM 3 – left and GEM 4 – right.

Table 11 - Magnetic base station locations.

Station Name	Easting/Northing	Latitude/Longitude	Datum/Projection
GEM 5 S/N 1094678	700,620 m E 5,483,219 m N	49° 28' 6.42" N 120° 13' 51.28" W	WGS 84, Zone 10N
GEM 6 S/N 5087249	700,614 m E 5,483,223 m N	49° 28' 6.56" N 120° 13' 51.56" W	WGS 84, Zone 10N

5.0 DATA ACQUISITION AND PROCESSING

After all data were collected, several procedures were undertaken to ensure that the data met a high standard of quality. All magnetic data recorded by the AGIS were converted into Geosoft or ASCII file formats using Nuvia Dynamics software. Further processing was carried out using Geosoft Oasis Montaj 9.7 geophysical processing software along with proprietary processing algorithms.

5.1 DATA ACQUISITION EQUIPMENT CHECKS

Equipment tests and calibrations were conducted for the laser altimeter and magnetometers at the start of the survey to ensure compliance with contract specifications and to deliver high quality airborne geophysical data. A lag test was conducted for all sensors. For the airborne magnetometers, compensation and heading error test flights were flown.

5.2 LASTER ALTIMETER CALIBRATION

The Opti-Logic RS-800 laser altimeter used on the survey helicopter was tested and calibrated in accordance with manufacturer's instructions prior to starting the survey. This ensured that heights reported by the laser were accurate within the normal survey operating range.

5.3 LAG TEST

A lag test was performed to determine the difference in time the digital reading was recorded for the magnetometers and laser altimeter with the position fix time that the fiducial of the reading was obtained by the GPS system resulting from a combination of system lag and different locations of the various sensors and the GPS antenna. The test was flown in the four orthogonal survey headings in two directions over identifiable features at survey speed and height. The resulting data (Table 12) were used to correct for time and position.

Table 12 – Survey lag correction values. Magnetic data at 20 Hz; laser altimeter was resampled to 20 Hz.

Instrument	Source	Lag Fiducial	Correction (sec)
Mag 1	Logging equipment	7	0.35
Mag 2	Logging equipment	9	0.45
Mag 3	Logging equipment	11	0.55
Laster	Sharp Gully	16	0.80

5.4 MAGNETOMETER TESTS

The magnetometers were tested and calibrated with a series of dedicated flights specifically for removing instrument offset errors and undesired effects of aircraft movement, speed, and heading direction.

5.4.1 Compensation Flight Test

During aeromagnetic surveying, a small but significant amount of noise is introduced to the magnetic data by the aircraft itself, as the magnetometers are within the aircraft's magnetic field. Changes in aircraft attitude combined with the permanent magnetization of certain aircraft parts (in particular the engine and other ferrous magnetic objects) contribute to this noise. The aircraft was degaussed using proprietary technology prior to starting the survey and the remaining magnetic noise was removed by a process called magnetic compensation.

A magnetic compensation flight was completed for this survey. The process consists of a series of prescribed maneuvers ($\pm 10^\circ$ roll, $\pm 10^\circ$ pitch, and $\pm 10^\circ$ yaw) where the aircraft flies in the four orthogonal headings required ($000^\circ/090^\circ/180^\circ/270^\circ$ in the case of this survey) at a sufficient altitude (typically $> 2,500$ m AGL) in an area of low magnetic gradient where Earth's magnetic field becomes nearly uniform at the scale of the compensation flights. In each heading direction, three specified roll, pitch, and yaw maneuvers (total 36) are performed by the pilot at constant elevation so that any magnetic variation recorded by the airborne magnetometers can be attributed to aircraft movement. These maneuvers are determined by the airborne fluxgate magnetometer and provide the data that are required to calculate the necessary parameters for compensating the magnetic data to remove aircraft noise from survey data. Compensation flight test results are summarized in Table 13, Table 14, and Table 15.

Table 13 – Results of compensation flight for Mag 1.

Pre-compensation					Post-compensation				
Heading	Roll	Pitch	Yaw	Total	Heading	Roll	Pitch	Yaw	Total
000°	1.5828	0.3602	0.3535	2.2965	000°	0.2718	0.3068	0.2745	0.8531
090°	1.2691	0.7776	0.7521	2.7988	090°	0.1701	0.1647	0.1820	0.5168
180°	0.8110	0.5913	0.4304	1.8327	180°	0.2270	0.2392	0.1900	0.6562
270°	0.9121	0.5877	0.4252	1.9250	270°	0.3001	0.3255	0.3194	0.9450
FOM (nT) = 8.8530					FOM (nT) = 2.9711				

Table 14 – Results of compensation flight for Mag 2

Pre-compensation					Post-compensation				
Heading	Roll	Pitch	Yaw	Total	Heading	Roll	Pitch	Yaw	Total
000°	0.3544	0.9193	0.3236	1.5973	000°	0.1405	0.1317	0.1235	0.3957
090°	0.2587	0.8528	0.4095	1.5210	090°	0.1451	0.1564	0.1839	0.4854
180°	0.2498	0.4006	0.1955	0.8459	180°	0.1504	0.1438	0.1226	0.4168
270°	0.2611	0.6819	0.3525	1.2955	270°	0.1285	0.1286	0.1272	0.3843
FOM (nT) = 5.2597					FOM (nT) = 1.6822				

Table 15 – Results of compensation flight for Mag 3

Pre-compensation					Post-compensation				
Heading	Roll	Pitch	Yaw	Total	Heading	Roll	Pitch	Yaw	Total
000°	2.6327	0.7073	0.4864	3.8264	000°	0.3128	0.2987	0.2373	0.8488
090°	0.8874	0.7145	0.6231	2.2250	090°	0.2038	0.1901	0.2115	0.6054
180°	0.6368	0.7187	0.3077	1.6626	180°	0.2467	0.2578	0.2161	0.7206
270°	1.1702	0.6608	0.5304	2.3614	270°	0.3434	0.3526	0.2991	0.9951
FOM (nT) = 10.0754					FOM (nT) = 3.1699				

5.4.2 Heading Correction Test

To determine heading errors and other offsets, a cloverleaf pattern flight test was conducted at high altitude to minimize the effect of natural magnetic gradient. The cloverleaf test was flown in the same orthogonal headings as the survey and tie lines (000°/090°/180°/270° in the case of this survey) at >2500 m AGL in an area with low magnetic gradient. For all four directions of the cloverleaf test the survey helicopter must pass over the same point, at the same elevation, with the aircraft in straight and level flight. The difference in magnetic values obtained in reciprocal headings is the heading error. Heading correction values derived from the test flight for each of the magnetometers are summarized in Table 16.

Table 16 – Magnetic sensor heading corrections for headings 000°/090°/180°/270°

Heading	Mag 1 Heading Correction (nT)	Mag 2 Heading Correction (nT)	Mag 3 Heading Correction (nT)
000°	-1.76	-0.34	-0.12
090°	-3.62	-0.93	-5.77
180°	-2.66	-0.06	-6.60
270°	8.04	1.33	12.49
Total:	0.00	0.00	0.00

5.5 FIELD PROCESSING AND QUALITY CONTROL

Survey data were transferred from the aircraft’s data acquisition system onto a USB memory stick and copied onto a field data processing laptop on a flight-by-flight basis. The raw data files in PEI binary data format were converted into Geosoft GDB database format. Using Geosoft Oasis Montaj 9.9.1, the data were inspected to ensure compliance with contract specifications (Table 17). Several sources of potential geophysical data interference from logging equipment were reported by the survey crew.

Table 17 – Contract survey specifications

Parameter	Specification	Tolerance
Position	Line Spacing	Flight line deviation within 8 m L/R from ideal flight path. No exceedance for more than 1 km.
	Height	Nominal flight height of 40 m above ground level (AGL) with tolerance of ± 10 m. No exceedance for more than 1 km, provided deviation is not due to tall trees, topography, mitigation of wildlife/livestock harassment, cultural features, or other obstacles beyond the pilot's control.
	GPS	GPS signals from four or more satellites must be received at all times, except where signal loss is due to topography. No exceedance for more than 1 km.
Magnetics	Temporal / Diurnal Variations	Non-linear temporal magnetic variations within 10 nT of a linear chord of length 5 minutes.
	Normalized 4 th Difference	Magnetic data within 0.01 nT peak to peak. No exceedance for distances greater than 1 km or more, provided noise is not due to geological or cultural features.

5.6 DATA PROCESSING

After all data were collected, several procedures were undertaken to ensure that the data met a high standard of quality. Magnetic data recorded by the AGIS were converted into Geosoft or ASCII file formats using Nuvia Dynamics software. Further processing (Figure 16) was carried out using Geosoft Oasis Montaj 9.9.1 geophysical processing software along with proprietary processing algorithms.

5.6.1 Position Corrections

To collect high resolution geophysical data, the location at which the data were collected and recorded must be accurate.

5.6.1.1 Lag Correction

A correction for lag error was applied to the geophysical data recorded at each individual sensor to compensate for the combination of lag in the recording system and the sensing instrument flying in a different location from the GPS antenna, as determined during the lag test. Validity of the lag corrections was confirmed by the absence of grid corrugations in adjoining reciprocal lines.

Geophysical Data Processing Flow

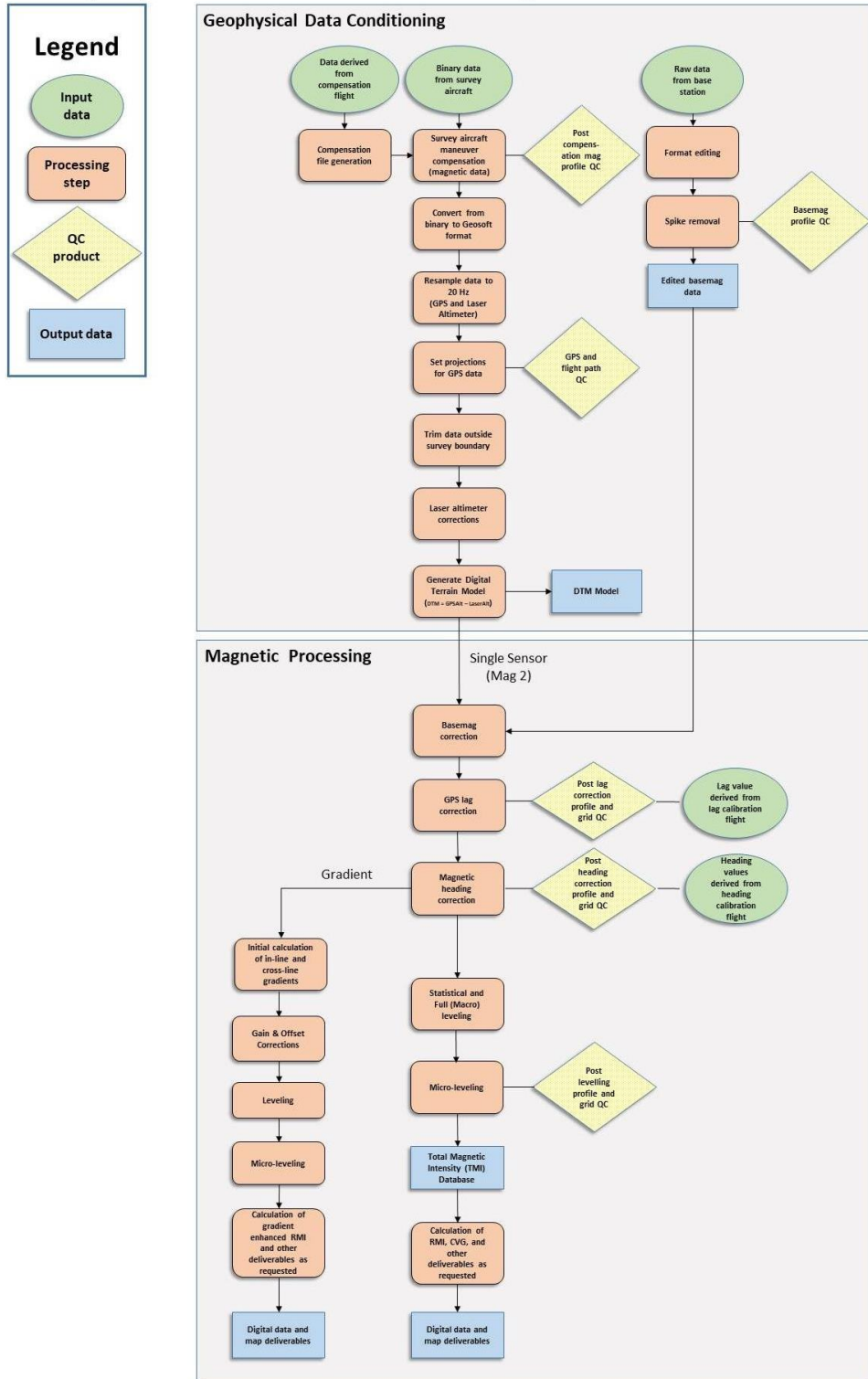


Figure 16 – Magnetic data processing flow.

5.6.2 Flight Height and Digital Terrain Model

Laser altimeters are unable to provide valid data over glassy water or fog which dissipate the laser so that a “zero” reading is obtained. In these cases, estimates of correct height are inserted manually. Dense vegetation generates high frequency variations from leaf and branch reflections. A Rolling Statistics filter is applied to the lag corrected (0.6 seconds lag) laser altimeter data to remove vegetation clutter followed by a Low Pass filter to smooth out the laser altimeter profile to eliminate isolated high frequency noise and generate a surface closely corresponding to the actual ground profile.

As the GPS antenna is on the tail of the helicopter, altitude data were corrected by subtracting 3.1 m to place it in the same plane as the laser altimeter. A Digital Terrain Model (DTM) was determined by subtracting the laser altimeter data from the filtered GPS altimeter data defined by the WGS 84 ellipsoidal height. DTM accuracy is affected by the attitude of the aircraft, slope of the ground, sample density, and satellite geometry. Small inconsistencies in recorded flight height at the intersection points of survey lines and tie lines resulted in small spatial variabilities in the digital terrain model. Conventional leveling and micro-leveling were applied to correct for these variations and a fully leveled digital terrain model was generated.

5.6.3 Magnetic Processing

Magnetic data from each individual sensor were corrected for temporal variations (including diurnal) and lag. The data were examined for magnetic noise and spikes, which were removed as required. Survey and tie line data of the resulting total magnetic field were leveled and the background magnetic field, International Geomagnetic Reference Field (IGRF) of the Earth was removed to derive the residual magnetic field. Magnetic gradients in the X and Y axes were determined to provide cross-line and in-line gradients, respectively.

5.6.3.1 Temporal Variation Correction

The intensity of Earth’s magnetic field varies with location and time. The time variable, known as diurnal or more correctly temporal variation, is removed from the recorded airborne data to provide the desired magnetic field at a specified location. Magnetic data from base station GEM 6 were used for correcting the airborne magnetic survey data, and GEM 5 data were retained for backup. The data were edited, plotted, and merged into a Geosoft database (.GDB) on a daily basis.

Base station measurements were averaged to establish a magnetic reference datum of 54657.64 nT. Magnetic deviations relative to the reference datum were used to calculate the observed variations of the Earth’s magnetic field during the time it took to complete the survey. The airborne magnetic data were then corrected for temporal variations by subtracting the base station deviations from the data collected on the aircraft, effectively removing the effects of diurnal and other temporal variations.

5.6.3.2 Heading Correction

For each survey heading, changes in the apparent magnetic field due to instrumental heading error are measured and recorded. These values are used to construct a heading table (.TBL) file. For the entire dataset, the overall average magnetic field value was calculated. For each of the four headings, the averages were calculated and then compared to the overall average to determine four values which were used to correct heading and offset errors in each flight direction for each magnetometer.

5.6.3.3 Leveling and Micro-leveling

Small inconsistencies in flight height and line orientation result in small spatial variabilities in magnetic intensity measured at the intersection points of survey lines and tie lines. Using the initial Total Magnetic Intensity (TMI) data from Mag 2, data from survey and tie lines were leveled to each other. Two types of leveling were applied to the corrected data: conventional leveling and micro-leveling. There were two components to conventional leveling: statistical leveling to level tie lines and full leveling to level survey lines. The statistical leveling method corrected the SL/TL intersection errors that follow a specific pattern or trend. Through the error channel, an algorithm calculated a least-squares trend line and derived a trend error curve, which was then added to the channel to be leveled. The second component was full leveling. This adjusted the magnetic value of the survey lines so that all lines matched the trended tie lines at each intersection point.

Following statistical and full leveling, micro-leveling was applied to the corrected conventional leveled data. This iterative grid-based process removed low amplitude components of flight line noise that still remained in the data after tie line and survey line leveling and resulted in fully leveled TMI data.

5.6.3.4 IGRF Removal

The International Geomagnetic Reference Field (IGRF) model is the empirical representation of Earth's dynamic magnetic field (main core field without external sources) collected and disseminated from satellite data and from magnetic observatories around the world. The IGRF has historically been revised and updated every five years by a group of modellers associated with the International Association of Geomagnetism and Aeronomy (IAGA).

The leveled Residual Magnetic Intensity (RMI) was calculated by taking the difference between the 13th generation IGRF (IGRF-13, released in December 2019) and the leveled Total Magnetic Intensity (TMI) to create a more valid model of individual near-surface magnetic anomalies. This model is independent of time to allow for other magnetic data (previous or future) to be more easily incorporated into each survey database.

5.6.4 Magnetic Gradient

When magnetic values are obtained simultaneously from two or more sensors at a fixed separation, gradient of the magnetic field can be measured. Dividing the difference in magnetic values between the sensors by the distance between the sensors yields the magnetic gradient. The units are commonly reported as nT/m and, by convention, positive magnetic polarity is defined as to the north and east, and negative to the south and west. For vertical gradient, positive is defined as downwards. The sensors and the separations that were used to determine the various gradients are listed in Table 18.

Table 18 – Magnetic sensor relationship used to calculate magnetic gradients. Total magnetic intensity (TMI) was determined from Mag 2, and successive values of the TMI were used to determine the longitudinal (Y axis) gradient.

Direction	Sensors	Separation (m)
Lateral (X)	Mag 1 and Mag 3	11.5
Longitudinal (Y)	Sequential TMI values (Mag 2)	2.07*

*average separation between sequential TMI values shown; actual value varied according to aircraft speed.

5.6.4.1 Horizontal Gradients

Horizontal magnetic gradients were determined in the in-line (Y axis) and cross-line (X axis) directions. Gradients were calculated with respect to the magnetometer array with units provided as nT/m.

In-line gradient (iLG) is determined from successive magnetic values of Mag 2 referenced to the distance between data points in accordance with the following formula:

$$iLG = \frac{a(i + 1) - a(i - 1)}{d(i + 1) + d(i - 1)}$$

where: a is the average total magnetic intensity of Mag 2

d is the distance between measurements

i is the record number for the location

Cross-line gradient (xLG) is measured directly by dividing the difference between Mag 1 and Mag 3 by the sensor separation in accordance with the following formula:

$$xLG = \frac{\text{Mag 1} - \text{Mag 3}}{d_x}$$

where: d_x is the transverse sensor separation, 11.5 m

5.6.4.1.1 Gain Correction

Gain corrections were applied to the initial cross-line gradient. If the ratio of the TMI between Mag 1 and Mag 3 does not equal one, a gain correction needs to be applied to account for instrument error and asymmetric magnetic fields. The mean of the ratio between the TMI values for Mag 1 and Mag 3 for each line was calculated and applied to each Mag 3 value along the line. The cross line gradient was then re-calculated from the gain-corrected Mag 3 values.

5.6.4.1.2 Offset Correction

Offset corrections were then applied to the cross-line gradient to reduce line-to-line errors (striping) in the gradient grid. The resulting data were then micro-leveled to remove any remaining striping.

5.6.4.1.3 Total Horizontal Gradient

Total Horizontal Gradient (HG) is the magnitude of the combined in-line and cross-line gradients. It is used to estimate contact locations of magnetic bodies at shallow depths, reveal anomaly textures, and highlight anomaly-pattern discontinuities.

Horizontal Gradient (HG) is calculated as:

$$HG(x, y) = \sqrt{iLG^2 + xLG^2}$$

where: iLG is the in-line gradient

xLG is the cross-line gradient

5.6.4.2 Calculation of Vertical Gradient

Calculated Vertical Gradient (CVG) is the first order vertical derivative of the leveled Residual Magnetic Intensity (RMI) data determined from Mag 2. It is the vertical rate of change in the magnetic field per unit distance (m). The vertical gradient is used to enhance shorter wavelength signals; therefore, edges of magnetic anomalies are highlighted, and deep geologic sources in the data are suppressed.

The filter, L , used to produce the n th vertical derivative is described by:

$$L(r) = r^n$$

where: r is the radial component in the wavenumber domain

5.6.4.3 Gradient Enhanced Magnetic Intensity

Total magnetic intensity was gridded using a bi-directional method, which allowed horizontal gradient data to be incorporated to create a gradient enhanced Total Magnetic Intensity (TMIge) grid. The TMIge grid was imported back into the final database to be available for alternative gridding methods. The gradient enhanced Residual Magnetic Intensity (RMIge) was derived by taking the difference between the gradient enhanced Total Magnetic Intensity (TMIge) and IGRF.

5.6.4.4 Gradient Enhanced Reduction to Magnetic Pole

Gradient enhanced Reduced to Magnetic Pole (RTPge) data were determined from the gradient enhanced Residual Magnetic Intensity (RMIge) data. The RTP filter was applied in the Fourier domain and rotates the observed magnetic inclination and declination field to what the field would look like at the north magnetic pole, to allow observation of magnetic trends and patterns independent of magnetic inclination and declination.

Inclination and declination were calculated by using the “Date” channel. The derived values were used in the following formula:

$$RTP(\theta) = \frac{[\sin(I) - I \cdot \cos(I) \cdot \cos(D - \theta)]^2}{[\sin^2(I_a) + \cos^2(I_a) \cdot \cos^2(D - \theta)] \cdot [\sin^2(I) + \cos^2(I) \cdot \cos^2(D - \theta)]}$$

where: I is geomagnetic inclination in ° from horizontal.

D is geomagnetic declination in ° azimuth from magnetic north.

I_a is the inclination for amplitude correction (never less than I). Default is $\pm 20^\circ$. If $|I_a|$ is specified to be less than $|I|$, it is set to I .

6.0 RESULTS

The TMI is presented in Figure 17, gradient enhanced TMI in Figure 18, residual magnetic field (RMI) in Figure 19, gradient enhanced RMI in Figure 20, and gradient enhanced reduced-to-pole RMI in Figure 21.

The principle gradients (in-line, cross-line, and calculated vertical) are presented in Figure 22, Figure 23, and Figure 24. The total horizontal gradient is presented in Figure 25.

The digital terrain model (DTM) is presented in Figure 26.

All figures have a shading effect oriented north (178° declination) and with a 60° inclination.

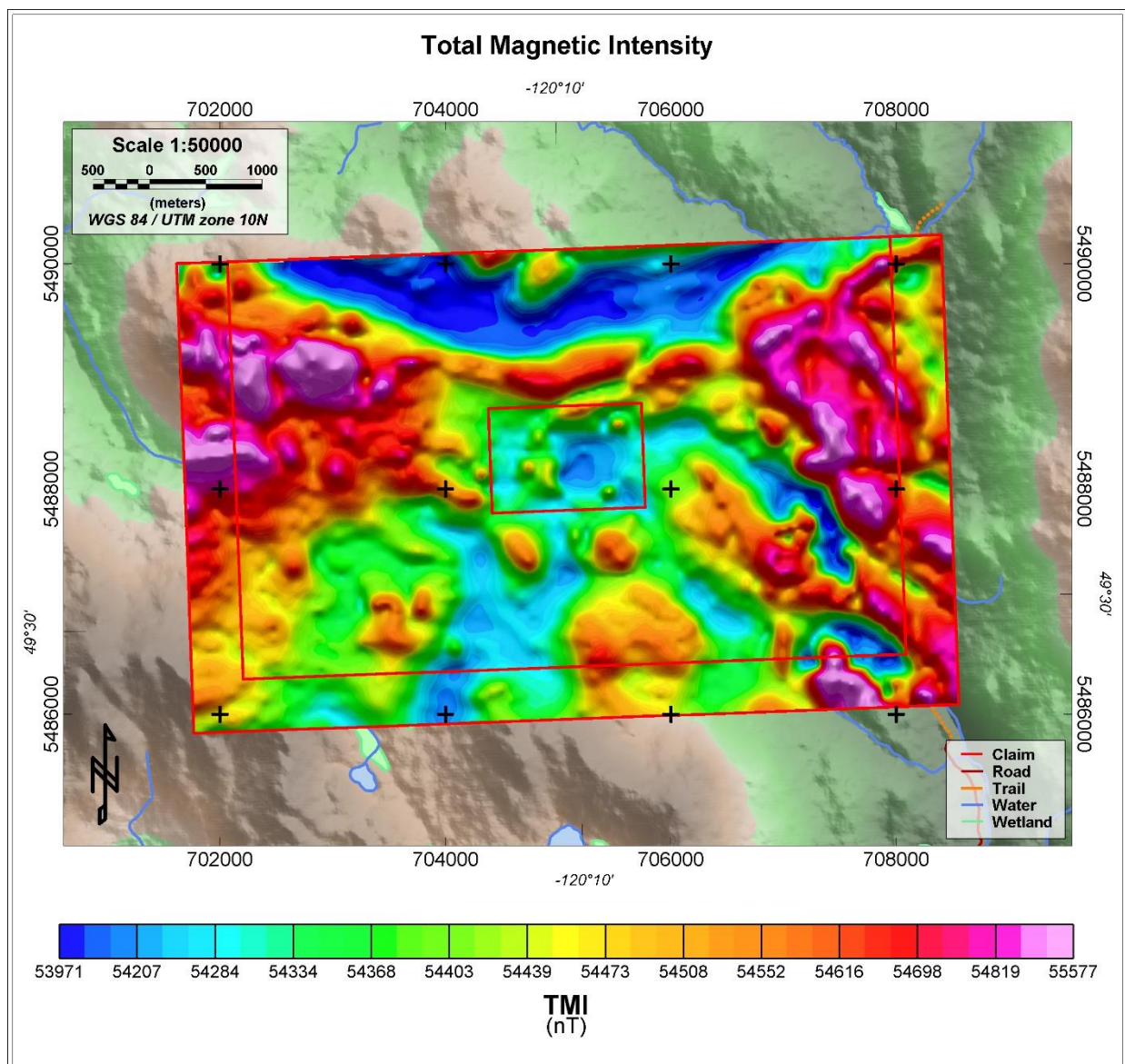


Figure 17 - Shaded image of the Total Magnetic Intensity (TMI) over the survey block.

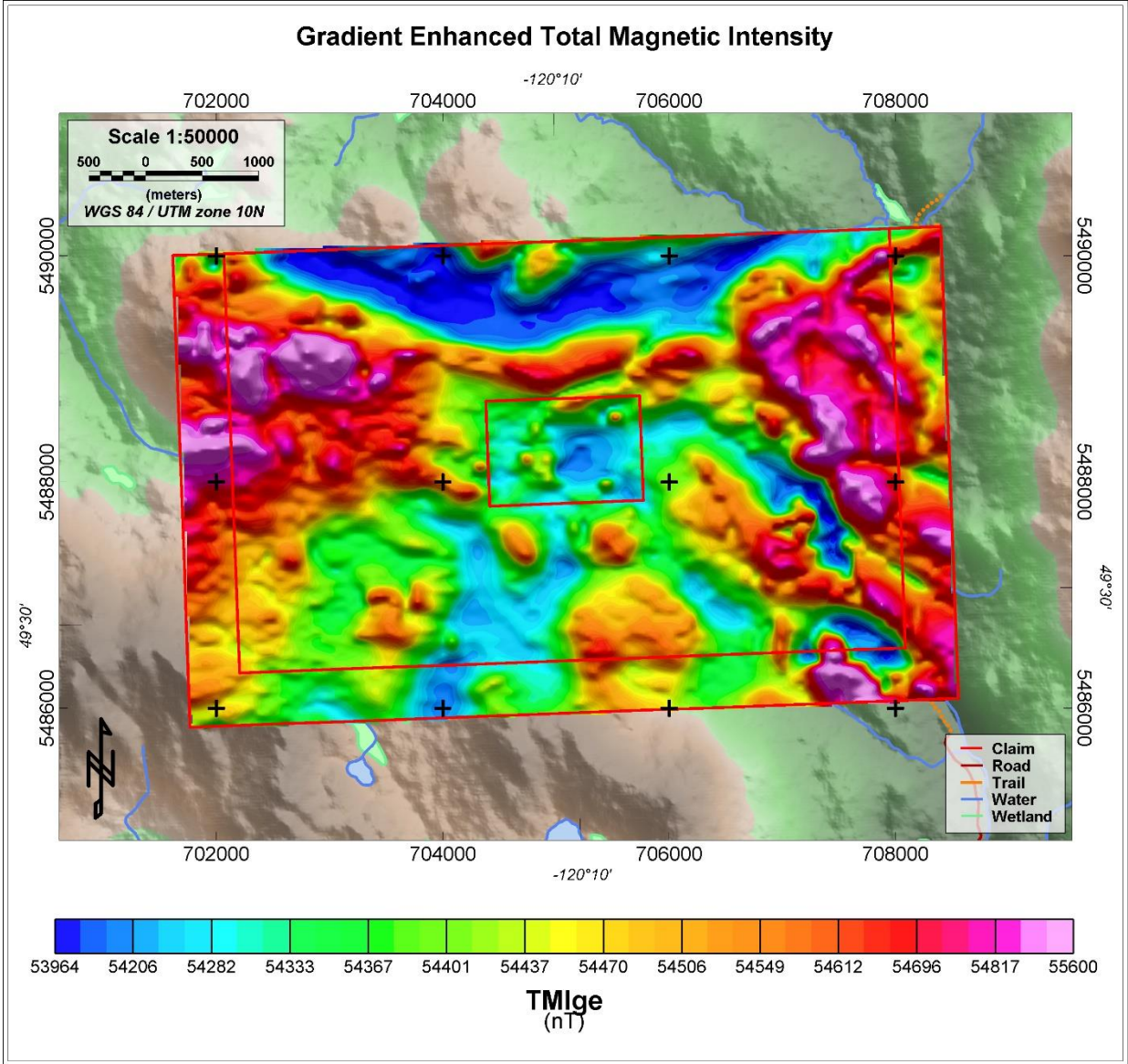


Figure 18 - Shaded image of the Gradient Enhanced Total Magnetic Intensity (TMI) over the survey block.

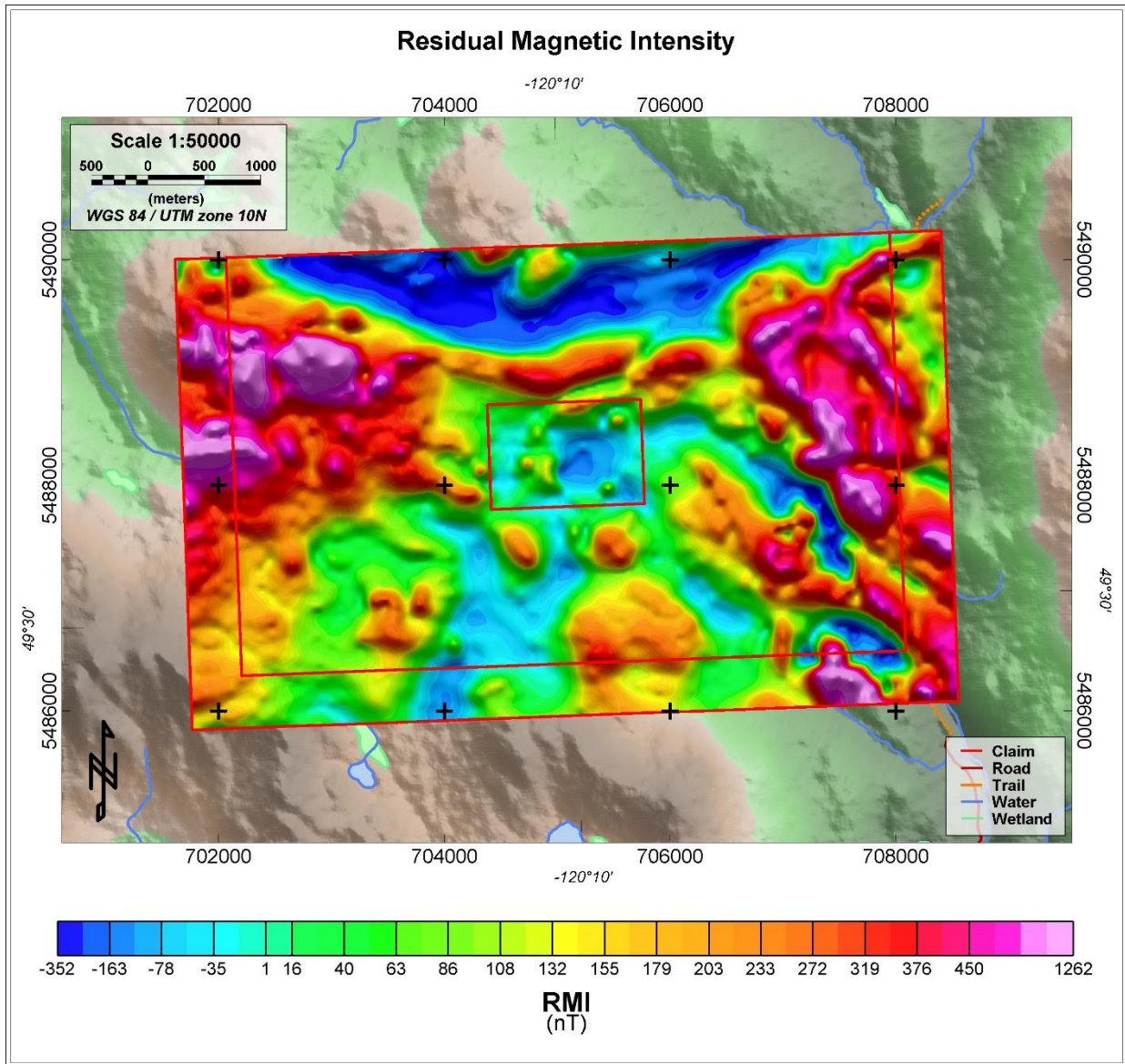


Figure 19 - Shaded image of the Residual Magnetic Intensity (RMI) over the survey block.

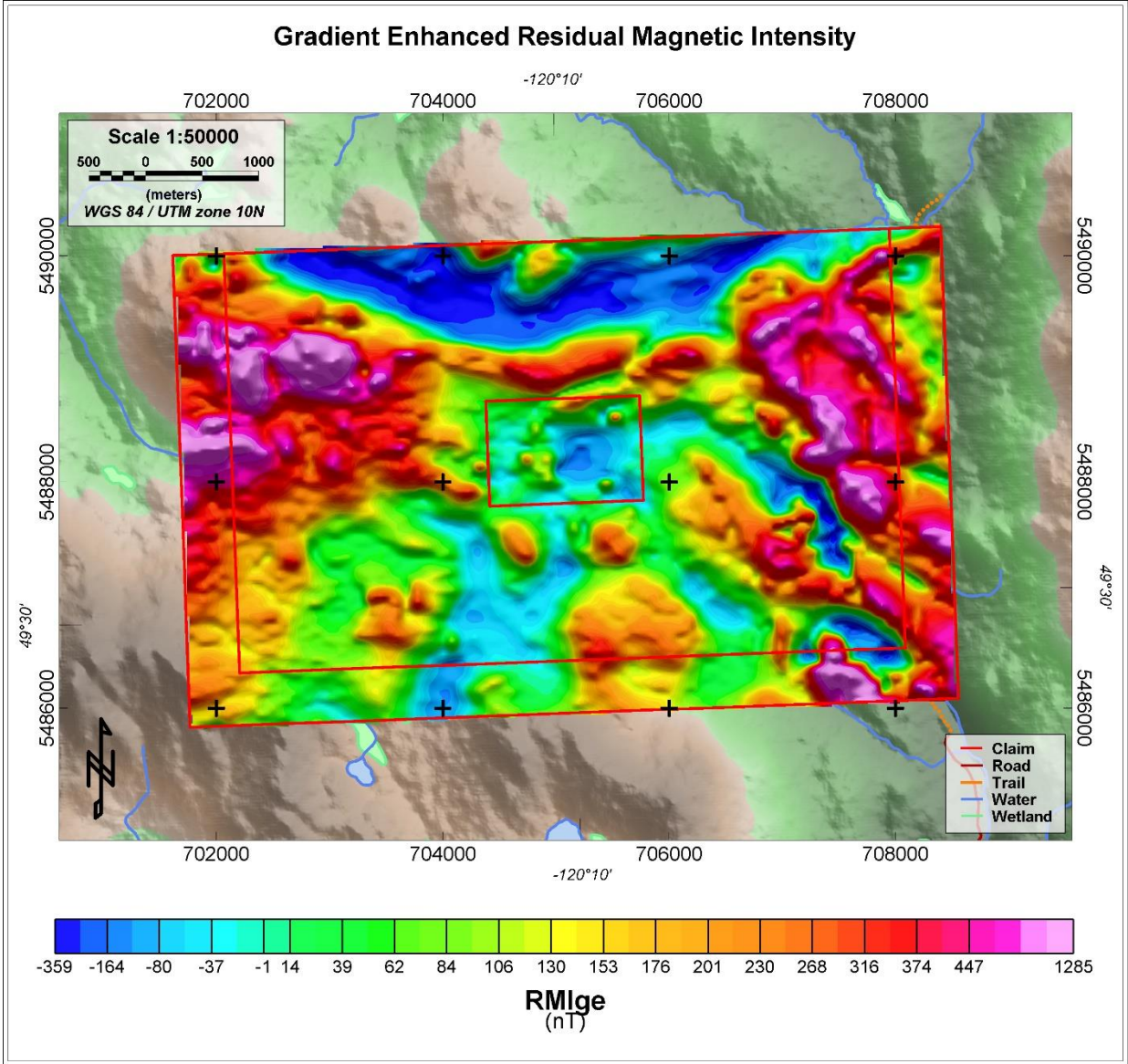


Figure 20 - Shaded image of the Gradient Enhanced Residual Magnetic Intensity (RMI) over the survey block.

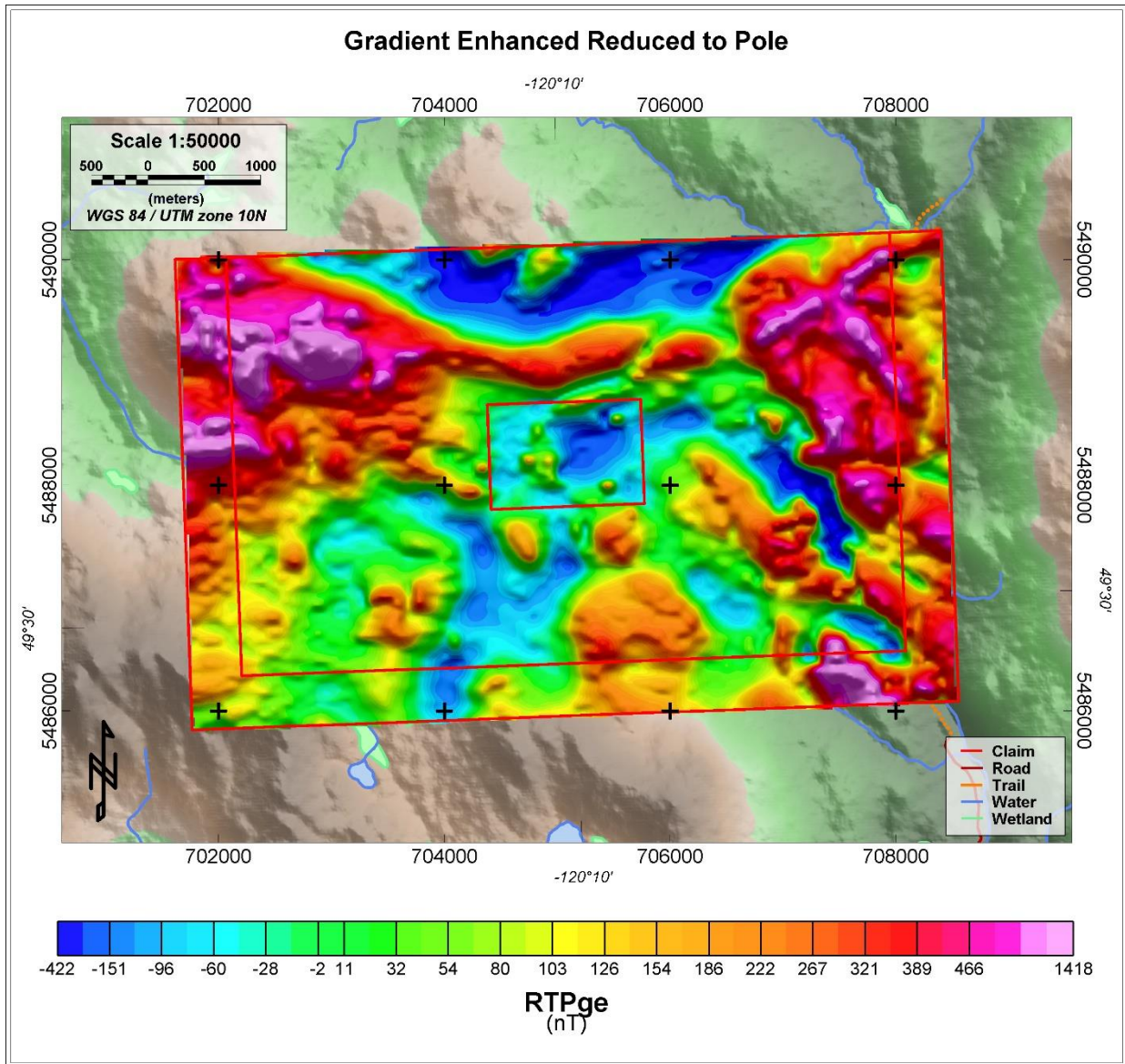


Figure 21 - Shaded image of the Gradient Enhanced Reduced-To-Pole (RTP) over the survey block.

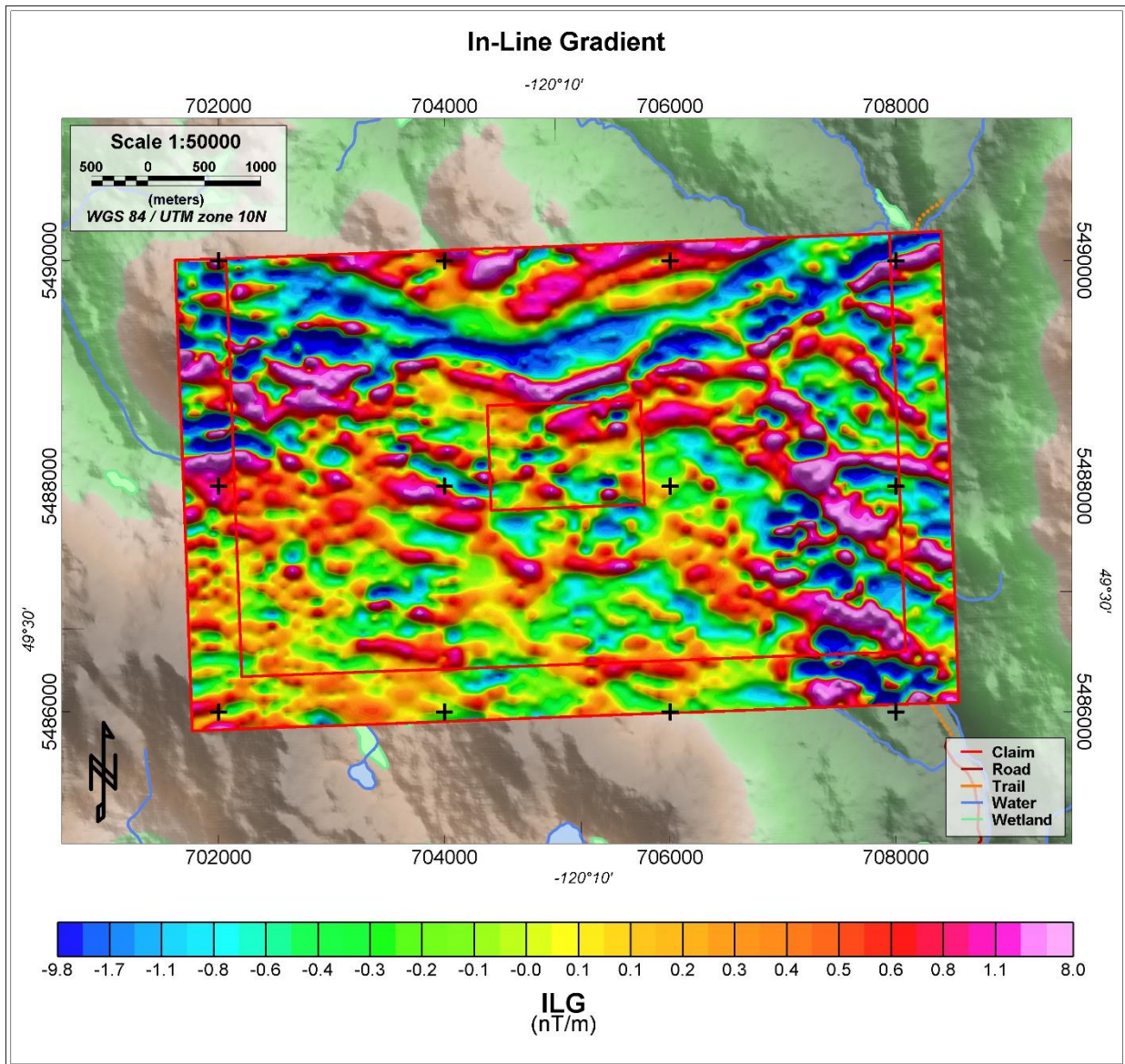


Figure 22 – Shaded image of the In-Line Horizontal Gradient over the survey block.

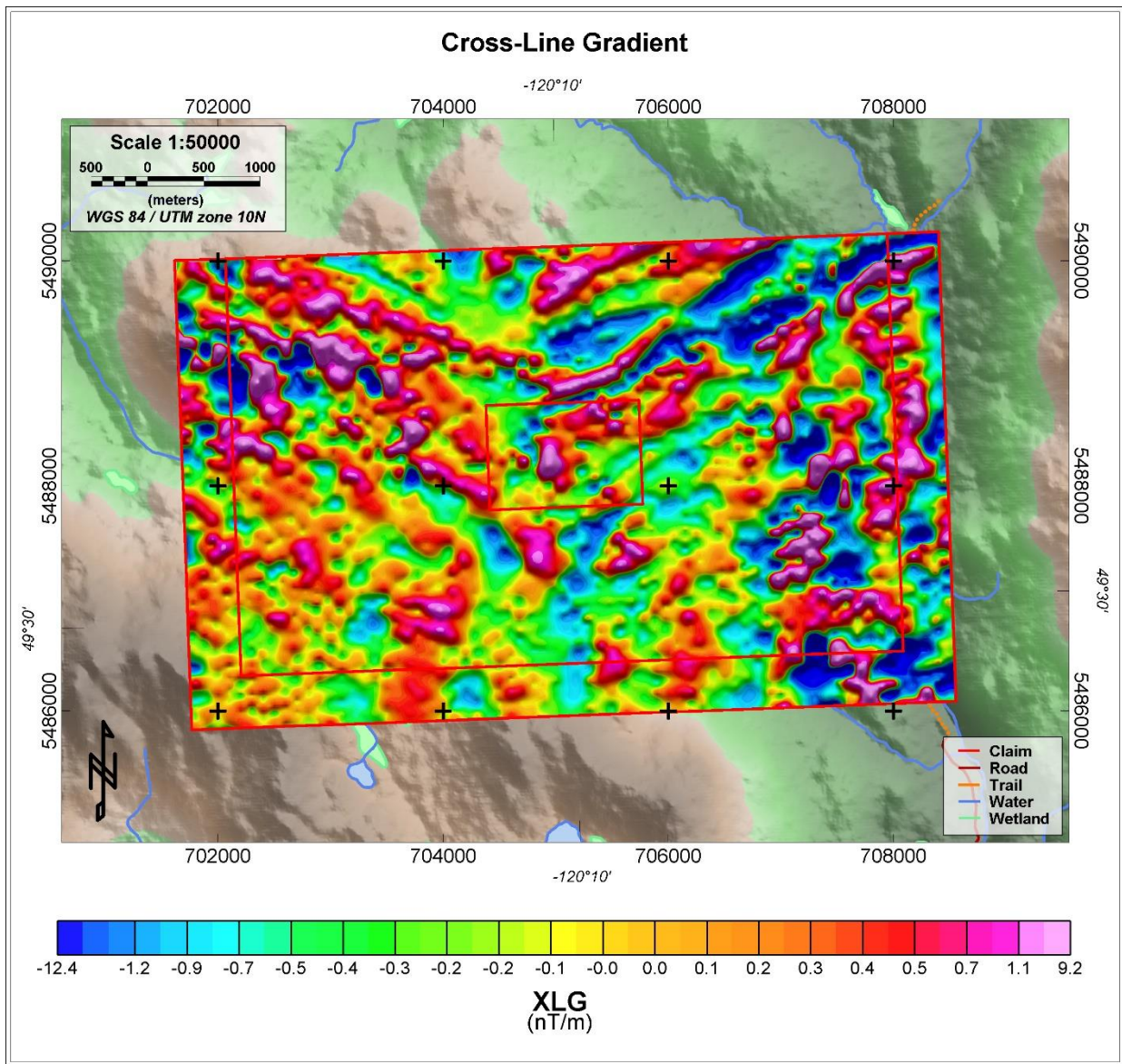


Figure 23 – Shaded Image of the Cross-Line Horizontal Gradient over the survey block.

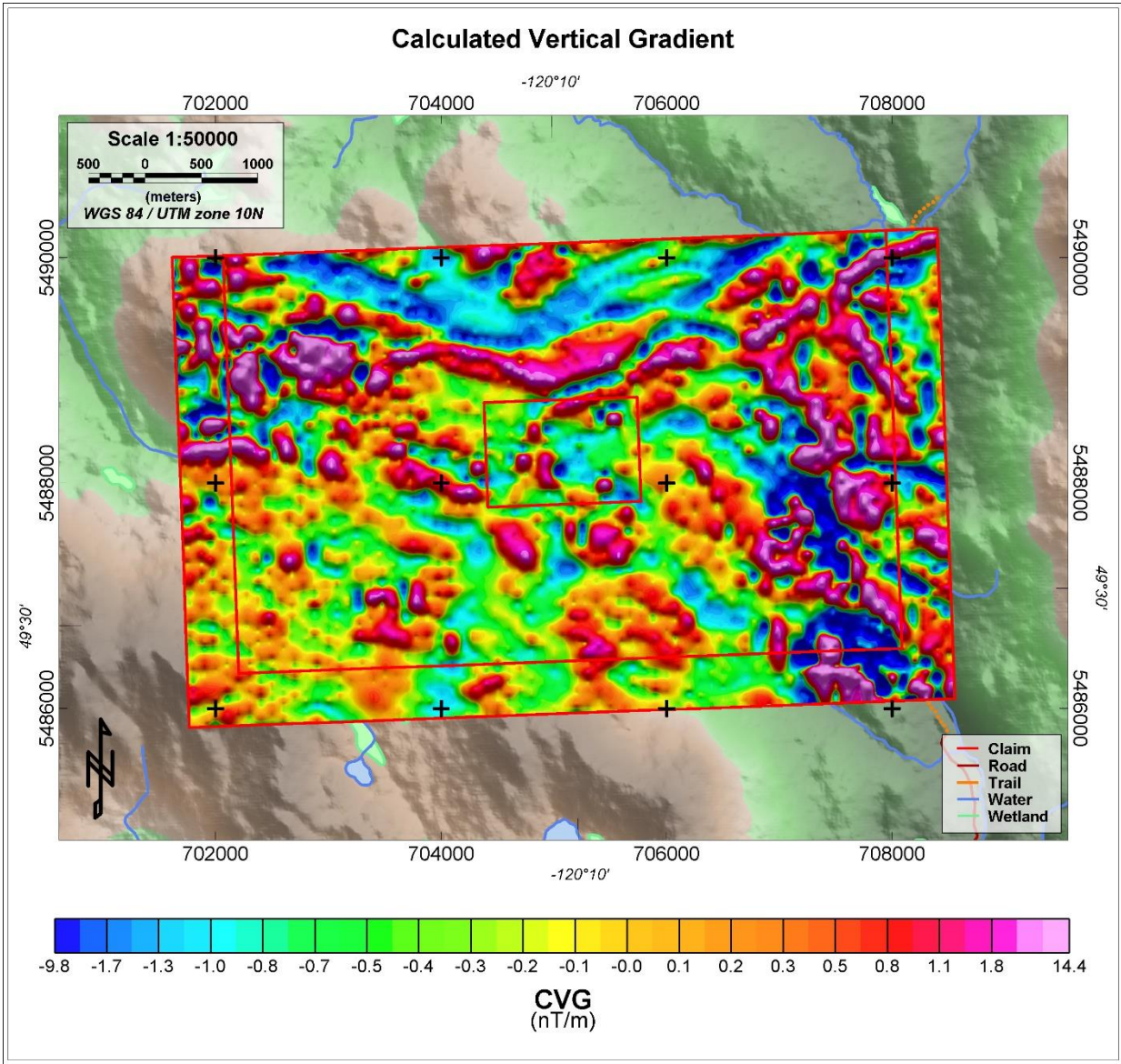


Figure 24 – Shaded image of the Vertical Gradient over the survey block.

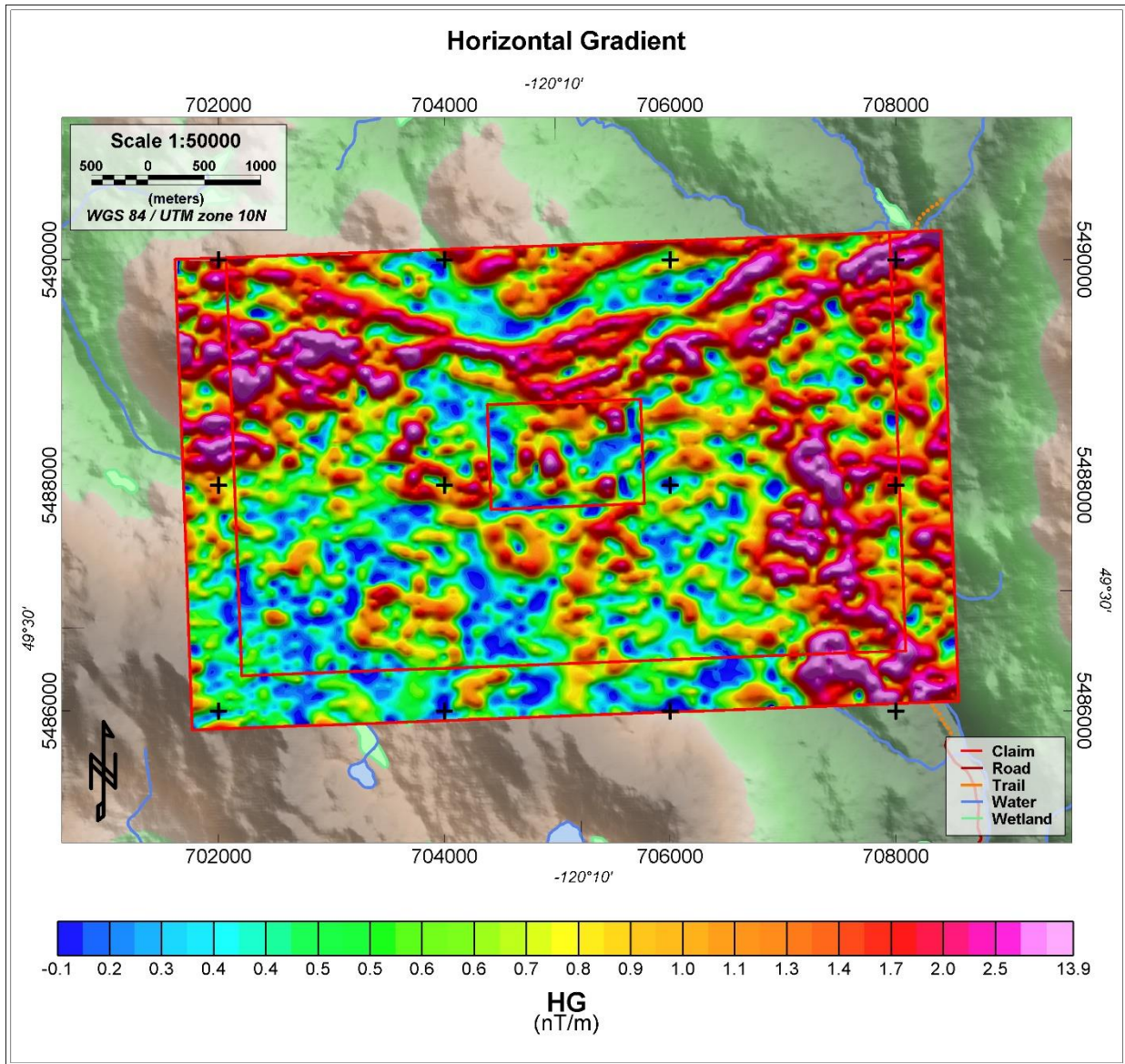


Figure 25 – Shaded image of the Total Horizontal Gradient over the survey block.

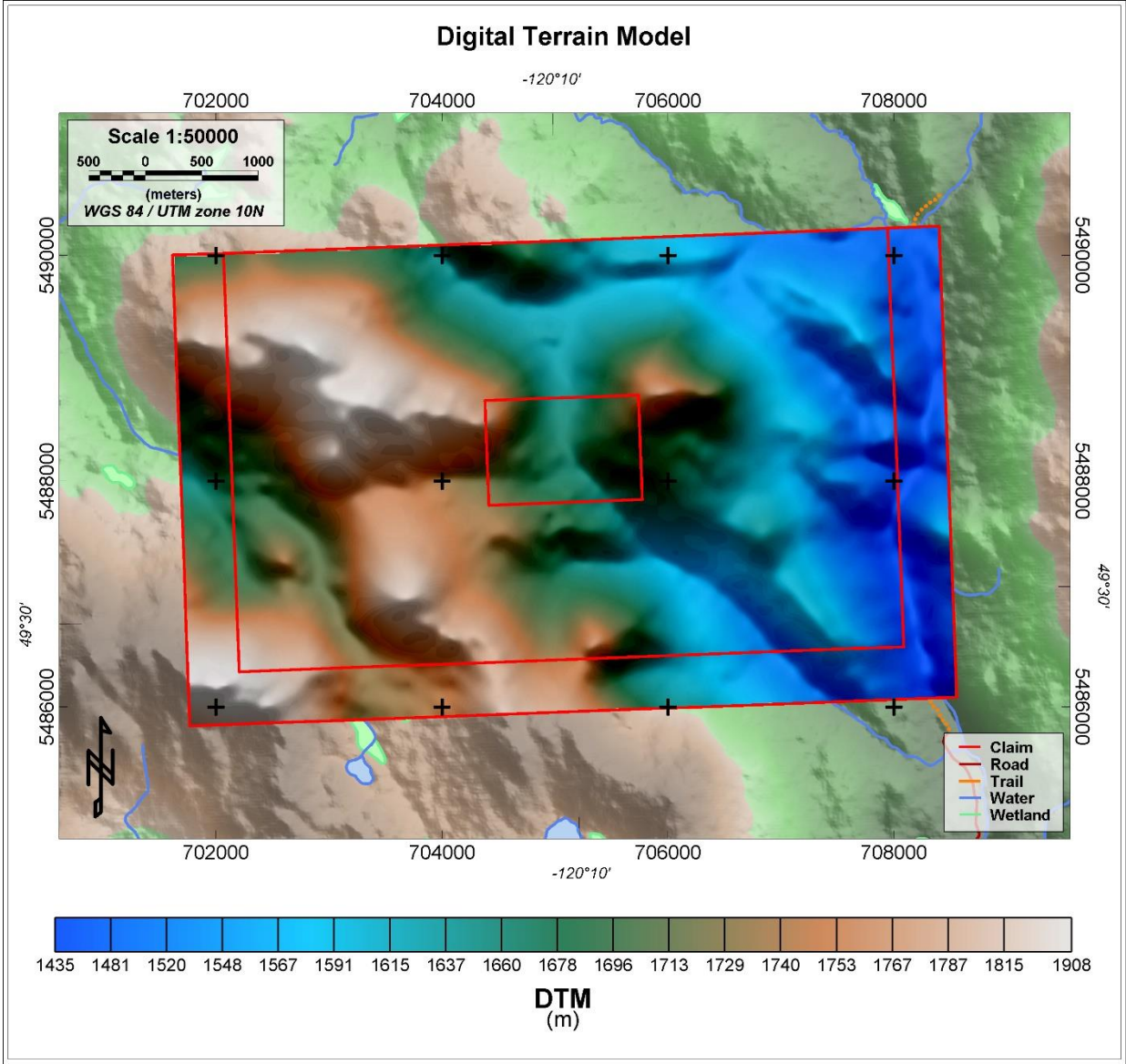


Figure 26 - Image of the DTM over the survey block.

7.0 INTERPRETATION

7.1 OVERVIEW

Little historical work has been performed over the McNulty block, however there are at least four former or active mines within a 40 km range of the McNulty property. Bedrock geology over the region has also been interpreted. See Figure 27.

Approximately 15 km southeast are four gold bearing skarn deposits, which were mined at the Nickel Plate and Mascot mines near Hedley, BC. The mines were in operation between 1902 and 1955, with the Nickel Plate mine operating again between 1987 and 1993.

The Hedley gold skarn camp is underlain predominantly by sedimentary facies of the Late Triassic Nicola Group. The facies can be subdivided into four sedimentary and one volcanoclastic formation, in a north trending, westward deepening, fault-controlled basin. Intrusive activity and associated mineralization's are: (1) Late Triassic Hedley intrusions (gold skarn); (2) Early Jurassic Bromley batholith (McNulty survey block region) (minor W-Cu and industrial garnet skarns), and (3) Middle Jurassic Cahill Creek pluton (W-Mo porphyry and skarn) (Dawson, 1994; Ray et al. 1996).

30 km southwest is the Copper Mountain mine, an alkalic porphyry copper-gold deposit also hosting minor silver resources. This deposit located on and near Triassic to Jurassic aged Diorite, Syenite, Monzonite, and Gabarro intrusive rocks and mafic breccia and tuffs (Collins et al. 2019).

35 km northwest is the Elk Gold mine is on Nicola Group volcanic units, primarily massive with locally porphyritic basalt and andesite units. Some volcanic rocks are silicified and were subject to carbonate or epidote alteration. Batholithic rocks to the east vary from granite to quartz monzonite to granodiorite and have been observed intruding the Nicola Group units. Gold mineralization occurs within quartz-sulphide veins and stringers within phyllic- and silica-altered. Pyrite is the most common sulphide (Laschiavo et al. 2020).

39 km north is the closed Brenda mine which contained plutonic porphyries associated with northern extension of the Okanagan complex hosting Copper, Molybdenum, Gold and Silver.

The McNulty survey area is situated on the Bromley Batholith, or Okanagan complex (there appears to be multiple names for this region). This forms a large body that intrudes the Nicola group, which extends from the McNulty block approximately 15 km west, 35 km north, 35 km east, and 1.5 km to 10 km south. The batholith hosts pale pink to grey, medium to coarse grained, equigranular granite, granodiorite, and minor amounts of syenite (Ray et al. 1996). The assemblage consists of hornblende, biotite, plagioclase, orthoclase, and quartz. Accessory minerals include sericite, apatite, epidote, carbonate, and opaque minerals. The edge of the batholith, generally granodiorite, is locally diorite to quartz diorite in composition. The batholith is dated between 173.4 Ma to 193 Ma. The Bromley batholith rocks are similar in texture and composition to those of the Mt. Riordan stock (195 Ma). (Dawson 1994). Neighbouring mafic and intermediate Triassic volcanic rocks (breccia, tuff, mafic flows, and volcanics) are mapped 5 km to 15 km south of the McNulty block.

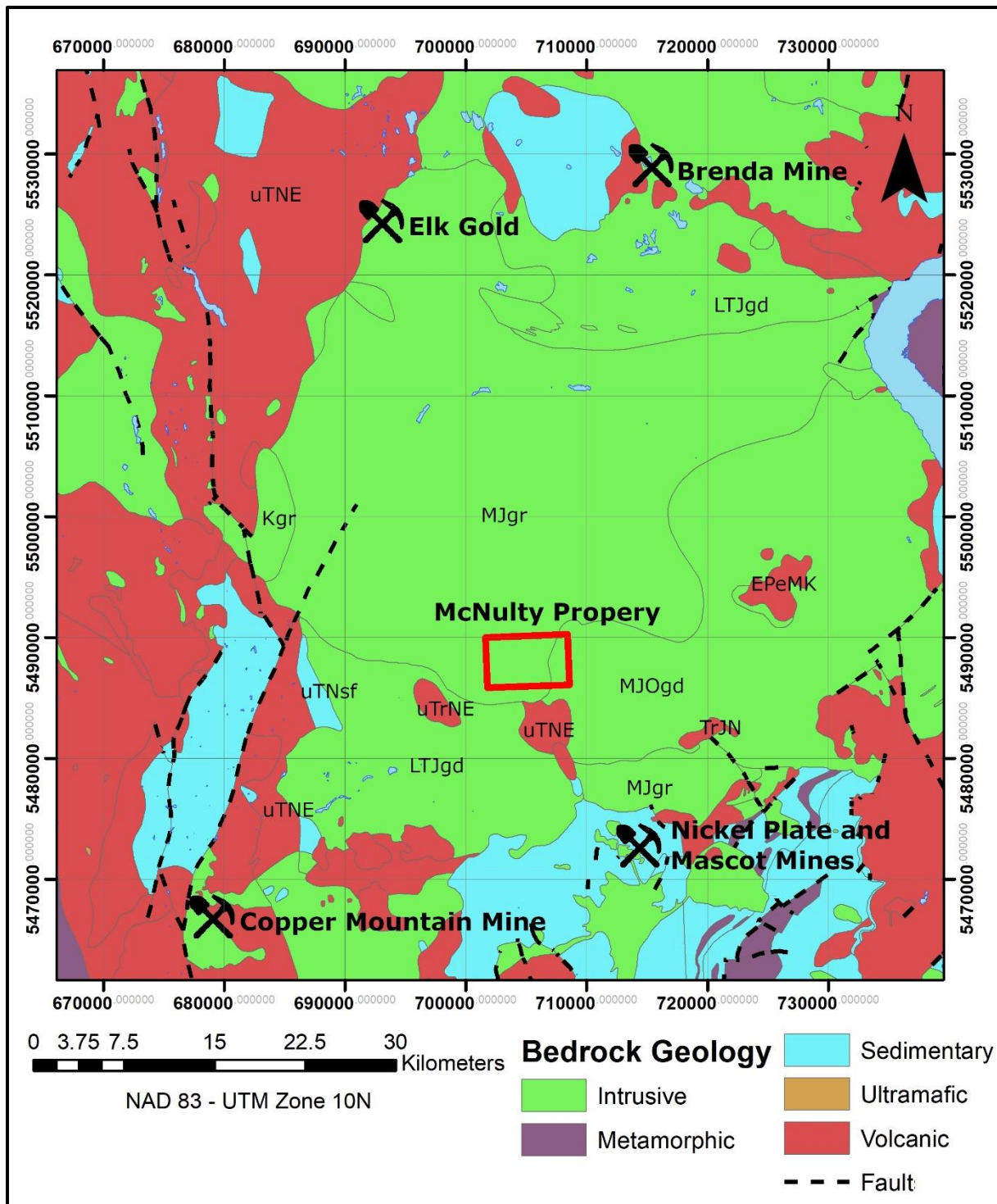


Figure 27 – Bedrock geology map of the McNulty survey block (red outline). Geological rock units near the McNulty property: EPeMK – Eocene undivided volcanic rocks; Kgr – Cretaceous granites; MJgr – Middle Jurassic Granite; MJOgd – Middle Jurassic granodiorite; LTJgd – Late Triassic to Early Jurassic granodiorite; TRJn – Triassic to Jurassic calc-alkaline volcanic rocks; uTrNE/uTNE – Upper Triassic basaltic volcanic rocks; uTNSf – Upper Triassic mudstone, siltstone, and shales;

7.2 MCNULTY MAGNETIC SURVEY

Due to the skarn type gold deposits at the Nickel Plate mine and prevalence of porphyry type deposits further way, it is reasonable to expect similar targets within the McNulty survey block. Magnetic surveying can delineate structural environments associated with stockworks and veins hosting magnetically susceptible minerals (magnetite, pyrrhotite).

Within the McNulty block there appear to be three observed magnetic regions (Figure 28 and Figure 29):

- (1) the north-south trending geological boundary between the Middle Jurassic granite rocks (moderate magnetic intensity) in the west and the Middle Jurassic granodiorite rocks (high magnetic intensity) in the east appears to separate appears to be near vertical northwest-southeast ($142^{\circ}/322^{\circ}$) trending dyke like structures. The magnetic intensity (Figure 30) varies by 450 nT from west to east and appears to be near vertical or steeply dipping to the west. Two potential areas of interest have been marked on Figure 28 and Figure 29 and are also listed in Table 19.
- (2) an east-west trending structure along the northern region of the McNulty (Figure 28 and Figure 29) appears to crosscut the dyke structures identified in (1) and could be a fault or later occurring intrusion. The magnetic intensity (Figure 30) varies across the structure by over 520 nT from north to south and appears to be near vertical or steeply dipping southward. A potential area of interest is marked on Figure 28 and Figure 29 and listed in Table 18.
- (3) a magnetic anomaly located in the north-west region (high magnetic intensity) of the McNulty block (Figure 28 and Figure 29). This region is difficult to interpret, but it could be a decrease in depth to bedrock geology or a contact between different intrusions. A magnetic intensity variation of 1,000 nT is observed. Investigation along the line marked by PT4 in Figure 28 and 29 and listed in Table 18 could shed light on this region.

Table 19 – Potential areas of interest locations in UTM Zone 10 and datum WGS84.

Target	Easting (m)	Northing (m)
PT1	706,808	5,488,483
PT2	706,630	5,487,715
PT3	705,120	5,488,635
PT4	702,919	5,488,630

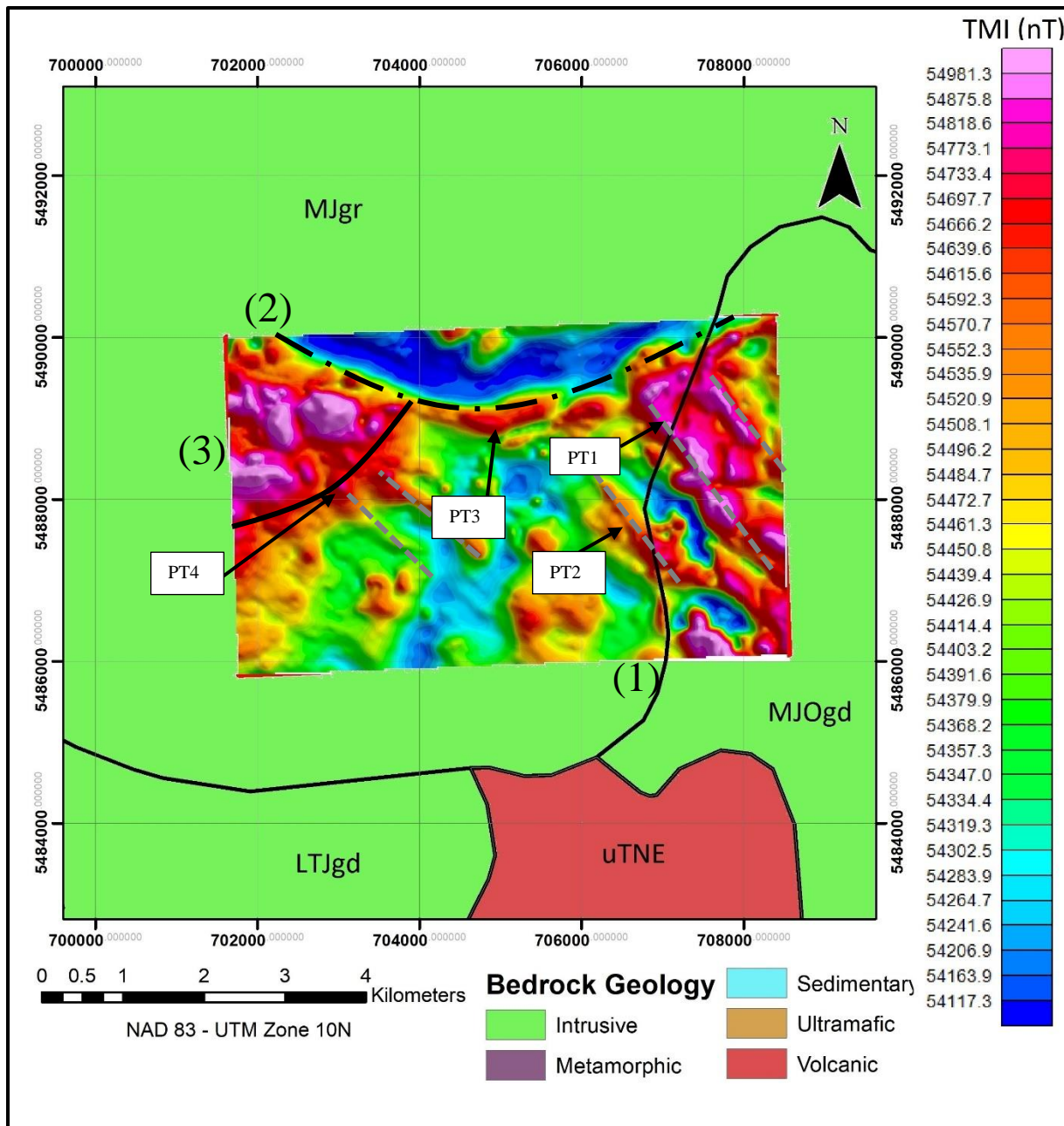


Figure 28 - Total magnetic intensity map of the McNulty block with bedrock geology: MJgr – Middle Jurassic Granite; MJOgd – Middle Jurassic granodiorite; LTJgd – Late Triassic to Early Jurassic granodiorite; and uTNE – Upper Triassic basaltic volcanic rocks. (1) Interpreted N-W trending structures near contact between MJgr and MJOgd. (2) E-W trending structure. (3) High magnetic region.

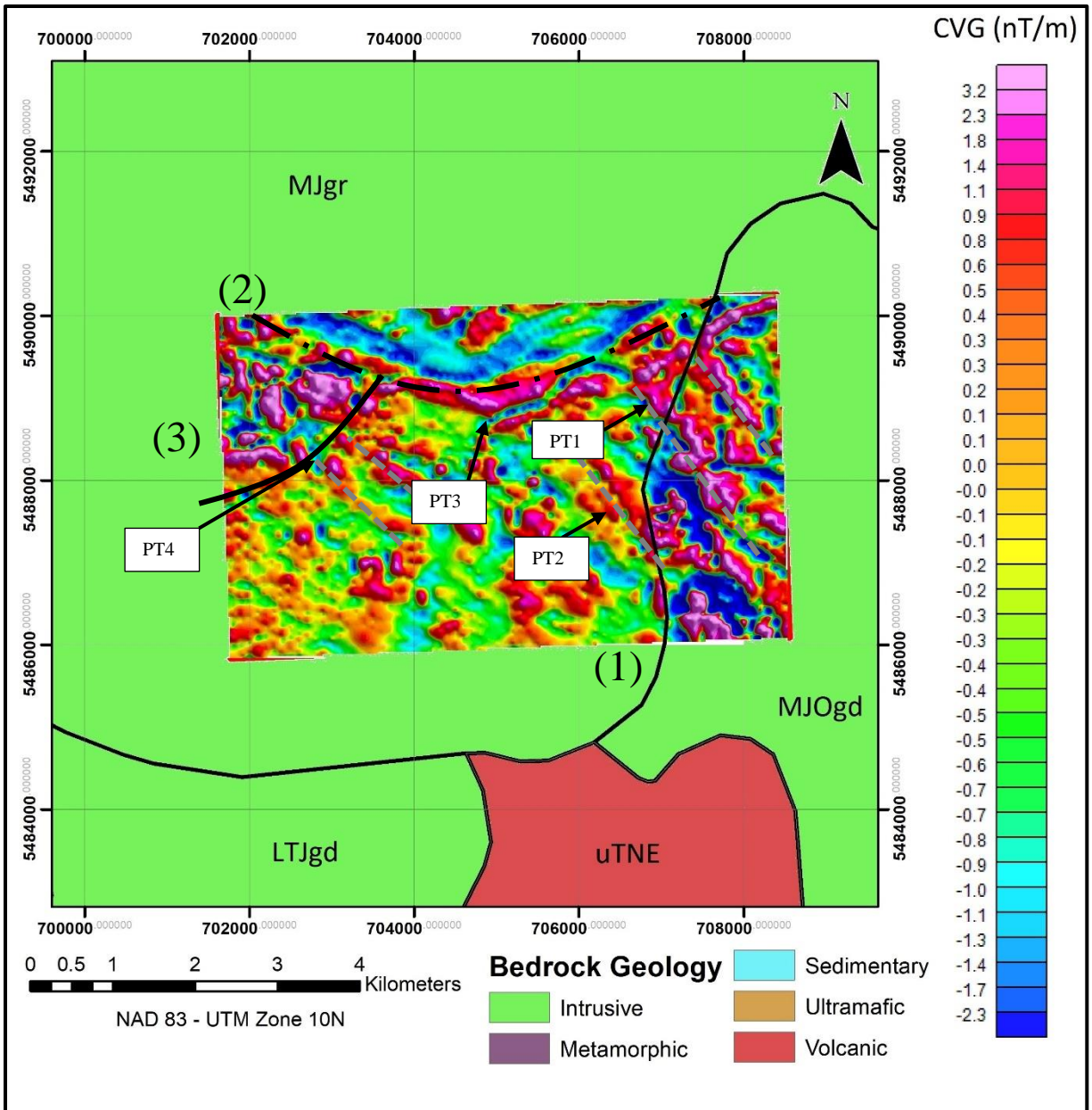


Figure 29 – Calculated vertical gradient map of the McNulty block with bedrock geology: MJgr – Middle Jurassic Granite; MJOgd – Middle Jurassic granodiorite; LTJgd – Late Triassic to Early Jurassic granodiorite; and uTNE – Upper Triassic basaltic volcanic rocks.

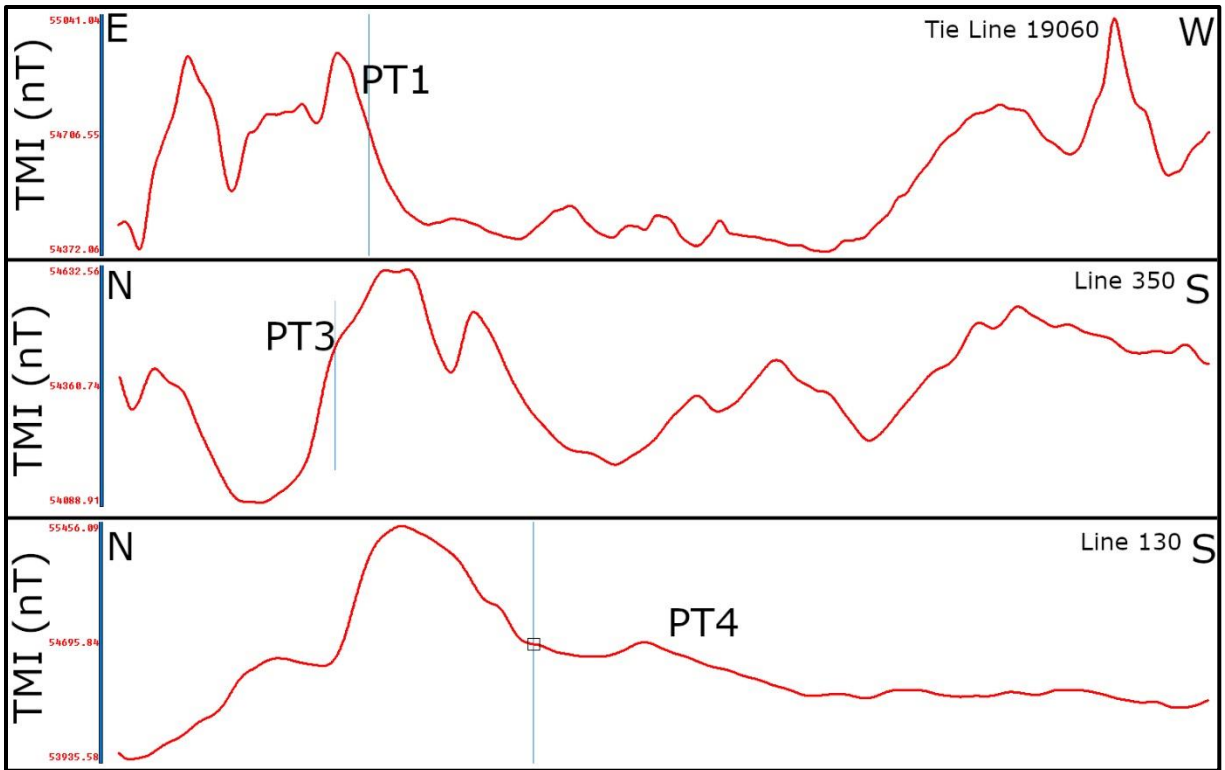


Figure 30 – total magnetic intensity profiles along three survey lines (T19060, L350, and L40) with some potential target regions (PT1, PT3, and PT4).

8.0 QUALIFICATIONS

I, Michael Cunningham, do hereby claim the following to be true:

1. I am a professional geoscientist (P.Ge.) in good standing, registered with the Association of Geoscientists of Ontario (#3007);
2. I am a graduate of Carleton University with a degree in Earth Sciences (Geophysics) (M.Sc, 2016);
3. I am a practicing exploration geophysicist with more than 5 years experience and reside at F-3070 Councillor's Way, Gloucester, Ontario, K1T 2S6;
4. I have no direct interest in the McNulty property, or Max Investments Ltd.;
5. I prepared this report and I am solely responsible for its contents.

Dated at Ottawa, Ontario this the 10th day of May, 2021.



Michael Cunningham, M.Sc., P.Ge.
Geophysicist
Balch Exploration Consulting Inc.

9.0 REFERENCES

- Collins, E., Holbek, P., Westendorf, M., and Strickland, D. 2019. Integrated life-of-mine NI 43-101 Technical report for the Coppter Mountain mine including New Ingerbelle. February 25, 2019.
- Dawson, G.L. 1994. Geological setting of the Hedley Gold Skarn camp with specific reference to the French Mine, south-central British Columbia. M.Sc. Thesis. University of British Columbia.
- Laschiavo, A., Wilson, R.G., Mosher, G.Z., and McLeod, K. 2020. NI 43-101 Technical Report – Preliminary economic assessment on the Elk Gold Project, Merritt, British Columbia, Canada.
- Poon, J. 2021. McNulty Survey Block. Princeton, BC. Precision GeoSurveys Inc. Job# 21142.
- Ray, G.E., Dawson, G.L., and Webster, I.C.L. 1996. The stratigraphy of the Nicola Group in the Hedley district, British Columbia, and the chemistry of its intrusions and Au skarns. *Canadian Journal of Earth Sciences*. 33 (8): 1105–1126.
- Schulze, C. 2010. Assessment report on Geological and Gechemical surveys on ‘block 4’ Copper Mountain Project Solitaire Minerals Inc. BC Geological Survey Assessment Report 31452.

APPENDIX A – OUTLINE OF SURVEY POLYGONS

Polygon corners are given in meters easting and northing, WGS-84, ZONE 10N (Table 19).

Table 20 – McNulty block polygon corners.

Easting (m)	Northing (m)
701,163	5,490,000
708,397	5,490,257
708,557	5,486,088
701,769	5,485,833

APPENDIX B - LIST OF DATABASE COLUMNS (.GDB FORMAT)

CHANNEL	UNITS	DESCRIPTION
X_WGS84	m	UTM Easting – WGS84 Zone 10N
Y_WGS84	m	UTM Northing – WGS84 Zone 10N
Lat_deg	Decimal degree	Latitude – WGS84
Lon_deg	Decimal degree	Longitude – WGS84
Date	yyyy/mm/dd	Dates of the survey flight(s) – Local
FLT		Flight Line numbers
LineNo		Line numbers
STL		Number of satellite(s)
GPSfix		1 = non-differential 2 = WAAS/SBAS differential
Ghead_Heading	degree	Heading of the aircraft
GPStime	HH:MM:SS	GPS time (UTC)
Geos_m	m	Geoidal separation
XTE_m	M	Cross track error
Galt	m	GPS height – WGS84 Zone 10N (ASL)
Lalt	m	Laser altimeter readings (AGL)
DTM	m	Digital Terrain Model
Sample_Density	m	Horizontal distance in meters between adjacent measurement locations; sample frequency is 20 Hz
Speed_km_hr	km/hr	Ground speed of aircraft in km/hr
basemag	nT	Base station temporal variation data
IGRF	nT	International Geomagnetic Reference Field, 2015
Declin	Decimal degree	Calculated declination of magnetic field
Inclin	Decimal degree	Calculated inclination of magnetic field
XFg_Step	step	X - fluxgate
YFg_Step	step	Y - fluxgate
ZFg_Step	step	Z - fluxgate
Mag1_Head	nT	Mag 1 – Diurnal, lag, and heading corrected
Mag2_Head	nT	Mag 2 - Diurnal, lag, and heading corrected
Mag3_Head	nT	Mag 3 - Diurnal, lag, and heading corrected
TMI	nT	Total Magnetic Intensity (Mag 2)
RMI	nT	Residual Magnetic Intensity (Mag 2)
iLG	nT/m	In-Line Gradient (Mag 2)
xLG	nT/m	Cross-Line Gradient (Mag 1 and Mag 3)
HG	nT/m	Total Horizontal Gradient (in-line and cross-line)
TMIge	nT	Gradient enhanced Total Magnetic Intensity
RMIge	nT	Gradient enhanced Residual Magnetic Intensity

**APPENDIX C – PRECISION GEOSURVEYS LOGISTICS
REPORT**

AIRBORNE GEOPHYSICAL SURVEY REPORT



McNulty Survey Block
Princeton, BC
Max Investments Inc.

Precision GeoSurveys Inc.

www.precisiongeosurveys.com
Hangar 42 Langley Airport
21330 - 56th Ave., Langley, BC
Canada V2Y 0E5
604-484-9402

Jenny Poon, B.Sc., P.Geo.
April 2021
Job# 21142

Table of Contents

Table of Contents	i
1.0 Introduction	1
1.1 Survey Area	1
1.2 Survey Specifications	3
2.0 Geophysical Data	3
2.1 Magnetic Data	4
2.1.1 Gradient Magnetic Data	4
3.0 Aircraft and Equipment	4
3.1 Aircraft	5
3.2 Geophysical Equipment	5
3.2.1 IMPAC	5
3.2.2 GPS Navigation System	7
3.2.3 Pilot Guidance Unit	7
3.2.4 Laser Altimeter	8
3.2.5 Magnetic Gradiometer	9
3.2.6 Fluxgate Magnetometer	9
3.2.7 Magnetic Base Station	10
4.0 Survey Operations	10
4.1 Operations Base and Crew	11
4.2 Magnetic Base Station Specifications	11
4.3 Field Processing and Quality Control	13
5.0 Data Acquisition Equipment Checks	14
5.1 Laser Altimeter Calibration	14
5.2 Lag Test	15
5.3 Magnetometer Tests	15
5.3.1 Compensation Flight Test	15
5.3.2 Heading Correction Test	17
6.0 Data Processing	17
6.1 Position Corrections	19
6.1.1 Lag Correction	19
6.2 Flight Height and Digital Terrain Model	19
6.3 Magnetic Processing	19
6.3.1 Temporal Variation Correction	20
6.3.2 Heading Correction	20
6.3.3 Leveling and Micro-leveling	20
6.3.4 IGRF Removal	21
6.4 Magnetic Gradient	21
6.4.1 Horizontal Gradients	22
6.4.2 Calculation of Vertical Gradient	23
6.4.3 Gradient Enhanced Magnetic Intensity	23
6.4.4 Gradient Enhanced Reduction to Magnetic Pole	23

7.0 Deliverables.....24

7.1 Digital Data24

7.1.1 Grids24

7.2 KMZ.....25

7.3 Maps25

7.4 Report26

8.0 Conclusions and Recommendations26

List of Figures

Figure 1: McNulty survey area located in southern British Columbia.	1
Figure 2: McNulty survey block east of Princeton, British Columbia.	2
Figure 3: Plan View – McNulty survey block with actual flight lines in yellow.....	2
Figure 4: Terrain View – McNulty survey block with actual flight lines displayed in yellow.....	3
Figure 5: Survey helicopter equipped with three magnetic sensors.....	5
Figure 6: IMPAC data acquisition system.....	6
Figure 7: AGIS operator display.....	6
Figure 8: Hemisphere R330 GPS receiver.....	7
Figure 9: PGU screen displaying navigation information.....	8
Figure 10: Opti-Logic RS800 Rangefinder laser altimeter.....	8
Figure 11: View of triple magnetic boom system.....	9
Figure 12: Billingsley TFM100G2 triaxial fluxgate magnetometer.....	10
Figure 13: GEM GSM-19T proton precession magnetometer.....	10
Figure 14: Location of GEM 5 and GEM 6.....	12
Figure 15: GEM 5 (L) and GEM 6 (R).....	12
Figure 16: Histogram showing survey elevation vertically above ground.....	13
Figure 17: Histogram showing magnetic sample density.....	14
Figure 18: Histogram showing cross track error of survey helicopter.....	14
Figure 19: Magnetic data processing flow.....	18

List of Tables

Table 1: Survey flight line specifications for McNulty.....	3
Table 2: Magnetometer details. Cross-line gradient measured between Mag 1 and Mag 3.....	9
Table 3: List of survey crew members.....	11
Table 4: Magnetic base station locations.....	11
Table 5: Contract survey specifications.....	13
Table 6: Survey lag correction values.....	15
Table 7: Results of compensation flight for Mag 1.....	16
Table 8: Results of compensation flight for Mag 2.....	16
Table 9: Results of compensation flight for Mag 3.....	16
Table 10: Magnetic sensor heading corrections for headings 000°/090°/180°/270°.....	17
Table 11: Magnetic sensor relationship used to calculate magnetic gradients.....	21

List of Appendices

- Appendix A: Polygon Coordinates
- Appendix B: Equipment Specifications
- Appendix C: Digital File Descriptions

List of McNulty Survey Block Plates

Plate 1: McNulty – Actual Flight Lines (FL)

Plate 2: McNulty – Digital Terrain Model (DTM)

Plate 3: McNulty – Total Magnetic Intensity with Actual Flight Lines (TMI_wFL)

Plate 4: McNulty – Total Magnetic Intensity (TMI)

Plate 5: McNulty – Residual Magnetic Intensity (RMI)

Plate 6: McNulty – In-Line Gradient (ILG)

Plate 7: McNulty – Cross-Line Gradient (XLG)

Plate 8: McNulty – Horizontal Gradient (HG)

Plate 9: McNulty – Calculated Vertical Gradient (CVG) of RMI

Plate 10: McNulty – Gradient Enhanced Total Magnetic Intensity (TMIge)

Plate 11: McNulty – Gradient Enhanced Residual Magnetic Intensity (RMIge)

Plate 12: McNulty – Gradient Enhanced Reduced to Magnetic Pole (RTPge) of RMIge

1.0 Introduction

This report outlines the geophysical survey operations and data processing procedures taken during the high resolution helicopter-borne magnetic gradiometer survey flown over the McNulty survey block for Max Investments Inc. The survey block is located in southern British Columbia (Figure 1) and it was flown on April 13 and 14, 2021.

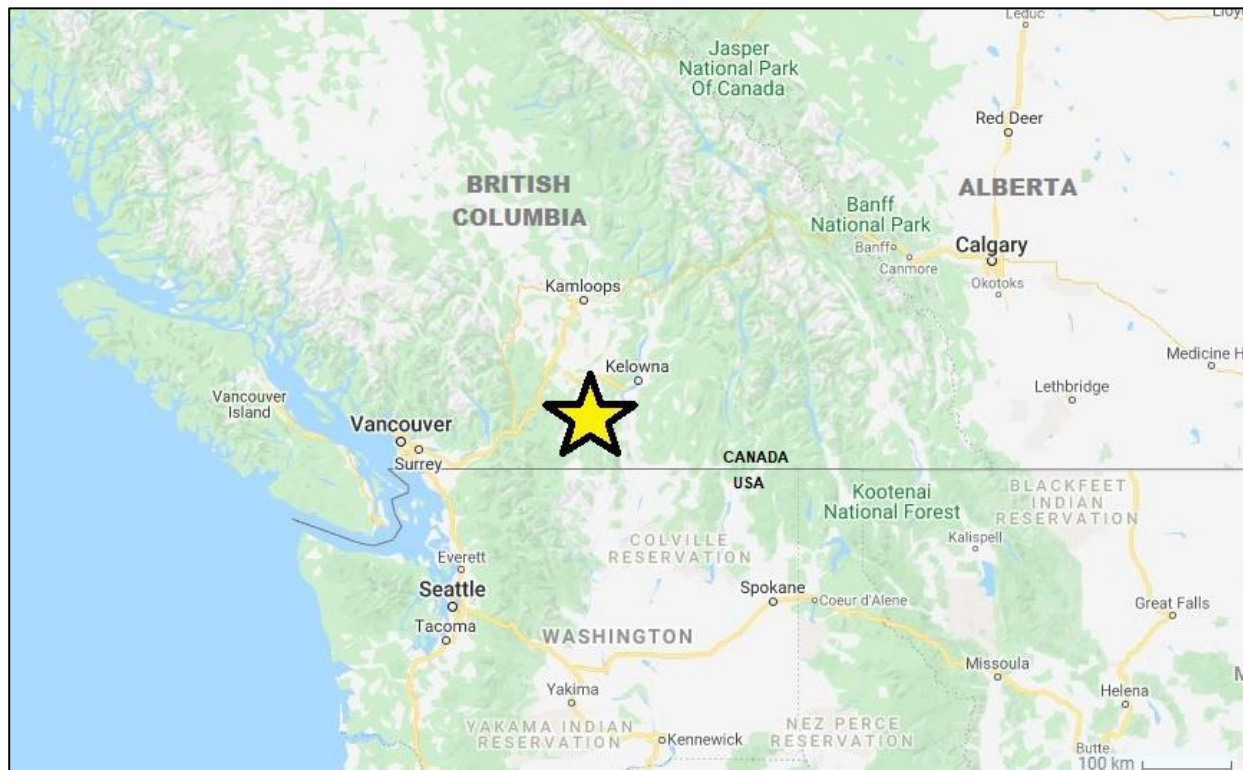


Figure 1: McNulty survey area located in southern British Columbia.

1.1 Survey Area

The McNulty survey block is centered approximately 26 km east of Princeton, British Columbia (Figure 2).

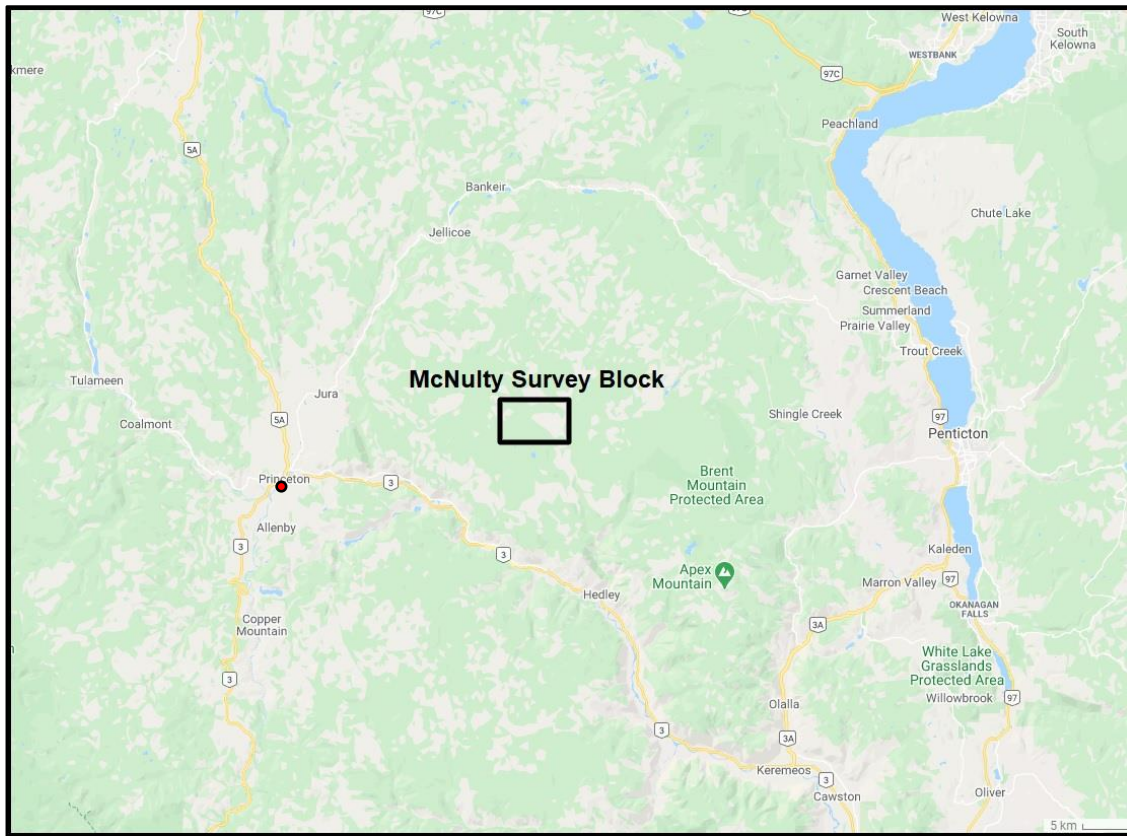


Figure 2: McNulty survey block east of Princeton, British Columbia.

The McNulty survey block was flown at 100 m line spacing at a heading of 178°/358°; tie lines were flown at 500 m spacing at a heading of 088°/268° (Figures 3 and 4).

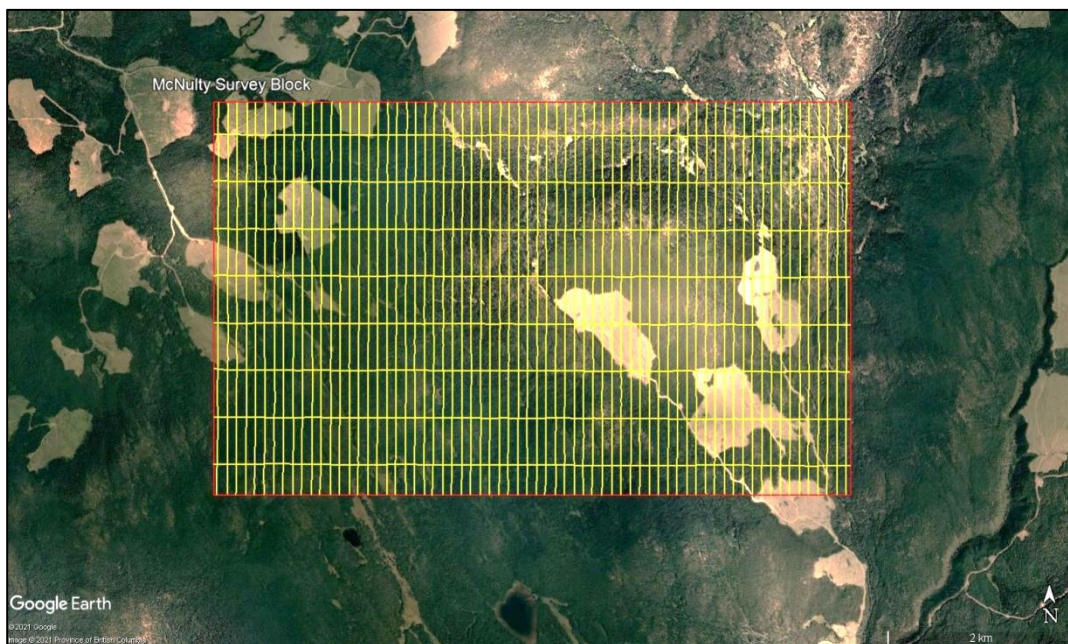


Figure 3: Plan View – McNulty survey block with actual flight lines in yellow and survey block boundary in red.

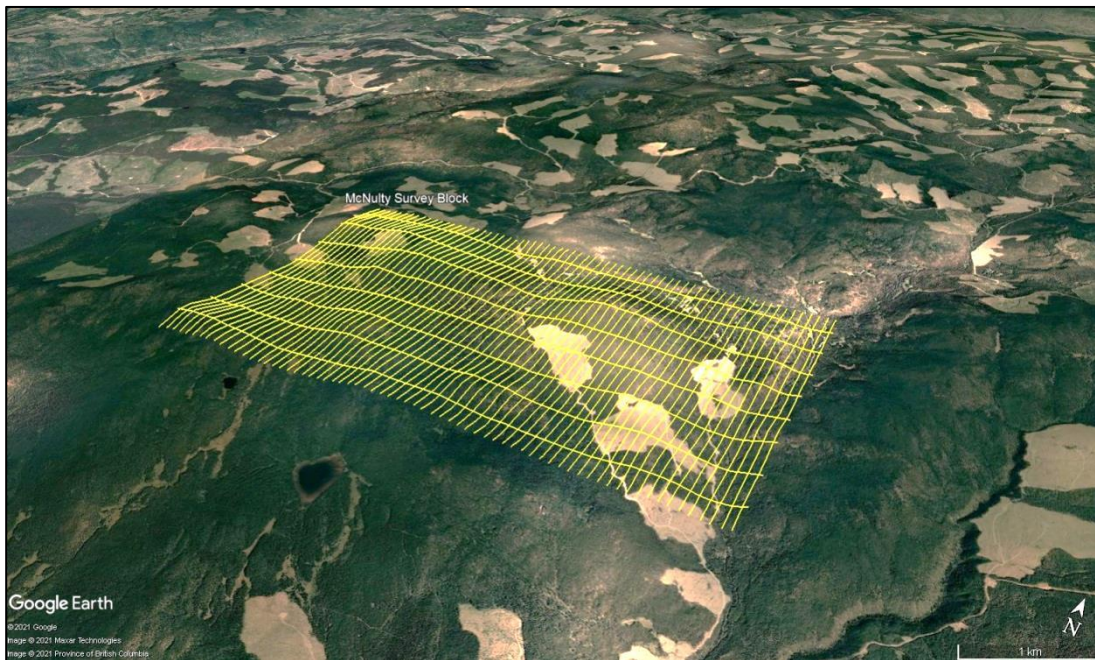


Figure 4: Terrain View – McNulty survey block with actual flight lines displayed in yellow.

1.2 Survey Specifications

The geodetic system used for the geophysical survey was WGS 84 in UTM Zone 10N. Polygon coordinates for the McNulty survey block are specified in Appendix A. A total of 338 line km was flown over an area of 28.3 km² (Table 1).

Survey Block	Area (km ²)	Line Type	No. of Lines Planned	No. of Lines Completed	Line Spacing (m)	Line Orientation (UTM grid)	Total Planned Line km	Total Actual km Flown
McNulty	28.3	Survey	68	68	100	178°/358°	284	284
		Tie	8	8	500	088°/268°	54	54
		Total:	76	76			338	338

Table 1: Survey flight line specifications for McNulty.

2.0 Geophysical Data

Geophysical data are collected in a variety of ways and are used for many purposes including aiding in the determination of geology, mineral deposits, oil and gas deposits, geotechnical investigations, contaminated land sites, and UXO (unexploded ordnance) detection.

For the purposes of this survey, airborne gradient magnetic data were collected to serve in geological mapping and exploration for mineral deposits.

2.1 Magnetic Data

Magnetic surveying is the most common airborne geophysical technology used for both mineral and hydrocarbon exploration. Aeromagnetic surveys measure and record the total intensity of the magnetic field at the magnetometer sensor, which is a combination of the desired geomagnetic field as well as influences from the constantly varying solar wind and the aircraft's magnetic field. By subtracting temporal and aircraft magnetic effects, the resulting aeromagnetic maps show the spatial distribution and relative abundance of magnetic minerals - most commonly the iron oxide mineral magnetite - in the upper levels of Earth's crust, which in turn are related to lithology, structure, and alteration of bedrock. Survey specifications, instrumentation, and interpretation procedures depend on the objectives of the survey. Magnetic surveys are typically performed for:

- Geological Mapping - to aid in mapping lithology, structure, and alteration.
- Depth to Basement Mapping - for exploration in sedimentary basins or mineralization associated with the basement surface.

2.1.1 Gradient Magnetic Data

In addition to high resolution total magnetic field data, horizontal magnetic gradient data were collected by using a triple magnetic gradient boom with 3 axis compensation. Direct measurement of the magnetic gradient is particularly useful for:

- Enhanced definition of near-surface anomalies.
- Emphasis on short wavelength spatial components of magnetic anomalies from horizontal variations of the gradients.
- Attenuation of long wavelength spatial components associated with regional trends and large scale anomalies.
- Reduction of high frequency temporal variations in the Earth's magnetic field due to micro-pulsations.
- Immunity to diurnal fluctuations.
- Reduction of aircraft/sensor movement errors.

3.0 Aircraft and Equipment

All geophysical and subsidiary equipment were carefully installed on an aircraft by Precision GeoSurveys to collect gradient magnetic data.

3.1 Aircraft

Precision GeoSurveys flew the survey using an Airbus AS350 helicopter, registration C-GSVY.

3.2 Geophysical Equipment

The survey aircraft (Figure 5) was equipped with a data acquisition system, GPS navigation system, pilot guidance unit (PGU), laser altimeter, triple magnetic gradient boom system, and fluxgate magnetometer. In addition, two magnetic base stations were used to record temporal magnetic variations. Technical specifications for the geophysical equipment are provided in Appendix B.



Figure 5: Survey helicopter equipped with three magnetic sensors for gradient magnetic data acquisition.

3.2.1 IMPAC

The Integrated Multi-Parameter Acquisition Console (IMPAC) (Figure 6), manufactured by Nuvia Dynamics Inc. (previously Pico Envirotec Inc.), is the main computer used in integrated data recording, data synchronizing, providing real-time quality control data for the geophysical operator display, and the generation of navigation information for the pilot and operator display systems.



Figure 6: IMPAC data acquisition system.

IMPAC uses the Microsoft Windows operating system and geophysical parameters are based on Nuvia's Airborne Geophysical Information System (AGIS) software. Depending on survey specifications, information such as magnetic field, electromagnetic response, total gamma count, counts of various radioelements (K, U, Th, etc.), cosmic radiation, barometric pressure, atmospheric humidity, temperature, aircraft attitude, navigation parameters, and GPS status can all be monitored on the AGIS on-board display (Figure 7).

While in flight, raw magnetic response, magnetic fourth difference, compensated and uncompensated data, radiometric spectra, aircraft position, survey altitude, cross track error, and other parameters are recorded and can be viewed by the geophysical operator for immediate QC (quality control). Additional software allows for post or real time magnetic compensation and radiometric calibration.

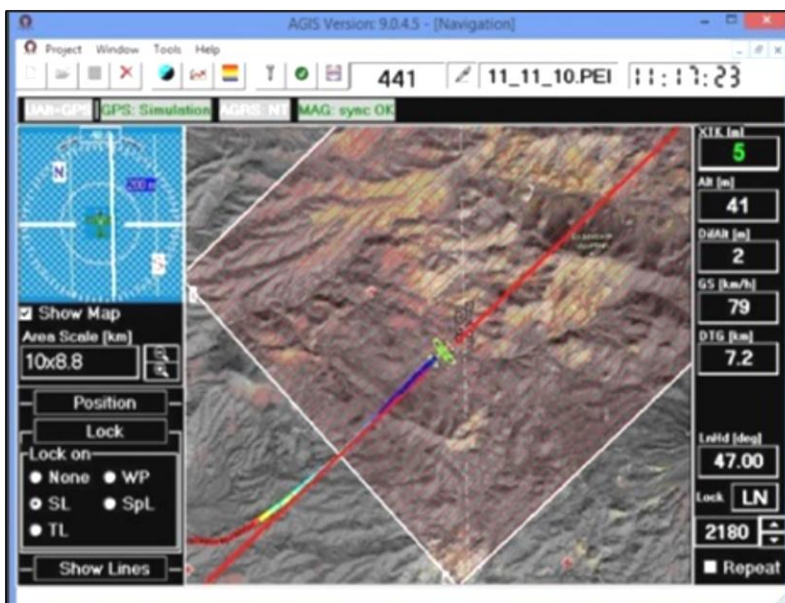


Figure 7: AGIS operator display showing real time flight line recording and navigation parameters. Additional windows display real-time geophysical data to operator.

3.2.2 GPS Navigation System

A Hemisphere R330 GPS receiver (Figure 8) and a Novatel GPS antenna on the tail of the aircraft integrated with the AGIS navigation system and pilot display (PGU) provide accurate navigational information and position control. The R330 GPS receiver supports fast updates at a rate of up to 10 Hz (10 times per second); delivering sub-meter positioning accuracy in three dimensions. It receives GNSS (GPS/GLONASS) L1 and L2 signals.

The receiver supports differential correction methods including L-Band, RTK, SBAS, and Beacon. The R330 employs innovative Hemisphere GPS Eclipse SureTrack technology, which allows it to model the phase on satellites that the airborne unit is currently tracking. With SureTrack technology, dropouts are reduced and speed of the signal reacquisitions is increased; enhancing accurate positioning when base corrections are not available.

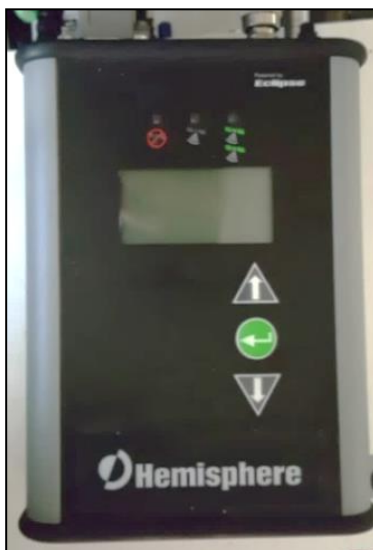


Figure 8: Hemisphere R330 GPS receiver.

3.2.3 Pilot Guidance Unit

Steering and elevation (ground clearance) information is continuously provided to the pilot by the Pilot Guidance Unit (PGU). The graphical display is mounted on top of the aircraft's instrument panel, remotely from the data acquisition system. The PGU is the primary navigation aid (Figure 9) to assist the pilot in keeping the aircraft on the planned flight path, heading, speed, and at the desired ground clearance.

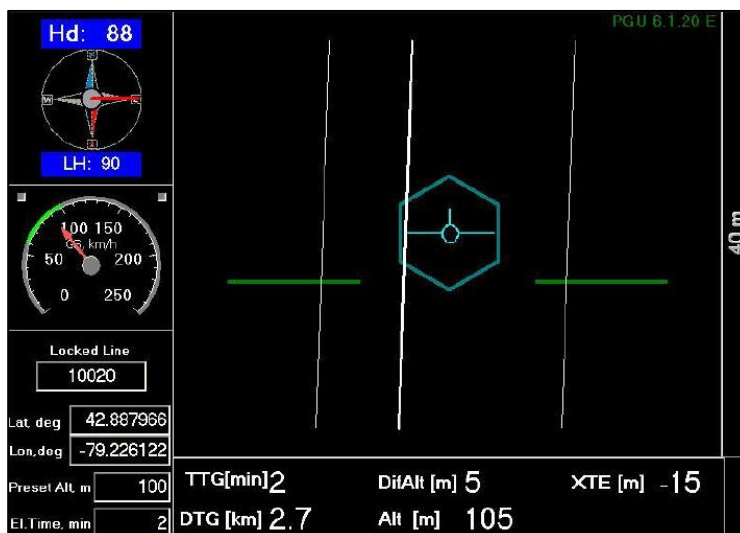


Figure 9: PGU screen displaying navigation information.

PGU information is displayed on a full VGA 600 x 800 pixel 7 inch (17.8 cm) LCD display. The CPU for the PGU is contained in a PC-104 console and uses Microsoft Windows operating system control, with input from the GPS antenna on the aircraft, laser altimeter, and AGIS.

3.2.4 Laser Altimeter

Terrain clearance is measured by an Opti-Logic RS800 Rangefinder laser altimeter (Figure 10) attached to the belly of the forward magnetometer boom. The RS800 laser is a time-of-flight sensor that measures distance by a rapidly modulated and collimated laser beam that creates a dot on the target surface. The maximum range of the laser altimeter is 700 m off natural surfaces with accuracy of ± 1 m on 1 x 1 m diffuse target with 50% ($\pm 20\%$) reflectivity. Within the sensor unit, reflected signal light is collected by the lens and focused onto a photodiode. Through serial communications and digital outputs, ground clearance data are transmitted to an RS-232 compatible port and recorded and displayed by the AGIS and PGU at 10 Hz in meters.

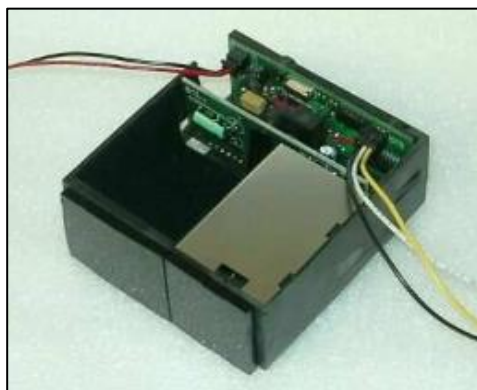


Figure 10: Opti-Logic RS800 Rangefinder laser altimeter.

3.2.5 Magnetic Gradiometer

The primary geophysical technology used on this survey was a magnetic gradiometer system (Figure 11). Three widely-spaced split-beam cesium vapor magnetometers mounted in a non-magnetic and non-conductive triple boom configuration provide total magnetic intensity as well as magnetic gradient in the cross-line (X or lateral or transverse) and in-line (Y or longitudinal) directions (Table 2). The magnetometer sensors were orientated at 45 degrees with respect to the horizontal to couple with local magnetic field at the McNulty survey block.



Figure 11: View of triple magnetic boom system.

Magnetometer	Model	Serial No.	Gradient Direction	Separation (m)
Mag 1	Geometrics G-822A	75656	X or Cross-line	11.5
Mag 2	Scintrex CS-3	612211	Total Field and In-line	7.3
Mag 3	Geometrics G-822A	823063	X or Cross-line	11.5

Table 2: Magnetometer details. Cross-line gradient measured between Mag 1 and Mag 3.

3.2.6 Fluxgate Magnetometer

As the survey helicopter flies along a survey line, small attitude changes (pitch, roll, and yaw) are recorded by a triaxial fluxgate magnetometer (Figure 12). The fluxgate consists of three magnetic sensors, X, Y, and Z, operating independently and simultaneously. Each sensor has an analog output corresponding to the component of the ambient magnetic field along its axis. Response of the sensors is proportional to the cosine of the angle between the applied field and the sensor's sensitive axis.



Figure 12: Billingsley TFM100G2 triaxial fluxgate magnetometer.

3.2.7 Magnetic Base Station

Temporal variations of Earth's magnetic field, particularly diurnal, were monitored and recorded by two GEM GSM-19T base station magnetometers. They were operated at all times while airborne data were being collected. The base stations were located in an area with low magnetic gradient, away from electric power transmission lines and moving ferrous objects, such as motor vehicles, that could affect the survey data integrity.

The GEM GSM-19T magnetometer (Figure 13) with integrated GPS time synchronization uses proton precession technology with absolute accuracy of ± 0.20 nT and sensitivity of 0.15 nT at 1 Hz. Base station magnetic data were recorded on internal solid-state memory and downloaded onto a field laptop computer using a serial cable and GEMLink 5.4 software. Profile plots of the base station readings were generated, updated, and reviewed at the end of each survey day.



Figure 13: GEM GSM-19T proton precession magnetometer.

4.0 Survey Operations

The McNulty geophysical survey was flown on April 13 and 14, 2021 in dry and sunny weather conditions. The experience of the pilots ensured that data quality objectives were met, and that safety of the flight crew was never compromised given the potential risks involved in airborne geophysical surveying. Field processing and quality control checks were performed daily.

4.1 Operations Base and Crew

The base of operation for the McNulty survey was at Princeton airport, British Columbia, west of the survey block.

Precision's geophysical crew consisted of three members (Table 3):

Crew Member	Position
Harmen Keyser, P.Geo.	Helicopter pilot and project manager
Melissa Sparrow	Helicopter pilot and geophysical operator
Jenny Poon, B.Sc., P.Geo.	Geophysicist – data processor, mapping, and reporting (off-site)

Table 3: List of survey crew members.

4.2 Magnetic Base Station Specifications

Changes in the Earth's magnetic field over time, such as diurnal variations, magnetic pulsations, and geomagnetic storms, were measured and recorded by two stationary GEM GSM-19T proton precession magnetometers. The magnetic base stations were installed southwest of the survey block in an area (Table 4; Figures 14 and 15) of low magnetic noise away from metallic items such as ferromagnetic objects, vehicles, and power lines that could affect the base stations and ultimately the survey data.

Station Name	Easting/Northing	Latitude/Longitude	Datum/Projection
GEM 5 S/N 1094678	700620 m E 5483219 m N	49° 28' 6.42" N 120° 13' 51.28" W	WGS 84, Zone 10N
GEM 6 S/N 5087249	700614 m E 5483223 m N	49° 28' 6.56" N 120° 13' 51.56" W	WGS 84, Zone 10N

Table 4: Magnetic base station locations.

Magnetic readings were reviewed at regular intervals to ensure that no airborne data were collected during periods of high magnetic activity (in excess of 10 nT from a linear chord of five minutes).



Figure 14: Location of GEM 5 and GEM 6 magnetic base stations southwest of McNulty survey block.



Figure 15: GEM 5 (L) and GEM 6 (R) magnetic base stations.

4.3 Field Processing and Quality Control

Survey data were transferred from the aircraft's data acquisition system onto a USB memory stick and copied onto a field data processing laptop on a flight-by-flight basis. The raw data files in PEI binary data format were converted into Geosoft GDB database format. Using Geosoft Oasis Montaj 9.9.1, the data were inspected to ensure compliance with contract specifications (Table 5; Figures 16 to 18). Several sources of potential geophysical data interference from logging equipment were reported by the survey crew.

Parameter	Specification	Tolerance
Position	Line Spacing	Flight line deviation within 8 m L/R from ideal flight path. No exceedance for more than 1 km.
	Height	Nominal flight height of 40 m above ground level (AGL) with tolerance of ± 10 m. No exceedance for more than 1 km, provided deviation is not due to tall trees, topography, mitigation of wildlife/livestock harassment, cultural features, or other obstacles beyond the pilot's control.
	GPS	GPS signals from four or more satellites must be received at all times, except where signal loss is due to topography. No exceedance for more than 1 km.
Magnetics	Temporal/Diurnal Variations	Non-linear temporal magnetic variations within 10 nT of a linear chord of length 5 minutes.
	Normalized 4 th Difference	Magnetic data within 0.01 nT peak to peak. No exceedance for distances greater than 1 km or more, provided noise is not due to geological or cultural features.

Table 5: Contract survey specifications.

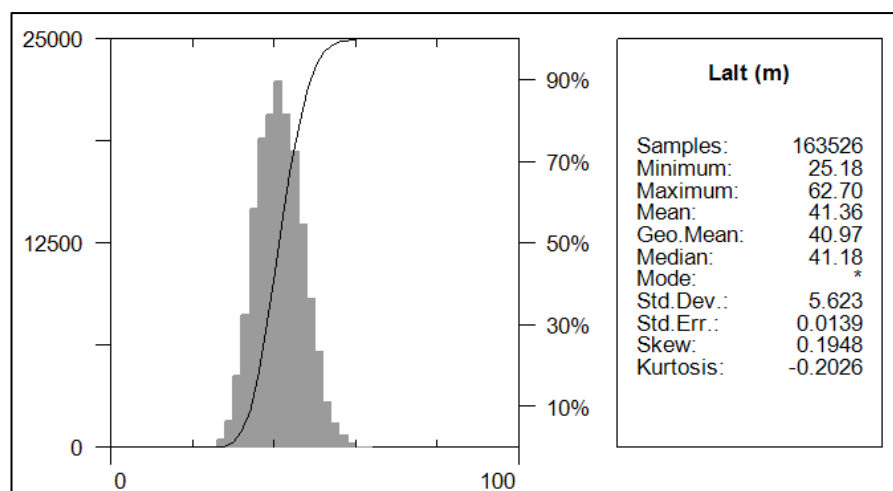


Figure 16: Histogram showing survey elevation vertically above ground.

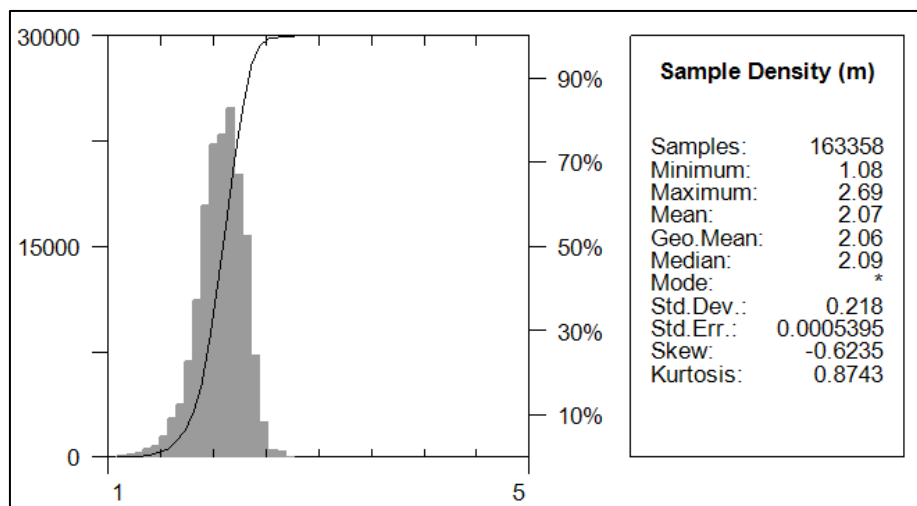


Figure 17: Histogram showing magnetic sample density. Horizontal distance in meters between adjacent measurement locations; magnetic sample frequency 20 Hz.

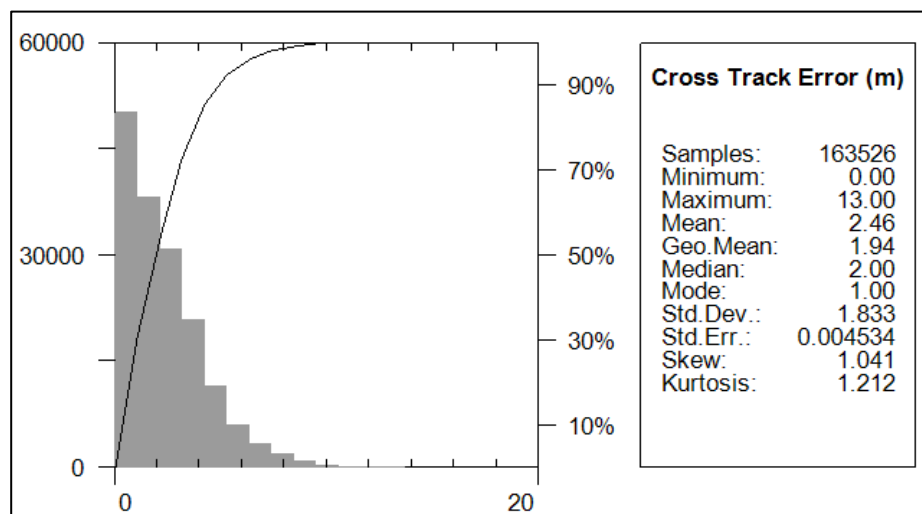


Figure 18: Histogram showing cross track error of survey helicopter.

5.0 Data Acquisition Equipment Checks

Equipment tests and calibrations were conducted for the laser altimeter and magnetometers at the start of the survey to ensure compliance with contract specifications and to deliver high quality airborne geophysical data. A lag test was conducted for all sensors. For the airborne magnetometers, compensation and heading error test flights were flown.

5.1 Laser Altimeter Calibration

The Opti-Logic RS-800 laser altimeter used on the survey helicopter was tested and calibrated in accordance with manufacturer's instructions prior to starting the survey. This ensured that heights reported by the laser were accurate within the normal survey operating range.

5.2 Lag Test

A lag test was performed to determine the difference in time the digital reading was recorded for the magnetometers and laser altimeter with the position fix time that the fiducial of the reading was obtained by the GPS system resulting from a combination of system lag and different locations of the various sensors and the GPS antenna. The test was flown in the four orthogonal survey headings in two directions over identifiable features at survey speed and height. The resulting data (Table 6) were used to correct for time and position.

Instrument	Source	Lag Fiducial	Correction (sec)
Mag 1	Logging equipment	7	0.35
Mag 2	Logging equipment	9	0.45
Mag 3	Logging equipment	11	0.55
Laser	Sharp gully	16	0.80

Table 6: Survey lag correction values. Magnetic data at 20 Hz; laser altimeter was resampled to 20 Hz.

5.3 Magnetometer Tests

The magnetometers were tested and calibrated with a series of dedicated flights specifically for removing instrument offset errors and undesired effects of aircraft movement, speed, and heading direction.

5.3.1 Compensation Flight Test

During aeromagnetic surveying, a small but significant amount of noise is introduced to the magnetic data by the aircraft itself, as the magnetometers are within the aircraft's magnetic field. Changes in aircraft attitude combined with the permanent magnetization of certain aircraft parts (in particular the engine and other ferrous magnetic objects) contribute to this noise. The aircraft was degaussed using proprietary technology prior to starting the survey and the remaining magnetic noise was removed by a process called magnetic compensation.

A magnetic compensation flight was completed for this survey. The process consists of a series of prescribed maneuvers ($\pm 10^\circ$ roll, $\pm 10^\circ$ pitch, and $\pm 10^\circ$ yaw) where the aircraft flies in the four orthogonal headings required ($000^\circ/090^\circ/180^\circ/270^\circ$ in the case of this survey) at a sufficient altitude (typically $> 2,500$ m AGL) in an area of low magnetic gradient where Earth's magnetic field becomes nearly uniform at the scale of the compensation flights. In each heading direction, three specified roll, pitch, and yaw maneuvers (total 36) are performed by the pilot at constant elevation so that any magnetic variation recorded by the airborne magnetometers can be attributed to aircraft movement. These maneuvers are determined by the airborne fluxgate magnetometer and provide the data that are required to calculate the necessary parameters for

compensating the magnetic data to remove aircraft noise from survey data. Compensation flight test results are summarized in Tables 7 to 9.

Pre-Compensation					Post-Compensation				
Heading	Roll	Pitch	Yaw	Total	Heading	Roll	Pitch	Yaw	Total
000°	1.5828	0.3602	0.3535	2.2965	000°	0.2718	0.3068	0.2745	0.8531
090°	1.2691	0.7776	0.7521	2.7988	090°	0.1701	0.1647	0.1820	0.5168
180°	0.8110	0.5913	0.4304	1.8327	180°	0.2270	0.2392	0.1900	0.6562
270°	0.9121	0.5877	0.4252	1.9250	270°	0.3001	0.3255	0.3194	0.9450
FOM (nT) = 8.8530					FOM (nT) = 2.9711				

Table 7: Results of compensation flight for Mag 1.

Pre-Compensation					Post-Compensation				
Heading	Roll	Pitch	Yaw	Total	Heading	Roll	Pitch	Yaw	Total
000°	0.3544	0.9193	0.3236	1.5973	000°	0.1405	0.1317	0.1235	0.3957
090°	0.2587	0.8528	0.4095	1.5210	090°	0.1451	0.1564	0.1839	0.4854
180°	0.2498	0.4006	0.1955	0.8459	180°	0.1504	0.1438	0.1226	0.4168
270°	0.2611	0.6819	0.3525	1.2955	270°	0.1285	0.1286	0.1272	0.3843
FOM (nT) = 5.2597					FOM (nT) = 1.6822				

Table 8: Results of compensation flight for Mag 2.

Pre-Compensation					Post-Compensation				
Heading	Roll	Pitch	Yaw	Total	Heading	Roll	Pitch	Yaw	Total
000°	2.6327	0.7073	0.4864	3.8264	000°	0.3128	0.2987	0.2373	0.8488
090°	0.8874	0.7145	0.6231	2.2250	090°	0.2038	0.1901	0.2115	0.6054
180°	0.6368	0.7181	0.3077	1.6626	180°	0.2467	0.2578	0.2161	0.7206
270°	1.1702	0.6608	0.5304	2.3614	270°	0.3434	0.3526	0.2991	0.9951
FOM (nT) = 10.0754					FOM (nT) = 3.1699				

Table 9: Results of compensation flight for Mag 3.

5.3.2 Heading Correction Test

To determine heading errors and other offsets, a cloverleaf pattern flight test was conducted at high altitude to minimize the effect of natural magnetic gradient. The cloverleaf test was flown in the same orthogonal headings as the survey and tie lines (000°/090°/180°/270° in the case of this survey) at >2500 m AGL in an area with low magnetic gradient. For all four directions of the cloverleaf test the survey helicopter must pass over the same point, at the same elevation, with the aircraft in straight and level flight. The difference in magnetic values obtained in reciprocal headings is the heading error. Heading correction values derived from the test flight for each of the magnetometers are summarized in Table 10.

Heading	Mag 1 Heading Correction (nT)	Mag 2 Heading Correction (nT)	Mag 3 Heading Correction (nT)
000°	-1.76	-0.34	-0.12
090°	-3.62	-0.93	-5.77
180°	-2.66	-0.06	-6.60
270°	8.04	1.33	12.49
Total:	0.0000	0.0000	0.0000

Table 10: Magnetic sensor heading corrections for headings 000°/090°/180°/270°.

6.0 Data Processing

After all data were collected, several procedures were undertaken to ensure that the data met a high standard of quality. Magnetic data recorded by the AGIS were converted into Geosoft or ASCII file formats using Nuvia Dynamics software. Further processing (Figure 19) was carried out using Geosoft Oasis Montaj 9.9.1 geophysical processing software along with proprietary processing algorithms.

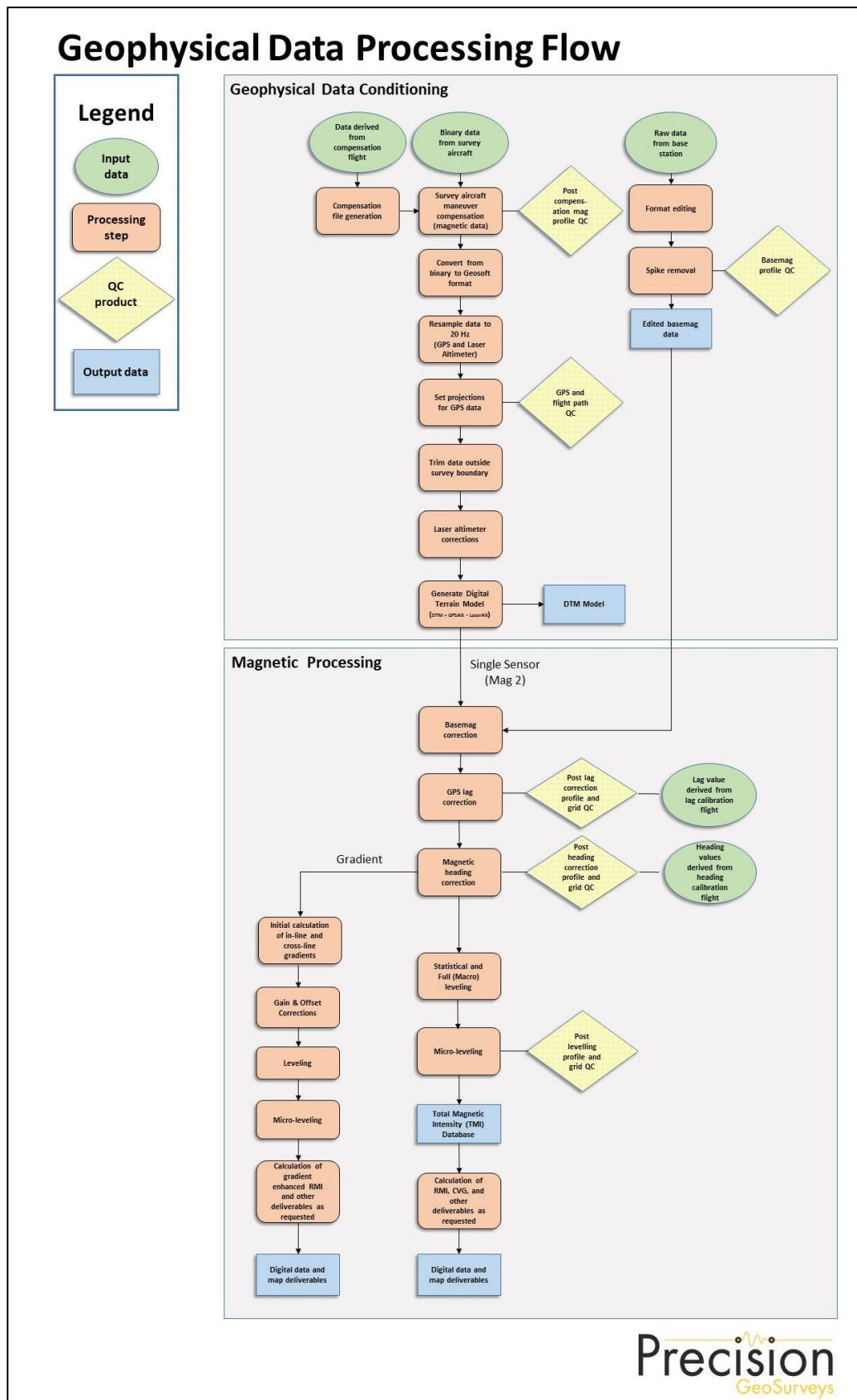


Figure 19: Magnetic data processing flow.

6.1 Position Corrections

In order to collect high resolution geophysical data, the location at which the data were collected and recorded must be accurate.

6.1.1 Lag Correction

A correction for lag error was applied to the geophysical data recorded at each individual sensor to compensate for the combination of lag in the recording system and the sensing instrument flying in a different location from the GPS antenna, as determined during the lag test. Validity of the lag corrections was confirmed by the absence of grid corrugations in adjoining reciprocal lines.

6.2 Flight Height and Digital Terrain Model

Laser altimeters are unable to provide valid data over glassy water or fog which dissipate the laser so that a “zero” reading is obtained. In these cases, estimates of correct height are inserted manually. Dense vegetation generates high frequency variations from leaf and branch reflections. A Rolling Statistics filter is applied to the lag corrected (0.80 seconds lag) laser altimeter data to remove vegetation clutter followed by a Low Pass filter to smooth out the laser altimeter profile to eliminate isolated high frequency noise and generate a surface closely corresponding to the actual ground profile.

As the GPS antenna is on the tail of the helicopter, altitude data were corrected by subtracting 3.1 m to place it in the same plane as the laser altimeter. A Digital Terrain Model (DTM) was determined by subtracting the laser altimeter data from the filtered GPS altimeter data defined by the WGS 84 ellipsoidal height. DTM accuracy is affected by the attitude of the aircraft, slope of the ground, sample density, and satellite geometry. Small inconsistencies in recorded flight height at the intersection points of survey lines and tie lines resulted in small spatial variabilities in the digital terrain model. Conventional leveling and micro-leveling were applied to correct for these variations and a fully leveled digital terrain model was generated.

6.3 Magnetic Processing

Magnetic data from each individual sensor were corrected for temporal variations (including diurnal) and lag. The data were examined for magnetic noise and spikes, which were removed as required. Survey and tie line data of the resulting total magnetic field were leveled and the background magnetic field, International Geomagnetic Reference Field (IGRF) of the Earth was removed to derive the residual magnetic field. Magnetic gradients in the X and Y axes were determined to provide cross-line and in-line gradients, respectively.

6.3.1 Temporal Variation Correction

The intensity of Earth's magnetic field varies with location and time. The time variable, known as diurnal or more correctly temporal variation, is removed from the recorded airborne data to provide the desired magnetic field at a specified location. Magnetic data from base station GEM 6 were used for correcting the airborne magnetic survey data, and GEM 5 data were retained for backup. The data were edited, plotted, and merged into a Geosoft database (.GDB) on a daily basis.

Base station measurements were averaged to establish a magnetic reference datum of 54657.64 nT. Magnetic deviations relative to the reference datum were used to calculate the observed variations of the Earth's magnetic field during the time it took to complete the survey. The airborne magnetic data were then corrected for temporal variations by subtracting the base station deviations from the data collected on the aircraft, effectively removing the effects of diurnal and other temporal variations.

6.3.2 Heading Correction

For each survey heading, changes in the apparent magnetic field due to instrumental heading error are measured and recorded. These values are used to construct a heading table (.TBL) file. For the entire dataset, the overall average magnetic field value was calculated. For each of the four headings, the averages were calculated and then compared to the overall average to determine four values which were used to correct heading and offset errors in each flight direction for each magnetometer.

6.3.3 Leveling and Micro-leveling

Small inconsistencies in flight height and line orientation result in small spatial variabilities in magnetic intensity measured at the intersection points of survey lines and tie lines. Using the initial Total Magnetic Intensity (TMI) data from Mag 2, data from survey and tie lines were leveled to each other. Two types of leveling were applied to the corrected data: conventional leveling and micro-leveling. There were two components to conventional leveling: statistical leveling to level tie lines and full leveling to level survey lines. The statistical leveling method corrected the SL/TL intersection errors that follow a specific pattern or trend. Through the error channel, an algorithm calculated a least-squares trend line and derived a trend error curve, which was then added to the channel to be leveled. The second component was full leveling. This adjusted the magnetic value of the survey lines so that all lines matched the trended tie lines at each intersection point.

Following statistical and full leveling, micro-leveling was applied to the corrected conventional leveled data. This iterative grid-based process removed low amplitude components of flight line

noise that still remained in the data after tie line and survey line leveling and resulted in fully leveled TMI data.

6.3.4 IGRF Removal

The International Geomagnetic Reference Field (IGRF) model is the empirical representation of Earth's dynamic magnetic field (main core field without external sources) collected and disseminated from satellite data and from magnetic observatories around the world. The IGRF has historically been revised and updated every five years by a group of modellers associated with the International Association of Geomagnetism and Aeronomy (IAGA).

The leveled Residual Magnetic Intensity (RMI) was calculated by taking the difference between the 13th generation IGRF (IGRF-13, released in December 2019) and the leveled Total Magnetic Intensity (TMI) to create a more valid model of individual near-surface magnetic anomalies. This model is independent of time to allow for other magnetic data (previous or future) to be more easily incorporated into each survey database.

6.4 Magnetic Gradient

When magnetic values are obtained simultaneously from two or more sensors at a fixed separation, gradient of the magnetic field can be measured. Dividing the difference in magnetic values between the sensors by the distance between the sensors yields the magnetic gradient. The units are commonly reported as nT/m and, by convention, positive magnetic polarity is defined as to the north and east, and negative to the south and west. For vertical gradient, positive is defined as downwards. The sensors and the separations that were used to determine the various gradients are listed in Table 11.

Direction	Sensors	Separation (m)
Lateral (X)	Mag 1 and Mag 3	11.5
Longitudinal (Y)	Sequential TMI values (Mag 2)	2.07*

Table 11: Magnetic sensor relationship used to calculate magnetic gradients. Total magnetic intensity (TMI) was determined from Mag 2, and successive values of the TMI were used to determine the longitudinal (Y axis) gradient.

*average separation between sequential TMI values shown; actual value varied according to aircraft speed.

6.4.1 Horizontal Gradients

Horizontal magnetic gradients were determined in the in-line (Y axis) and cross-line (X axis) directions. Gradients were calculated with respect to the magnetometer array with units provided as nT/m.

In-line gradient (ILG) is determined from successive magnetic values of Mag 2 referenced to the distance between data points in accordance with the following formula:

$$ILG = \frac{a(i + 1) - a(i - 1)}{d(i + 1) + d(i - 1)}$$

where: a is the total magnetic intensity of Mag 2
 d is the distance between measurements
 i is the record number for the location

Cross-line gradient (XLG) was measured directly by dividing the difference between Mag 1 and Mag 3 by the sensor separation in accordance with the following formula:

$$XLG = \frac{\text{Mag 1} - \text{Mag 3}}{d_x}$$

where: d_x is the transverse sensor separation, 11.5 m

Gain corrections were applied to the initial cross-line gradient. If the ratio of the TMI between Mag 1 and Mag 3 does not equal one, a gain correction needs to be applied to account for instrument error and asymmetric magnetic fields. The mean of the ratio between the TMI values for Mag 1 and Mag 3 for each line was calculated and applied to each Mag 3 value along the line. The cross line gradient was then re-calculated from the gain-corrected Mag 3 values.

Offset corrections were then applied to the cross-line gradient to reduce line-to-line errors (striping) in the gradient grid. The resulting data were then micro-leveled to remove any remaining striping.

Total Horizontal Gradient (HG) is the magnitude of the combined in-line and cross-line gradients. It is used to estimate contact locations of magnetic bodies at shallow depths, reveal anomaly textures, and highlight anomaly-pattern discontinuities.

Horizontal Gradient (HG) is calculated as:

$$HG(x, y) = \sqrt{ILG^2 + XLG^2}$$

where: *ILG* is the in-line gradient
XLG is the cross-line gradient

6.4.2 Calculation of Vertical Gradient

Calculated Vertical Gradient (CVG) is the first order vertical derivative of the leveled Residual Magnetic Intensity (RMI) data determined from Mag 2. It is the vertical rate of change in the magnetic field per unit distance (m). The vertical gradient is used to enhance shorter wavelength signals; therefore, edges of magnetic anomalies are highlighted, and deep geologic sources in the data are suppressed.

The filter, *L*, used to produce the n^{th} vertical derivative is described by:

$$L(r) = r^n$$

where: *r* is the radial component in the wavenumber domain

6.4.3 Gradient Enhanced Magnetic Intensity

Total magnetic intensity was gridded using a bi-directional method, which allowed horizontal gradient data to be incorporated to create a gradient enhanced Total Magnetic Intensity (TMIge) grid. The TMIge grid was imported back into the final database to be available for alternative gridding methods. The gradient enhanced Residual Magnetic Intensity (RMIge) was derived by taking the difference between the gradient enhanced Total Magnetic Intensity (TMIge) and IGRF.

6.4.4 Gradient Enhanced Reduction to Magnetic Pole

Gradient enhanced Reduced to Magnetic Pole (RTPge) data were determined from the gradient enhanced Residual Magnetic Intensity (RMIge) data. The RTP filter was applied in the Fourier domain and rotates the observed magnetic inclination and declination field to what the field would look like at the north magnetic pole, to allow observation of magnetic trends and patterns independent of magnetic inclination and declination.

Inclination and declination were calculated by using the “Date” channel. The derived values were used in the following formula:

$$RTP(\theta) = \frac{[\sin(I) - I \cdot \cos(I) \cdot \cos(D - \theta)]^2}{[\sin^2(I_a) + \cos^2(I_a) \cdot \cos^2(D - \theta)] \cdot [\sin^2(I) + \cos^2(I) \cdot \cos^2(D - \theta)]}$$

where: I is geomagnetic inclination in ° from horizontal

D is geomagnetic declination in ° azimuth from magnetic north

I_a is the inclination for amplitude correction (never less than I). Default is $\pm 20^\circ$. If $|I_a|$ is specified to be less than $|I|$, it is set to I

7.0 Deliverables

McNulty survey block data are presented as digital databases, grids, maps, and a logistics report.

7.1 Digital Data

Digital files have been provided in three formats, the first is a .GDB file for use in Geosoft Oasis Montaj, the second format is a text (.XYZ) file, and the third format is an excel comma separated (.CSV) file. Full descriptions of the digital data and contents are included in the report (Appendix B).

7.1.1 Grids

The digital data were represented as grids as listed below:

- Digital Terrain Model (DTM)
- Total Magnetic Intensity (TMI)
- Residual Magnetic Intensity (RMI) – removal of IGRF from TMI
- In-Line Gradient (ILG)
- Cross-Line Gradient (XLG)
- Horizontal Gradient (HG) – total magnitude of the horizontal gradients (in-line and cross-line)
- Calculated Vertical Gradient (CVG)
- Gradient enhanced Total Magnetic Intensity (TMIge)
- Gradient enhanced Residual Magnetic Intensity (RMIge) – subtraction of IGRF
- Gradient enhanced Reduced to Magnetic Pole (RTPge) – reduced to magnetic pole of RMIge

Non-gradient magnetic digital data were gridded and displayed using the following Geosoft parameters:

- Gridding method: minimum curvature
- Grid cell size: 25 m
- Low-pass desampling factor: 2

- Tolerance: 0.001
- % pass tolerance: 99.99
- Maximum iterations: 100

Gradient-enhanced magnetic grids were generated and displayed using the following Geosoft parameters:

- Gridding method: gradient enhanced bi-directional
- Grid cell size: 12.5 m
- Gradient noise level: 5.0

The gradient magnetic grids (ILG and XLG) were drawn with a linear wet-look colour shade and all other magnetic grids were drawn with a histogram-equalized colour shade. All maps were shaded with the sun illumination inclination at 45° and declination at 045°. DTM grid was drawn with a linear topographic colour scale.

7.2 KMZ

Gridded digital data were exported into .KMZ files which can be displayed using Google Earth. The grids can be draped onto topography and rendered to give a 3D view.

7.3 Maps

Digital maps were created for the McNulty survey block. The following map products were prepared:

Overview Maps (colour images with elevation contour lines and topographic features):

- Actual flight lines
- DTM

Magnetic Maps (colour images with elevation contour lines):

- TMI, with actual flight lines and topographic features
- TMI
- RMI
- ILG
- XLG
- HG
- CVG

Gradient Enhanced Magnetic Maps (colour images with elevation contour lines):

- TMIge
- RMIge
- RTPge

All survey maps were prepared in WGS 84 and UTM Zone 10N.

7.4 Report

A .PDF copy of the logistics report is included along with digital data and maps. The report provides information on acquisition, processing, and presentation of the McNulty survey block data.

8.0 Conclusions and Recommendations

The McNulty survey resulted in the collection of 338 line km of high resolution gradient magnetic data over one survey block. The data have been processed and plotted on maps as a representation of the magnetic features of the survey area.

Geophysical data processing, particularly leveling and data interpolation routines, may tend to smooth the original data so that resolution is reduced. In addition, gridding algorithms are not always able to properly calculate grids where flight height between adjacent flight lines varied due to cultural obstacles or steep terrain, where geological structures are acute to flight lines, where line spacing exceeds the size of the causative anomaly, or near grid margins as in “edge effects.” Therefore, subtle geophysical features in gridded and derivative-enhanced products or near the survey margins may introduce artifacts and must be evaluated with discretion.

The airborne geophysical data were acquired to map the geophysical characteristics of the survey area, which are in turn related to the distribution and concentration of magnetic minerals in the Earth. Geophysical data are rarely a direct indication of mineral deposits and therefore interpretation and careful integration with existing and new geological, geochemical, and other geophysical data are recommended to maximize value from the survey investment.

Respectfully submitted,
Precision GeoSurveys Inc.

Jenny Poon, P.Geo.
April 2021

Appendix A

Polygon Coordinates

- McNulty Survey Block

McNulty Survey Block – WGS 84 Zone 10N

Latitude (deg N)	Longitude (deg W)	Easting (m)	Northing (m)
49.52904	120.21376	701613	5490000
49.52906	120.11999	708397	5490257
49.49155	120.11999	708557	5486088
49.49155	120.21374	701769	5485833

Appendix B

Equipment Specifications

- GEM GSM-19T Proton Precession Magnetometer (Magnetic Base Station)
- Hemisphere R330 GPS Receiver
- Opti-Logic RS800 Rangefinder Laser Altimeter
- Scintrex CS-3 Survey Magnetometer
- Geometrics G-822A Survey Magnetometer
- Billingsley TFM100G2 Ultra Miniature Triaxial Fluxgate Magnetometer
- Nuvia Dynamics IMPAC data recorder system (for navigation and geophysical data acquisition)

GEM GSM-19T Proton Precession Magnetometer (Magnetic Base Station)

Sensitivity	0.15 nT @ 1 Hz
Resolution	0.01 nT (gamma), magnetic field and gradient
Absolute Accuracy	±0.2 nT @ 1 Hz
Operating Range	20,000 nT to 120,000 nT
Gradient Tolerance	Over 7,000 nT/m
Operating Ranges	Temperature: -40°C to +50°C Battery Voltage: 10.0 V minimum to 15 V maximum Humidity: up to 90% relative, non-condensing
Storage Temperature	-50°C to +50°C
Dimensions	Console: 223 x 69 x 40 mm Sensor Staff: 4 x 450 mm sections Sensor: 170 x 71 mm dia. Weight: console 2.1 kg, sensor and staff assembly 2.2 kg
Integrated GPS	Yes

Hemisphere R330 GPS Receiver

GPS Sensor	Receiver Type	L1 and L2 RTK with carrier phase	
	Channels	12 L1CA GPS 12 L1P GPS 12 L2P GPS 12 L2C GPS 12 L1 GLONASS (with subscription code) 12 L2 GLONASS (with subscription code) 3 SBAS or 3 additional L1CA GPS	
	Update Rate	10 Hz standard, 20 Hz available	
	Cold Start Time	<60 s	
	Warm Start Time 1	30 s (valid ephemeris)	
	Warm Start Time 2	30 s (almanac and RTC)	
	Hot Start Time	10 s typical (valid ephemeris and RTC)	
	Reacquisition	<1 s	
	Differential Options	SBAS, Autonomous, External RTCM, RTK, OmniSTAR (HP/XP)	
	Horizontal Accuracy		RMS (67%)
RTK ^{1,2}		10 mm + 1 ppm	20 mm + 2 ppm
OmniSTAR HP ^{1,3}		0.1 m	0.2 m
SBAS (WAAS) ¹		0.3 m	0.6 m
Autonomous, no SA ¹		1.2 m	2.5 m
L-Band Sensor	Channel	Single channel	
	Frequency Range	1530 MHz to 1560 MHz	
	Satellite Selection	Manual or Automatic (based on location)	
	Startup and Satellite Reacquisition Time	15 seconds typical	
Communications	Serial Ports	2 full duplex RS232	
	Baud Rates	4800 – 115200	
	USB Ports	1 Communications, 1 Flash Drive data storage	
	Correction I/O Protocol	Hemisphere GPS proprietary, RTCM v2.3 (DGPS), RTCM v3 (RTK), CMR, CMR+NMEA 0183, Hemisphere GPS binary	
	Timing Output	1 PPS (HCMOS, active high, rising edge sync, 10 kΩ, 10 pF load)	
	Event Marker Input	HCMOS, active low, falling edge sync, 10 kΩ	
Environmental	Operating Temperature	-40°C to +70°C	
	Storage Temperature	-40°C to +85°C	
	Humidity	95% non-condensing	
Power GPS Sensor	Input Voltage Range	8 to 36 VDC	
	Consumption, RTK	<3.5 W (0.30 A @ 12 VDC typical)	
	Consumption, OmniSTAR	<4.3 W (0.36 A @ 12 VDC typical)	

¹ Depends on multipath environment, number of satellites in view, satellite geometry and ionospheric activity.

² Depends also on baseline length.

³ Requires a subscription from OmniSTAR.

Opti-Logic RS800 Rangefinder Laser Altimeter

Accuracy	±1 m on 1x1 m ² diffuse target with 50% reflectivity, up to 700 m
Resolution	0.2 m
Communication Protocol	RS232-8, N, 1 ASCII characters
Baud Rate	19200
Data Raw Counts	~200 Hz
Data Calibrated Range	~10 Hz
Data Rate	~200 Hz raw counts for un-calibrated operation; ~10 Hz for calibrated operation (averaging algorithm seeks 8 good readings)
Calibrated Range Units	Feet, Meters, Yards
Laser	Class I (eye-safe), 905 nm ± 10 nm
Power	7 - 9 VDC conditioned required, current draw at full power (~ 1.8 W)
Laser Wavelength	RS100 905 nm ± 10 nm
Laser Divergence	Vertical axis – 3.5 mrad half-angle divergence; Horizontal axis – 1 mrad half-angle divergence; (approximate beam “footprint” at 100 m is 35 cm x 5 cm)
Dimensions	32 x 78 x 84 mm (lens face cross section is 32 x 78 mm)
Weight	<227 g (8 oz)
Casing	RS100/RS400/RS800 units are supplied as OEM modules consisting of an open chassis containing optics and circuit boards. Custom housings can be designed and built on request.

Scintrex CS-3 Magnetometer

Operating Principal	Self-oscillating split-beam Cesium Vapor (non-radioactive ^{133}Cs)
Operating Range	15,000 nT to 105,000 nT
Gradient Tolerance	40,000 nT/m
Operating Zones	15° to 75° and 105° to 165°
Hemisphere Switching	a) Automatic b) Electronic control actuated by the control voltage levels (TTL/CMOS) c) Manual
Sensitivity	0.0006 nT $\sqrt{\text{Hz}}$ rms
Noise Envelope	Typically 0.002 nT peak to peak, 0.1 to 1 Hz bandwidth
Heading Error	± 0.20 nT (inside the optical axis to the field direction angle range 15° to 75° and 105° to 165°)
Absolute Accuracy	<2.5 nT throughout range
Output	a) Continuous signal at the Larmor frequency which is proportional to the magnetic field (proportionality constant 3.49857 Hz/nT) sine wave signal amplitude modulated on the power supply voltage b) Square wave signal at the I/O connector, TTL/CMOS compatible
Information Bandwidth	Only limited by the magnetometer processor used
Sensor Head	Diameter: 63 mm (2.5") Length: 160 mm (6.3") Weight: 1.15 kg (2.6 lb)
Sensor Electronics	Diameter: 63 mm (2.5") Length: 350 mm (13.8") Weight: 1.5 kg (3.3 lb)
Cable, Sensor to Sensor Electronics	3 m (9' 8"), lengths up to 5 m (16' 4") available
Operating Temperature	-40°C to +50°C
Humidity	Up to 100%, splash proof
Supply Power	24 to 35 VDC
Supply Current	Approx. 1.5 A at start up, decreasing to 0.5 A at 20°C
Power Up Time	Less than 15 minutes at -30°C

Geometrics G-822A Magnetometer

Operating Principal	Self-oscillating split-beam Cesium Vapor (non-radioactive ^{133}Cs)
Operating Range	20,000 nT to 100,000 nT
Operating Zones	Earth's field vector should be at an angle greater than 6° from the sensor's equator and greater than 6° away from the sensor's long axis.
Hemisphere Switching	Automatic
Sensitivity	<0.0005 nT $\sqrt{\text{Hz}}$ rms.
Noise Envelope	Typically 0.002 nT peak to peak at a 0.1 second sample rate (90% of all readings falling within the peak to peak envelope) using a 822A super-counter
Heading Error	<0.15 nT over entire 360° polar and equatorial spin
Absolute Accuracy	Better than 3 nT throughout range
Output	Cycle of Larmor frequency = 3.498572 Hz/nT, RS-232 data at 9600 baud, concatenated data streams from up to 6 sensors
Sensor Head	Diameter: 60.32 mm (2.375") Length: 158.75 mm (6.25") Weight: 680 g (24 oz)
Sensor Electronics	Diameter: 63.5 mm (2.5") Length: 279.4 mm (11") Weight: 680 g (24 oz)
Cable, Sensor to Electronics	Standard: 2.77 m (109") Cable length can be increased by 1.10 m (43") for a total length of 3.87 m (152")
Cable, Sensor Electronics to Counter	Standard: 10 m (33') Cable length can be increased up to 50 m (164')
Operating Temperature	-35°C to +50°C (-30°F to +122°F)
Storage Temperature	-45°C to +70°C (-48°F to +158°F)
Altitude	Up to 9,000 m (30,000 ft)
Water Tight	Sealed for up to 0.9 m (2 ft) water depth
Supply Power	24 to 35 VDC, 0.75 amp at turn-on and 0.5 amp thereafter

Billingsley TFM100G2 Ultra Miniature Triaxial Fluxgate Magnetometer

Axial Alignment	Orthogonality better than $\pm 1^\circ$
Input Voltage Options	15 to 34 VDC @ 30 mA
Field Measurement Range Options	$\pm 100 \mu\text{T} = \pm 10 \text{ V}$
Accuracy	$\pm 0.75\%$ of full scale (0.5% typical)
Linearity	$\pm 0.015\%$ of full scale
Sensitivity	100 $\mu\text{V/nT}$
Scale Factor Temperature Shift	0.007% full scale/ $^\circ\text{C}$
Noise	$\leq 12 \text{ pT rms}/\sqrt{\text{Hz}}$ @ 1 Hz
Output Ripple	3 mV peak to peak @ 2 nd harmonic
Analog Output at Zero Field	$\pm 0.025 \text{ V}$
Zero Shift with Temperature	$\pm 0.6 \text{ nT}/^\circ\text{C}$
Susceptibility to Perming	$\pm 8 \text{ nT}$ shift with $\pm 5 \text{ Gs}$ applied
Output Impedance	$332 \Omega \pm 5\%$
Frequency Response	3 dB @ $> 500 \text{ Hz}$ (to $> 4 \text{ kHz}$ wide band)
Over Load Recovery	$\pm 5 \text{ Gs}$ slew $< 2 \text{ ms}$
Random Vibration	$> 20 \text{ G rms}$ 20 Hz to 2 kHz
Temperature Range	-55°C to $+85^\circ\text{C}$
Acceleration	$> 60 \text{ G}$
Weight	100 g
Size	3.51 cm x 3.23 cm x 8.26 cm
Connector	Chassis mounted 9 pin male "D" type

Nuvia Dynamics IMPAC data recorder system

(for navigation and geophysical data acquisition)

Functions	Integrated Multi-Parameter Airborne Console (IMPAC) with integrated dual Global Positioning System Receiver (GPS) and all necessary navigation guidance software. Inputs for geophysical sensors - portable gamma ray spectrometer GRS-10/AGRS, MMS4/MMS8 Magnetometer, Totem 2A EM, A/D converter, temperature/humidity probe, barometric pressure probe, and laser/radar altimeter. Output for the multi-parameter PGU (Pilot Guidance Unit)
Display	Monitor display 600 x 800 pixels; customized keypad and operator keyboard. Multi-screen options for real-time viewing of all data inputs, fiducial points, flight line tracking, and GPS channels by operator
Navigation	Pilot/operator navigation guidance. Software supports preplanned survey flight plan, along survey lines, way-points, preplanned drape profile surfaces
Data Sampling	Sensor dependent
Data Synchronization	Synchronized to GPS position. Supports dual GPS
Data File	PEI Binary data format
Storage	80 GB
Software	PEIView: Allows fast data verification and conversion of PEI binary data to Geosoft GBN or ASCII formats PEIConv: For survey preparation, calibration and conversion of maps, and survey plot after data acquisition PEIComp: For calculation of magnetic compensation coefficients AGRS/GRS10 Calibration: High voltage adjustment, linearity correction coefficients calculation, and communication test support AGIS: Real time data acquisition and navigation system. Displays chart/spectrum view in real-time for fast data Quality Control (QC)
Electrical	Multiple ethernet connections, RS232 serial ports, USB ports, and 16-bit differential analog input channels. It can support up to 4 magnetometer sensors
Power Requirement	24 VDC

Appendix C

Digital File Descriptions

- Magnetic Database
- Geosoft Grids
- Maps

Magnetic Database:

Abbreviations used in the GDB/XYZ/CSV files listed below:

CHANNEL	UNITS	DESCRIPTION
X_WGS84	m	UTM Easting – WGS84 Zone 10N
Y_WGS84	m	UTM Northing – WGS84 Zone 10N
Lat_deg	Decimal degree	Latitude – WGS84
Lon_deg	Decimal degree	Longitude – WGS84
Date	yyyy/mm/dd	Dates of the survey flight(s) – Local
FLT		Flight Line numbers
LineNo		Line numbers
STL		Number of satellite(s)
GPSfix		1 = non-differential 2 = WAAS/SBAS differential
Heading	degree	Heading of the aircraft
GPStime	HH:MM:SS	GPS time (UTC)
Geos_m	m	Geoidal separation
XTE_m	m	Cross track error
Galt	m	GPS height – WGS84 Zone 10N (ASL)
Lalt	m	Laser altimeter readings (AGL)
DTM	m	Digital Terrain Model
Sample_Density	m	Horizontal distance in meters between adjacent measurement locations; sample frequency is 20 Hz
Speed_km_hr	km/hr	Ground speed of aircraft in km/hr
basemag	nT	Base station temporal variation data
IGRF	nT	International Geomagnetic Reference Field, IGRF-13
Declin	Decimal degree	Calculated declination of magnetic field
Inclin	Decimal degree	Calculated inclination of magnetic field
XFg_Step	step	X - fluxgate
YFg_Step	step	Y - fluxgate
ZFg_Step	step	Z - fluxgate
Mag1_Head	nT	Mag 1 – Diurnal, lag, and heading corrected
Mag2_Head	nT	Mag 2 – Diurnal, lag, and heading corrected
Mag3_Head	nT	Mag 3 – Diurnal, lag, and heading corrected
TMI	nT	Total Magnetic Intensity (Mag 2)
RMI	nT	Residual Magnetic Intensity (Mag 2)
ILG	nT/m	In-Line Gradient (Mag 2)
XLG	nT/m	Cross-Line Gradient (Mag 1 and Mag 3)
HG	nT/m	Total horizontal gradient (in-line and cross-line)
TMIge	nT	Gradient enhanced Total Magnetic Intensity
RMIge	nT	Gradient enhanced Residual Magnetic Intensity

Grids:

McNulty, WGS 84 Datum, Zone 10N, cell size at 25 m

FILE NAME	DESCRIPTION
21142_McNulty_DTM_25m.grd	Digital Terrain Model gridded at 25 m cell size
21142_McNulty_TMI_25m.grd	Total Magnetic Intensity gridded at 25 m cell size
21142_McNulty_RMI_25m.grd	Residual Magnetic Intensity gridded at 25 m cell size
21142_McNulty_ILG_25m.grd	Measured In-Line Gradient (Mag 1 and Mag 2) gridded at 25 m cell size
21142_McNulty_XLG_25m.grd	Measured Cross-Line Gradient (Mag 1 and Mag 2) gridded at 25 m cell size
21142_McNulty_HG_25m.grd	Total Horizontal Gradient (in-line and cross-line) gridded at 25 m cell size
21142_McNulty_CVG_25m.grd	Calculated Vertical Gradient of RMI gridded at 25 m cell size
21142_McNulty_TMIge_25m.grd	Gradient enhanced Total Magnetic Intensity (in-line, cross-line, and vertical gradients) gridded at 25 m cell size
21142_McNulty_RMIge_25m.grd	Gradient enhanced Residual Magnetic Intensity (in-line, cross-line, and vertical gradients) gridded at 25 m cell size
21142_McNulty_RTPge_25m.grd	Gradient enhanced Reduced to Magnetic Pole of RMIge gridded at 25 m cell size

*Grids are exported as Geotiffs (.tiff)

Maps:

McNulty, WGS 84 Datum, Zone 10N (jpegs, pdfs, and georeferenced pdf)

Plate Number	Plate Name	FILE NAME	DESCRIPTION
1	FL	21142_McNulty_ActualFlightLines	Plotted actual flown flight lines
2	DTM	21142_McNulty_DTM_25m	Digital Terrain Model gridded at 25 m cell size
3	TMI_wFL	21142_McNulty_TMI_wFL_25m	Total Magnetic Intensity gridded at 25 m cell size with actual flown flight lines
4	TMI	21142_McNulty_TMI_25m	Total Magnetic Intensity gridded at 25 m cell size
5	RMI	21142_McNulty_RMI_25m	Residual Magnetic Intensity gridded at 25 m cell size
6	ILG	21142_McNulty_ILG_25m	Measured In-Line Gradient gridded at 25 m cell size
7	XLG	21142_McNulty_XLG_25m	Measured Cross-Line Gradient gridded at 25 m cell size
8	HG	21142_McNulty_HG_25m	Total Horizontal Gradient gridded at 25 m cell size
9	CVG	21142_McNulty_CVG_25m	Calculated Vertical Gradient of RMI gridded at 25 m cell size
10	TMIge	21142_McNulty_TMIge_25m	Gradient enhanced Total Magnetic Intensity gridded at 25 m cell size
11	RMIge	21142_McNulty_RMIge_25m	Gradient enhanced Residual Magnetic Intensity gridded at 25 m cell size
12	RTPge	21142_McNulty_RTPge_25m	Gradient enhanced Reduced to Magnetic Pole of RMIge gridded at 25 m cell size

Plates

McNulty Survey Block

- Plate 1: McNulty – Actual Flight Lines (FL)
- Plate 2: McNulty – Digital Terrain Model (DTM)
- Plate 3: McNulty – Total Magnetic Intensity with Actual Flight Lines (TMI_wFL)
- Plate 4: McNulty – Total Magnetic Intensity (TMI)
- Plate 5: McNulty – Residual Magnetic Intensity (RMI)
- Plate 6: McNulty – In-Line Gradient (ILG)
- Plate 7: McNulty – Cross-Line Gradient (XLG)
- Plate 8: McNulty – Horizontal Gradient (HG)
- Plate 9: McNulty – Calculated Vertical Gradient (CVG) of RMI
- Plate 10: McNulty – Gradient Enhanced Total Magnetic Intensity (TMIge)
- Plate 11: McNulty – Gradient Enhanced Residual Magnetic Intensity (RMIge)
- Plate 12: McNulty – Gradient Enhanced Reduced to Magnetic Pole (RTPge) of RMIge